Cretaceous Research

Macrofauna and biostratigraphy of the Rollrock Section, northern Ellesmere Island, Canadian Arctic Islands – a comprehensive high latitude archive of the Jurassic–Cretaceous transition

--Manuscript Draft--

Manuscript Number:	YCRES_2020_5R1
Article Type:	Full Length Article
Keywords:	Berriasian; Tithonian; Valanginian; Buchia; ammonites; belemnites
Corresponding Author:	Simon Schneider CASP Cambridge, United Kingdom
First Author:	Simon Schneider
Order of Authors:	Simon Schneider
	Simon R. A. Kelly
	Joerg Mutterlose
	Jens Herrle
	Peter Hülse
	David Jolley
	Claudia Schroder-Adams
	Berta Lopez-Mir
Abstract:	The Rollrock Section in the Sverdrup Basin, Arctic Canada, is one of the northernmost outcrops where the Jurassic-Cretaceous transition is accessible. The over 500 m thick sedimentary succession exposes the Oxfordian to Valanginian Ringnes and Deer Bay formations. Macrofauna from 15 discrete horizons includes ammonites, Buchia bivalves and belemnites. These fossils improve the biostratigraphy of the Tithonian and Berriasian in the Sverdrup Basin, provide correlation to the remainder of the Boreal Realm and set reliable calibration points. The occurrence of Buchia rugosa in the Ringnes Formation moves the upper formation boundary of from the top of the Kimmeridgian into the lower Tithonian. Dorsoplanites maximus and D. sachsi document the middle Tithonian Dorsoplanites maximus Zone in Arctic Canada for the first time. The late Tithonian to early Berriasian Buchia terebratuloides is considered to be the best approximate indicator of the Jurassic-Cretaceous transition in the Rollrock Section. The middle early Berriasian Praetollia maynci and the late early Berriasian Borealites fedorovi tie the respective horizons to the successive Chetaites sibiricus and Hectoroceras kochi zones. Two species of the belemnite Arctoteuthis, collected from an interval with glendonites, suggest a Valanginian age for the upper Deer Bay Formation. The dearth of Late Jurassic to earliest Cretaceous macrofossils in the Sverdrup Basin is inferred to be predominantly a function of diagenetic carbonate loss. Abundant dropstones and glendonites in the middle Tithonian to middle Valanginian interval suggest cold climatic conditions, and make the Rollrock Section a prime candidate for studying the Arctic environmental perturbations of this time.
Suggested Reviewers:	Terry Poulton terry.poulton@canada.ca expert on biostratigraphy of study interval and on the Canadian Arctic
	Peter Alsen pal@geus.dk expert on biostratigraphy of study interval and on Boreal region
	Viktor Zakharov mzarctic@gmail.com expert on biostratigraphy of study interval and on Boreal region
Opposed Reviewers:	

Macrofauna and biostratigraphy of the Rollrock Section, northern Ellesmere Island, Canadian Arctic Islands – a comprehensive high latitude archive of the Jurassic–Cretaceous transition

[1]*Simon Schneider, [1]Simon R. A. Kelly, [2]Jörg Mutterlose, [3]Jens O. Herrle, [1]Peter Hülse, [4]David W. Jolley, [5]Claudia J. Schröder-Adams & [1]Berta Lopez-Mir

[1]CASP, West Building, Madingley Rise, Madingley Road, Cambridge, CB3 0UD, United Kingdom; *author for correspondence; e-mail: simon.schneider@casp.org.uk.

[2]Institut for Geologie, Mineralogy and Geophysics, Ruhr-Universität Bochum, Universitätsstrasse 150, 44801 Bochum, Germany.

[3]Institute of Geosciences, Goethe-University Frankfurt, Altenhoeferallee 1, 60438 Frankfurt am Main, Germany.

[4]School of Geosciences, Geology & Petroleum Geology, University of Aberdeen, Meston Building, King's College, Aberdeen, AB24 3UE, United Kingdom.

[5]Department of Earth Sciences, Carleton University, 1125 Colonel By Drive, Ottawa, Ontario, K1S 5B6, Canada.

Abstract

The Rollrock Section in the Sverdrup Basin of Arctic Canada is one of the northernmost outcrops where the Jurassic-Cretaceous transition is accessible. The over 500 m thick sedimentary succession

exposes the Oxfordian to Valanginian Ringnes and Deer Bay formations. Macrofauna from 15 discrete horizons includes ammonites, *Buchia* bivalves and belemnites. These fossils improve the biostratigraphy of the Tithonian and Berriasian in the Sverdrup Basin, provide correlation to the remainder of the Boreal Realm and set reliable calibration points. The occurrence of *Buchia rugosa* in the Ringnes Formation moves the upper formation boundary of from the top of the Kimmeridgian into the lower Tithonian. *Dorsoplanites maximus* and *D. sachsi* document the middle Tithonian *Dorsoplanites maximus* Zone in Arctic Canada for the first time. The late Tithonian to early Berriasian *Buchia terebratuloides* is considered to be the best approximate indicator of the Jurassic-Cretaceous transition in the Rollrock Section. The middle early Berriasian *Praetollia maynci* and the late early Berriasian *Borealites fedorovi* tie the respective horizons to the successive *Chetaites sibiricus* and *Hectoroceras kochi* zones. Two species of the belemnite *Arctoteuthis*, collected from an interval with common glendonites, suggest a Valanginian age for the upper Deer Bay Formation. The dearth of Late Jurassic to earliest Cretaceous macrofossils in the Sverdrup Basin is inferred to be predominantly a function of diagenetic carbonate loss. Abundant dropstones and glendonites in the middle Tithonian to middle Valanginian interval suggest cold climatic conditions, and make the Rollrock Section a prime candidate for studying the Arctic environmental perturbations of this time.

Key words: Tithonian, Berriasian, Valanginian, palaeoclimate, *Buchia*, Dorsoplanitidae, Craspeditinae, belemnites.

1 Introduction

The Jurassic–Cretaceous transition interval (Tithonian to Valanginian) is widely known as a phase of environmental perturbation and associated biotic turnover (see Tennant et al., 2017 for a summary). However, the magnitudes of extinction, recovery and ecosystem change remain poorly known (e.g.

Hallam 1986; Tennant et al., 2017). Notable is a global eustatic sea-level drop of 40–50 m close to the system boundary (latest Tithonian), followed by a second drop of similar magnitude during the latest Berriasian to mid Valanginian, resulting in the lowest sea-level of the entire Cretaceous Period (Haq, 2014). Both sea-level drops were associated with significant cold intervals, but whether the low temperatures corresponded to phases of polar glaciation is still a matter of debate (e.g. Price 1999; Price et al., 2013; Haq, 2014; O'Brien et al., 2017; Vickers et al., 2019).

Logically, one would turn to high latitude records when searching for evidence of cold snaps and ice caps, or more generally for an archive of pronounced climate fluctuations. The Mesozoic sedimentary succession of the Sverdrup Basin in Arctic Canada is one of the best candidates for investigating these topics (Kemper 1987; Galloway et al., 2020). Today, only the Wandel Sea Basin in northern Greenland has exposures of the Jurassic–Cretaceous boundary interval that lie at a higher latitude (e.g. Håkansson et al. 1981). However, the palaeo-latitude of the Sverdrup Basin during the Jurassic-Cretaceous transition was lower than today, but still Arctic to sub-Arctic, approximately between 60° and 70° N (van Hinsbergen et al., 2015). Moreover, cold climatic conditions during the deposition of the Tithonian to Valanginian Deer Bay Formation of the Sverdrup Basin are suggested by the occurrence of glendonites (Kemper and Schmitz 1975, 1981; Grasby et al., 2016) and abundant dropstones (Embry 1991).

In order to investigate palaeoecology and palaeoclimate in detail, a robust stratigraphy is first needed for the study interval. In 2015, we thus logged and sampled a more than 500 m thick, continuously exposed succession of Upper Jurassic to Lower Cretaceous mudstones, cropping out on the northern flank of the Rollrock River Valley, northern Ellesmere Island. This outcrop extends laterally over more than five kilometres (Figures 1, 2) and exposes the mudstone-dominated Ringnes and Deer Bay formations, grading into sandstones of the Isachsen Formation at the top. Based on its macrofossil content, the Rollrock Section was regarded as the biostratigraphically most important Jurassic–Cretaceous transition section of the Canadian Arctic by Jeletzky (1984). Furthermore, the

succession contains glendonites in several horizons and abundant dropstones over a large interval, and thus is likely to provide a direct record of Late Jurassic to Early Cretaceous Arctic cooling.

Discovered and briefly described by Wilson (1976), the Rollrock Section was logged and sampled by A. F. Embry and N. S. Ioannides in 1977 (personal communication A. F. Embry, 2017). Their results are expressed in the 1:250,000 scale geological map of the area, issued by the Geological Survey of Canada (Map no. 1886A, Tanquary Fiord; Mayr and Trettin 1996), and the macrofossils they collected were published by Jeletzky (1984). However, no detailed account of the succession is available, and the collected palynology data were never published.

Herein, we present a comprehensive log and brief sedimentological description of the succession exposed in the Rollrock Section, along with a lithostratigraphic framework. We further provide systematic descriptions of the macrofauna, together with an updated ammonite and bivalve biostratigraphy, which correlates the Jurassic-Cretaceous boundary succession of the Sverdrup Basin with the entire Boreal Realm.

2 Geological setting

2.1 The Sverdrup Basin

The Sverdrup Basin is located in the Queen Elizabeth Islands, Nunavut and the Northwest Territories, and covers an area of approximately 300,000 km^2 (e.g. Embry and Beauchamp, 2008; Pugh et al., 2014; Fig. 1). Basin development commenced in the Mississippian on Neoproterozoic to Devonian strata, and terminated with the onset of the Eurekan Orogeny in the latest Cretaceous (e.g. Hadlari et al., 2016).

The Sverdrup Basin is filled with up to 13 km of Carboniferous to Eocene sedimentary strata, which conform to eight major, unconformity-bounded depositional phases (Embry and Beauchamp, 2008, 2019). The Rhaetian to middle Valanginian phase five, which encompasses the study interval, was

characterised by a dominantly shallow marine depositional environment. Hadlari et al. (2016) characterised the Pliensbachian to mid Valanginian interval as a syn-rift stage. They inferred that rifting of the Sverdrup Basin started in the Pliensbachian and climaxed at around the Jurassic–Cretaceous transition. This is supported by the presence of Triassic to Jurassic extensional faults near the eastern basin margin, which were recently identified from cross-section restoration by Lopez-Mir et al. (2018). Increased subsidence and sediment supply, related to rift climax, resulted in the deposition of shoreline to shallow shelfal sandstones of the Awingak Formation (Oxfordian to Berriasian) along the southern and eastern basin margins (Fig. 2). A mudstone succession, comprising the Ringnes (Oxfordian to Kimmeridgian) and Deer Bay formations (Tithonian to Valanginian), persisted in the more distal part of the basin (Embry and Beauchamp, 2019) (Fig. 2), where passive salt diapirism played a significant role in the basin evolution (Harrison and Jackson, 2014).

2.2 Biostratigraphy

Traditionally, macrofossil biostratigraphy was employed to date the Upper Jurassic to Lower Cretaceous succession of the Sverdrup Basin, most commonly using ammonites and buchiid bivalves. However, in most sections, macrofossil-bearing horizons are sparse. In the Oxfordian to Kimmeridgian Ringnes Formation (Balkwill et al., 1977), scarce finds of *Cardioceras*, *Amoeboceras* and *Buchia concentrica* are the only stratigraphically relevant macrofossils (Frebold, 1961, 1964; Poulton, 1993). From the lowest ammonite level in the Deer Bay Formation, Tithonian *Dorsoplanites*, *Laugeites* and *Pavlovia*, associated with *Buchia fischeriana* were recorded (Frebold, 1961, 1964; Jeletzky, 1984). A higher, second level has yielded ammonites reported as *Craspedites* and *Subcraspedites* (Jeletzky, 1984). The third ammonite level, with *Taimyroceras canadensis*, straddles the Tithonian–Berriasian boundary, as interpreted herein. There is broad agreement now that the base of the *Calpionella alpina* Subzone defines the base of the Berriasian Stage in the Tethyan Realm

and beyond (Wimbledon, 2017). In the absence of calpionellids from the Boreal Realm, magnetostratigraphy is one of the most promising tools for precise correlation. The *Calpionella alpina* Subzone is confidently situated in the middle of magnetostratigraphic zone M19n.2n in various Tethyan localities (Wimbledon, 2017). Magnetostratigraphy of the Nordvik Section in northern Siberia suggests that zone M19n.2n is placed within the *Taimyroceras taimyrensis* Ammonite Zone (Houša et al., 2007; Schnabl et al., 2015). No magnetostratigraphic data are available from the Canadian Arctic. However, the *Taimyroceras taimyrensis* Zone is correlated with the level of *Taimyroceras canadensis* at Slidre Fiord on Fosheim Peninsula, Ellesmere Island, where it overlaps the upper part of the *Buchia unschensis* – *B. terebratuloides* Zone of Jeletzky (1966, 1984: fig. 9). As a working hypothesis, we adopt this interpretation of the Tithonian–Berriasian boundary for the present study. The boundary between the Volgian and Ryazanian regional Boreal stages, which are still widely in use, is situated slightly higher, at the top of the *Chetaites chetae* Zone (e.g. Rogov and Zakharov, 2009; Gradstein et al., 2012).

Two further Berriasian ammonite horizons, characterised by the occurrence of *Borealites fedorovi* and *Pseudocraspedites anglicus*, respectively, were documented (Jeletzky, 1984; see also Galloway et al., 2020). Rich Valanginian macrofossil assemblages are restricted to the Deer Bay Formation in the central part of the Sverdrup Basin, and mostly recorded from Amund Ringnes and Ellef Ringnes islands. Ten closely spaced ammonite levels corresponding to three *Buchia* zones provide a high-resolution biostratigraphy for most of this stage; locally also belemnites occur (Jeletzky, 1964, 1965b, 1973, 1979, 1986; Kemper, 1975, 1977; Kemper and Jeletzky, 1979; Jeletzky and Kemper, 1988; Galloway et al., 2020).

In the absence of macrofossils over large parts of the Upper Jurassic to lowermost Cretaceous succession, foraminifers and palynomorphs were utilised for biostratigraphy. Chamney (1968, 1971) first attempted to employ foraminifera to establish the Jurassic–Cretaceous boundary in the Canadian Arctic. Souaya (1976) produced a comprehensive scheme of Upper Jurassic to Valanginian

foraminifera zones, based on samples from a single well drilled on tiny Linckens Island, 10 miles SW of Amund Ringnes Island. Wall (1983) analysed samples from several outcrops and wells on Axel Heiberg and Ellesmere islands, and revised Souaya's (1976) foraminifer zones. He remarked that the majority of the foraminifera identified represent long-ranging species and are most useful for dating when integrated with the macrofauna (Wall, 1983). Later, the revised stratigraphy was used for dating well samples from Prince Patrick Island (Wall, 2004).

Palynomorph assemblages from the Upper Jurassic and Lower Cretaceous of the Sverdrup Basin were analysed in several studies (Pocock, 1967, 1976, Johnson and Hills, 1973; Brideaux and Fisher, 1976; Tan and Hills, 1978). Comprehensive zonal schemes for pollen and spores (Dörhöfer, 1979), and dinoflagellate cysts (Davies, 1983, 1985) were developed and applied (e.g. Pimpirev and Pavlishina, 2005). The most recent study on terrestrial palynomorphs, by Galloway et al. (2013), analysed Middle Jurassic to Early Cretaceous assemblages from the Hoodoo Dome H-37 well on Ellef Ringnes Island, but focused on palaeoclimate rather than biostratigraphy. So far, terrestrial and marine components of Late Jurassic to Early Cretaceous palynomorph assemblages from the Canadian Arctic have largely been analysed separately. To assess the full potential of palynomorphs for reconstructing palaeoecology and palaeoclimate, the integration of spore, pollen, dinoflagellate and microalgae occurrences is needed.

2.3 The Rollrock Section

The Rollrock Section is located in the northeastern part of the Sverdrup Basin (Fig. 1B) and exposes a slightly tilted, but not further disturbed, Upper Jurassic to Lower Cretaceous sedimentary succession (Wilson, 1976; Mayr and Trettin, 1996). During the Triassic, the area was part of a local topographic high, the Tanquary High, which is why strata older than Norian are absent (Nassichuk and Christie, 1966; Embry, 2019). The Mesozoic succession starts with the sandstone dominated Norian to Pliensbachian Heiberg Formation, which is overlain by sandstones of the Toarcian to Aalenian Sandy

Point Formation. Both units are exposed on the southeastern flank of the Rollrock River Valley (Fig. 1B). Middle to late Toarcian ammonites (*Dactylioceras*, *Pseudolioceras*; see Frebold, 1975 for biostratigraphic interpretation) constrain the age of the Sandy Point Formation. Palaeo-erosion has polished the surface of a massive sandstone bed at the top of the unit. Numerous 5 mm wide holes representing sub-vertical burrows are surrounded by a potentially biogenic vesicular crust (Fig. 3), which suggests long-term exposure of the lithified bed, most probably in a marine setting.

The overlying approximately 90 m thick interval is covered by vegetation and scree. As a result, the presence of Bajocian to Callovian strata is unconfirmed and the duration of the hiatus above the Sandy Point Formation is unclear. Potentially, the Sandy Point Formation is directly overlain by the Ringnes Formation in the Rollrock Valley, as has been reported from other, more marginal parts of the basin (Embry, 1984b).

The start of continuous outcrop on the northern flank of the Rollrock Valley, which consists of more than a dozen of individual ridges exposed over a distance of more than 5 km, defines the base of the Rollrock Section herein (Fig. 4).The lower, approximately 250 m thick part of the Upper Jurassic succession exposed in the Rollrock Section comprises mud- and siltstones with minor intervals of very fine- to fine-grained sandstones, and is attributed to the Ringnes Formation (Fig. 4; Balkwill et al., 1977; Balkwill, 1983). The following uninterrupted, approximately 270 m thick, mudstone succession is assigned to the Deer Bay Formation (Fig. 5; Heywood, 1955, 1957; Balkwill, 1983). Near the top, the mudstones quickly grade into sand- and siltstones with minor mudstone intercalations. The top of the Deer Bay Formation is positioned at the onset of sand-dominated sedimentation (524.5 m in Fig. 6). These sands are assigned to the Paterson Island Member of the Isachsen Formation (Embry, 1985a). The Isachsen Formation and the overlying Christopher Formation, which forms the top of the sedimentary succession exposed around Ekblaw Lake (Fig. 1), were not logged in detail and are not further considered herein.

3 Material and methods

The Rollrock Section was logged and sampled during five days in July 2015. The strata dip gently (17° on average) towards northwest (dip direction is 321° on average), which is approximately perpendicular to the slope. A telescopic walking pole, calibrated to 1.5 m length, was used for measuring thickness. We chose one of the easternmost ridges for logging, since it provided relatively easy access and had less scree cover in its lowest part (base near 81.61172°N, -75.58489°W, WGS84; top near 81.617447°N, -75.596306°W, WGS84 datum; Fig. 4). Judging from the relative positions of the macrofossil horizons published by Jeletzky (1984), our log starts approximately 175–200 m lower in the succession than A. F. Embry's log (personal communication, 2017). Access was difficult in the highest, steepest part of the exposure, and we twice had to move section along strike (Fig. 4). Most of the macrofossils described herein were collected along the measured section (Fig. 6). Sideritic concretions (Fig. 7) were carefully screened for fossils, level by level, and fossiliferous levels were tracked along the slopes of the logged ridge, and along several slopes further to the west.

All ammonites and bivalves from the Rollrock Section are preserved in sideritic mudstone concretions, which usually break into irregular fragments during weathering (Fig. 7C). Most of the collected specimens were cleaned with water and subsequently impregnated and re-assembled with Paraloid B liquid resin. In some specimens, part of the matrix was removed using a pneumatic chisel. For photographing, the specimens were whitened with ammonium chloride.

Most of the ammonite specimens are strongly compressed. Some of the shells were not entirely filled with sediment before they collapsed and/or were dissolved. As a result, often only one side of an ammonite is preserved three-dimensionally, and it is difficult to reconstruct cross-sections of the specimens.

4 Sedimentology

The lower 230 m of the Rollrock Section expose a succession of dark, thinly bedded or laminated clayey siltstones and mudstones, with rare intercalations of siltstone or fine-grained sandstone (Fig. 6). From 190 m upward, several horizons of sideritic concretions occur, some of which have yielded bivalves, a lobster and fossilised wood. Above 230 m, a 20 m thick interval of siltstones and fine-grained sandstones follows. At 251 m, the change back to mudstone sedimentation is sharp and sudden. Over the following 250 m, the succession consists of dark, thinly bedded or laminated mudstones, which are interrupted by a single sandstone bed with giant concretions (273 m) and a thin indurated siltstone interval (347 m) (Fig. 6). Above 295 m, numerous, irregularly spaced horizons of sideritic concretions occur (Fig. 7A). Several of them have yielded fossils, including ammonites, bivalves and crinoid columnals (Fig. 7C). Additionally, fossilised wood and belemnites occur scattered in the upper part of the succession (Fig. 6).

A persistent feature of the mudstone succession from 251 m onward is the occurrence of abundant, randomly distributed pebbles, up to 100 mm in size, most of which consist of greyish chert, often with a brownish-blackish weathered cortex, which is shiny and polished at its surface (Figs 7B, 8D–G); cloudy to milky white quartz pebbles are much less common. These pebbles are interpreted as dropstones (see discussion below). In addition, glendonites occur in at least eight horizons between 400 and 500 m (Fig. 7D). Above 520 m, several silty to slightly sandy horizons are intercalated. The first bed of clean, trough-cross-bedded sandstone occurs just below 525 m. Above this level, sandstones and siltstones start to dominate the succession. We stopped logging at 560 m.

5 Lithostratigraphy

The Ringnes Formation has its type section on central Amund Ringnes Island, and was defined as a succession of dark grey to black, very silty to slightly sandy shale with abundant, randomly distributed, giant, up to 5 m long, ellipsoidal, yellowish weathering, sideritic mudstone concretions (Balkwill et al., 1977; Balkwill, 1983). These characteristic concretions served to distinguish the unit

244 from the McConnell Island Formation below and the Deer Bay Formation above. Sparse macrofossils
245 indicate an Oxfordian to Kimmeridgian age for the Ringnes Formation (Frebold, 1961, 1964; Balkwill
246 et al., 1977; Poulton, 1993). In the Rollrock Section, similar sideritic concretions are present, and
247 some of them exceed 2 m in diameter, but they are less abundant than in the type region.
248 Moreover, concretions are not restricted to the Ringnes Formation. In fact, they are more common
249 and larger in the overlying Deer Bay Formation (Fig. 5). Consequently, it is impossible to distinguish
250 the Ringnes and Deer Bay formations based on lithology.

251 The upper, approximately 100 m thick mudstone-dominated interval of the Ringnes Formation has
252 several up to 4 m thick packages of very-fine- to fine-grained sand intercalated, and was assigned to
253 the Awingak Formation by Embry (in Mayr and Trettin, 1996). However, this interval comprises less
254 than 15 % of sandstone in total, and thus does not classify as a sand-dominated unit. Its assignment
255 to the Awingak Formation *sensu* Embry (1986) is not warranted. In proximal parts of the Sverdrup
256 Basin, the Awingak Formation is intercalated between the Ringnes and the Deer Bay formations
257 (Embry, 1986; Fig. 2). The 20 m thick siltstone and sandstone package in the Rollrock Section is likely
258 a distal equivalent of its upper member, the Slidre Member (see also the biostratigraphy presented
259 below), and provides sequence-stratigraphic correlation. Based on these considerations, the lower
260 250 m of the Rollrock Section are assigned to the Ringnes Formation herein.

261 At the top of the sandstone interval, the sharp transition to mudstone sedimentation is defined as
262 the base of the Deer Bay Formation herein. It coincides with the first occurrence of the chert pebbles
263 described above, which are interpreted as dropstones following Embry (1991; see discussion on
264 palaeoclimate below). The Deer Bay Formation was originally proposed by Heywood (1955, 1957).
265 Its type area is situated on Ellef Ringnes Island. Balkwill (1983) provided a comprehensive description
266 and redefinition of the unit, which he classified as a succession of mudstone and siltstone, with rare
267 intercalations of very-fine- to fine-grained sandstone. This rocks exposed in the Rollrock Section
268 match this description well. Kemper (1975) commented on the varying abundance of sideritic

concretions in the Deer Bay Formation throughout the basin, and stated that glendonites and fossilised wood were the most distinguishing features of its upper, Valanginian part.

The transition between the Deer Bay and Isachsen formations is gradual. The top of the Deer Bay Formation is placed at the base of a first clean, trough-cross-bedded sandstone bed, just below 525 m, which marks the onset of the Paterson Island Member of the Isachsen Formation. The higher parts of the Isachsen Formation and the overlying Christopher Formation are not considered in this study.

6 Systematic palaeontology

All fossils from the Rollrock Section are part of the Nunavut Collections of the Canadian Museum of Nature, Ottawa, Canada, and stored under registration numbers with the prefixes NUIF (for invertebrate fossils) and NUPB (for plant remains). Numbers NUIF 2979–3019, NUIF 3030–3046, NUIF 3061–3064, NUIF 3134–3140, NUIF 3158, NUIF 3165–3167 and NUPB 571, 572 and 575 are assigned to fossils from the Rollrock Section. Registration numbers for individual specimens are provided in the material paragraphs below, and in the figure captions.

The systematic arrangement of the Bivalvia is adopted from MolluscaBase (2019). Abbreviations used are: LV = left valve; RV = right valve; L = length; H = height. The systematic arrangement of the Ammonoidea is adapted from Wright et al. (1996), with additions from Igolnikov (2014) and Rogov (2014). The terminology follows Klug et al. (2015). Abbreviations used are: CSI = conch shape index; DM_1 = maximum diameter; IZR = imprint zone rate; UWI = umbilical width index; RC = rib coefficient; WER = whorl expansion rate; WWI = whorl width index. The taxonomy of the Belemnitida follows Saks and Nal´nayeva (1964, 1966) and Dzyuba (2011, 2012). The terminology of the belemnite rostral morphology is adapted from Doyle and Kelly (1988). For all taxa, synonymy only includes

reference to the original description of a species, to illustrated records from the Sverdrup Basin and to the most recent taxonomic revisions.

Class Bivalvia Linnaeus, 1758

Subclass Pteriomorphia Beurlen, 1944

Order Pectinida Gray, 1854

Family Buchiidae Cox, 1953

Genus *Buchia* Rouillier, 1845

Type species: *Avicula mosquensis* von Buch, 1844, by monotypy (Opinion 492; International Commission of Zoological Nomenclature, 1957).

Remarks: *Buchia* shells are strongly inequivalve. The left valve is obliquely ovate to rounded triangular in outline, more or less distinctly retrocrescent, moderately to strongly convex and inflated, with a prominently projecting, slightly prosogyrate to almost orthogyrate umbo and in most species markedly higher than long. The right valve is rounded-oval to sub-triangular in outline, weakly to strongly convex, with a barely projecting umbo and an anterior, tongue-shaped auricle, projecting over the commissural plane into a socket in the cardinal area of the left valve. A posterior auricle may occur in both valves. The cardinal area is triangular in outline and bears a single, shallow ligamental pit. Hinge teeth are lacking. The shell exhibits more or less strongly developed commarginal folds. Faint radial threads occur on the exterior of some species.

Buchiid bivalves are most common in the Oxfordian to earliest Hauterivian of the Boreal Realm, where they have considerable biostratigraphic merit (e.g. Jeletzky, 1964, 1965a, 1966, 1984; Zakharov, 1981; Rogov and Zakharov, 2009). Close to 200 species-level names were proposed for specimens now assigned to *Buchia* Rouillier, 1845 (first author's data). After decades of widespread

taxonomic splitting (most notably by Pavlow, 1907 and Sokolov, 1908a, b) due to the use of a typologic species concept, Jeletzky (1964, 1965a, 1966) and Zakharov (1981, 1987) gradually applied a biological species concept to *Buchia* and revised the taxonomy and biostratigraphy of the genus. Much of this work is still state-of-the-art, and the zonal scheme developed by these authors is also applied herein. A comprehensive overview of *Buchia* considering aspects of its taxonomy, distribution, biostratigraphic utility and life style is available from Sha and Fürsich (1994).

Like many bivalves, *Buchia* has shells with very few clearly delimited characters and morphologic boundaries between species are often not sharp. Grey et al. (2008, 2010) used Principal Component Analysis of linear and angular measurements for species discrimination, with mixed results. All specimens from the Rollrock Section are preserved as composite moulds and often are more or less strongly distorted. Thus, only simple size measurements (Fig. 9) were taken where feasible. Features of the ligament, anterior auricle and hinge region are not preserved in the specimens from the Rollrock Section. The species are described in the order of their stratigraphic occurrence in the section.

Buchia rugosa (Fischer von Waldheim, 1837)

Fig. 10C

*1837 *Inoceramus rugosus*, Bronn: Fischer von Waldheim, p. 175, pl. 19, fig. 5; pl. 46, fig. 2.

1981 *Buchia rugosa* (Fischer Waldheim, 1837): Zakharov, p. 81, pl. 9, figs 1–11.

Material: A distorted left valve from 192 m in the log (NUIF 2983); a strongly corroded left valve from 196.5 m (NUIF 2981); and a composite mould (NUIF 3019) and external cast (NUIF 3018) of a left valve from 196.8 m.

Measurements: LV, L = 21 mm; H = 23.5 mm.

Description: Left valve gryphaeoid; distinctly inequilateral and retrocrescent, markedly inflated; crest line curvoid. Umbo of left valve blunt, broad and prominent for genus. Shell ornamented with relatively widely spaced, pronounced, usually regular, sharp-crested commarginal folds.

Remarks: Typical specimens of *Buchia rugosa* are distinguished by their curvoid left valve with a broad and blunt umbo and widely-spaced, regular folds. Only *Buchia mosquensis* has a similarly shaped left valve, but more densely spaced, finer commarginal folds, which are less regularly arranged. In the Rollrock Section, *Buchia rugosa* occurs in three closely successive concretion horizons, all assigned to the Ringnes Formation. These are the lowest horizons with macrofossils in the section.

Associated fauna: Besides *Buchia rugosa*, a relatively poorly preserved decapod specimen, assigned to the genus *Glyphea* (personal communication Günter Schweigert, Stuttgart, 2018), was collected from one of these horizons. Furthermore, several specimens of the large pectinid *Mclearnia* were found, but were too poorly preserved to be collected.

Age: *Buchia rugosa* is the index of the lower Tithonian (lower Volgian) *Buchia rugosa* Zone (Zakharov, 1981; Rogov and Zakharov, 2009).

Buchia mosquensis (Buch, 1844)

Fig. 10A, B, E

*1844 *Avicula Mosquensis*: Buch, p. 537, pl. 6, figs 1, 4.

1981 *Buchia mosquensis* (Buch, 1844): Zakharov, p. 83, pl. 9, fig. 12; pl. 10, figs 1-4; pl. 11, figs 1-8; pl. 12, figs 1-5; pl. 13, figs 1-6; text-figs 12, 24d.

Material: A single slab with internal moulds of two specimens with valves in occlusion (NUIF 3003) and an external mould of a right valve (NUIF 3136) from 307 m log height.

Measurements: LV, L = 38.5 mm; H = 43.5 mm; RV, L = 32–34.5 mm; H = 33.5–37 mm.

Description: Left valve gryphaeoid; distinctly inequilateral and retrocrescent, markedly inflated; crest line curvoid. Umbo of left valve blunt, broad and prominent for genus. Right valve short-oval in outline, moderately inflated, with broad, low umbo. Both valves ornamented with distinct, rather irregularly and in places relatively closely spaced commarginal folds.

Remarks: Similar in shape to *Buchia rugosa*, *B. mosquensis* mainly differs from the latter in its slight recurvature and an irregular pattern of commarginal folds. *Buchia mosquensis* seems to be uncommon in Arctic Canada, and was not included in the zonal scheme of Jeletzky (1984). *Buchia mosquensis* was previously reported from Amund Ringnes Island (Balkwill, 1983) and *Buchia* cf. *mosquensis* from Ellef Ringnes and Axel Heiberg islands (Frebold in McMillan, 1963; Jeletzky in Stott, 1969), but no specimens were figured.

Age: *Buchia mosquensis* is the index of the lower to middle Tithonian (lower to middle Volgian) *Buchia mosquensis* Zone (Zakharov, 1981; Rogov and Zakharov, 2009). The upper part of this interval matches the age range of the co-occurring ammonites described below.

Buchia terebratuloides (Lahusen, 1888)

Fig. 10D, F–J

*1888 *Aucella terebratuloides* (Trautsch.) nov. sp. Lahusen, p. 18, pl. 4, figs 1–11.

1973 *Buchia terebratuloides* (Lahusen) f. typ.: Jeletzky, p. 47, pl. 4, fig. 3.

1973 *B. terebratuloides* var. *subuncitoides* (Bodylevsky): Jeletzky, p. 47, pl. 4, fig. 2.

1973 *B. terebratuloides* var. *obliqua* Tullberg: Jeletzky, p. 47, pl. 5, fig. 2.

1981 *Buchia terebratuloides* (Lahusen, 1888): Zakharov, p. 105, pl. 23, figs 4–6; pl. 24, figs 1–4; pl. 25, figs 1–10; text-fig. 24.

1984 *Buchia terebratuloides* (Lahusen 1888) var. *obliqua* (Tullberg 1881): Jeletzky, p. 221, pl. 5, fig. 4.

1984 *Buchia terebratuloides* (Lahusen 1888) var. *subuncitoides* (Bodylevsky 1936): Jeletzky, p. 227, pl. 8, fig. 7.

Material: Three slabs of a monospecific shell pavement (NUIF 3007–3009) and four additional matrix slabs with several specimens (NUIF 2986, 2988, 2991, 2998), all from the 333 m horizon.

Measurements: LV, L = 26–29 mm: H = 34.5–39 mm; RV, L = 17.5–22.5 mm; H = 19–25.5 mm.

Description: Left valve subtriangular in outline, distinctly inequilateral and retrocrescent, distinctly higher than long, slender, well inflated; crest line obliquoid. Umbo distinctly prosogyrate, relatively narrow. Right valve short-oval in outline, markedly inflated. Umbo narrow, almost pointed, projecting over commissure. Shell exterior in adults ornamented with weak, often diffuse, irregularly spaced commarginal folds. Folds more evenly spaced and distinct in young individuals. Some specimens from Rollrock Section with several growth halts, marked by deep commarginal incisions.

Remarks: The narrow umbo, almost pointed in the right valve, the high, slender shells, and particularly the rather widely and intermittently spaced, irregularly strong folds are distinctive of *Buchia terebratuloides*. Most specimens in the assemblage have rather feeble, irregular folds (Fig. 10G–I). However, some individuals (Fig. 10F), particularly juveniles (Fig. 10D, J), are more regularly and prominently ornamented, expressing the considerable intraspecific variability of *Buchia terebratuloides*. A peculiar feature of most specimens from the 333 m horizon is a number of rather deep growth interruptions. One of these growth halts, at a rather early, juvenile growth stage, is particularly distinctive and common to most adult specimens from this horizon, substantiating that these shells represent a single cohort.

Age: *Buchia terebratuloides* has a relatively long range, corresponding to the *Subcraspedites sowerbyi – Subcraspedites preplicomphalus* Zone and the overlying *Taimyroceras canadensis* Zone sensu Jeletzky (1984). Although *Buchia terebratuloides* is not a precise marker, the 333.5 m horizon

is certainly the macrofossil bed closest to the Jurassic-Cretaceous boundary in the Rollrock Section, as interpreted herein.

Buchia volgensis (Lahusen, 1888)

Fig. 11G, H

*1888 *Aucella volgensis* nov. sp.: Lahusen, p. 16, pl. 3, figs 1–17.

1970 *Buchia volgensis* (Lahusen) s. str.: Jeletzky, p. 655, pl. 23, fig. 5.

1981 *Buchia volgensis* (Lahusen, 1888): Zakharov, p. 125, pl. 37, figs 5–7; pl. 38, figs 1–3; pl. 39, figs 1–4; pl. 40, figs 1, 2, text-fig. 23.

1984 *Buchia volgensis* (Lahusen 1888) s.s.: Jeletzky, p. 227, pl. 8, fig. 14.

Material: A single compressed, double-valved specimen from the 355 m horizon (NUIF 3034).

Measurements: L = 52 mm; H = 63 mm.

Description: Shell relatively large, only moderately higher than long, moderately inflated, with moderately broad left valve umbo; crest line faintly curvoid. Umbo of right valve rather sharply triangular; anterior and posterior dorsal margins meeting more or less at right angles. Shells ornamented with relatively closely spaced, moderately regular, distinct but not very prominent or sharp commarginal folds.

Remarks: The specimen from the Rollrock Section is relatively poorly preserved and rather strongly compressed, and the left valve is barely interpretable. The right valve, however, shows the typical shape and ornamentation of the species rather well. Two prominent growth halts occur, one at a rather juvenile stage and one at mid height.

Age: *Buchia volgensis* has a relatively long, middle to late Berriasian (Ryazanian) range (Zakharov, 1981). Its co-occurrence with *Buchia unschensis* and *Praetollia maynci* (see below) indicates a position close to the lower limit of its range.

Buchia unschensis (Pavlow, 1907)

Fig. 11A, B

*1907 *Aucella unschensis* n. f.: Pavlow, p. 71, pl. 6, figs 12–14.

1966 *Buchia unschensis* (Pavlow, 1907) emend.: Jeletzky, p. 35, pl. 1, figs 1–4; pl. 5, figs 3–7; pl. 6, figs 1–4, 6–8.

1981 *Buchia unschensis* (Pavlow, 1907): Zakharov, p. 109, pl. 23, fig. 5; pl. 25, figs 11–13; pl. 26, figs 1–3; pl. 27, figs 1–6; pl. 28, figs 1–5; pl. 29, figs 1–4; pl. 30, figs 1–5; text-figs 24zh, 25a, 55.

1984 *Buchia unschensis* (Pavlow 1907) s.s.: Jeletzky, p. 221, pl. 5, figs 2, 6, 7; pl. 6, figs 2, 7; pl. 8, figs 1, 2, 4, 5, 10.

Material: One left valve and one right valve on the same slab (NUIF 3037), one external mould of a right valve (NUIF 3038), a poorly preserved double-valved specimen (NUIF 3035), and several juvenile specimens on one slab (NUIF 3039), all from the 355 m horizon.

Measurements: LV, L = 15 mm; H = 17.5 mm; RV, L = 13.5–30 mm; H = 14–30 mm.

Description: Shell stout, slightly higher than long; crest line obliquoid; posterior auricle, although not well preserved in the present material, distinct, angular and relatively large. Left valve moderately inflated; umbo moderately wide. Right valve broad, almost circular in adulthood, moderately but markedly inflated; umbonal region rather pointed initially (Fig. 11B), but much subdued and rounded at adult stage (Fig. 11A). Both valves ornamented with prominent, regularly and moderately widely

spaced commarginal folds, more strongly raised in central part of shell than towards anterior and posterior margins.

Remarks: *Buchia unschensis* differs from other *Buchia* species in the presence of a marked, angular posterior auricle. *Buchia okensis* is most similar, both with regard to the stout shell and the posterior auricle, which is, however, less prominent and pronounced than in *B. unschensis*. Furthermore, the commarginal folds in *B. okensis* are more widely spaced, and prominent and raised over their entire extent, while in *B. unschensis* they are less prominent towards the anterior and posterior ends.

Age: *Buchia unschensis* is a rather long-ranging early Berriasian (late Volgian to Ryazanian) species (Zakharov, 1981; Rogov and Zakharov, 2009). The specimens co-occur with *Buchia okensis* in the 355 m level (see below), corresponding to the *Buchia okensis* Zone of Jeletzky (1984), which is in good agreement with the age range of *Praetollia maynci* recorded from the same level (see below).

Buchia okensis (Pavlow, 1907)

Fig. 11D–F

*1907 *Aucella okensis* n. f.: Pavlow: p. 40, pl. 1, figs 10, 11.

1964 *Buchia okensis* (Pavlow, 1907): Jeletzky, p. 32, pl. 2, fig. 2.

1970 *Buchia okensis* (Pavlow): Jeletzky, p. 655, pl. 23, fig. 13.

1981 *Buchia okensis* (Pavlow, 1907): Zakharov, p. 116, pl. 31, figs 1–3; pl. 32, figs 1–4; pl. 33, figs 1, 2; pl. 34, figs 1–3; pl. 35, figs 1–4; text-figs 22, 24d. [with comprehensive synonymy]

1984 *Buchia* n. sp. aff. *okensis* (Pavlow, 1907): Jeletzky, p. 223, pl. 6, figs 3, 5, 6; pl. 8, figs 3, 8, 9, 12.

1984 *Buchia okensis* (Pavlow 1907) s.s.: Jeletzky, p. 227, pl. 8, fig. 13.

2020 *Buchia okensis* (Pavlow): Galloway et al., p. 5, fig. 3d.

Material: Three left valves, from 355 m (NUIF 3036), 356 m (NUIF 3033) and 363.5 m (NUIF 3042).

Measurements: LV, L = 27–31 mm; H = 32.5–36 mm.

Description: Shell stout, slightly to moderately higher than long, crest line obliquoid. Umbo of left valve relatively low, moderately inflated. Posterior auricle small and well rounded, but distinct. Shell ornamented with widely and relatively regularly spaced, prominent, sharp commarginal folds with deeply sunken interspaces.

Remarks: The specimens from the Rollrock Section, all left valves, have relatively low umbos, as common for *Buchia okensis*. However, the species is best distinguished by its ornament of prominent, widely spaced folds with deep interspaces, which are more pronounced than in any of the other species in *Buchia*. *Buchia okensis* is known from Mackenzie King Island and Axel Heiberg Island in the Sverdrup Basin (Jeletzky, 1984; Galloway et al., 2020). From the same localities, Jeletzky (1984) reported a similar, unnamed species, informally labelled as '*Buchia* n. sp. aff. *okensis* (Pavlow, 1907)'. In Arctic Canada, these forms only occur in the *Buchia okensis* Zone, in horizons together with *Buchia okensis* and *Borealites fedorovi* or *Pseudocraspedites anglicus* (Jeletzky, 1984). We think that the specimens figured by Jeletzky (1984: pl. 6, figs 3, 5, 6; pl. 8, figs 3, 8, 9, 12) fall into the variability of *Buchia okensis*. '*Buchia* cf. n. sp. aff. *okensis* (Pavlow, 1907)' (Jeletzky, 1984: pl. 8, fig. 11) is a poorly preserved specimen of unknown affinities. Presumably, '*Buchia* n. sp. aff. *okensis* (Pavlow, 1907)' *sensu* Jeletzky (1984) from other areas (California, SW British Columbia), reported from upper Tithonian strata, represents a different species.

Age: *Buchia okensis* is the index of the lower Berriasian (Ryazanian) *Buchia okensis* Zone of Jeletzky (1984), and co-occurs with *Praetollia maynci*, *Borealites fedorovi* and *Borealites* sp. in the Rollrock Section. In eastern Greenland, *Buchia okensis* occurs in association with *Hectoroceras kochi* in beds above those that contain *Praetollia maynci* (Surlyk and Zakharov, 1982).

Family Entoliidae Teppner, 1922

Genus *Entolium* Meek, 1865

Type species: *Pecten demissus* Phillips, 1829, by original designation.

Entolium sp.

Fig. 11I

Material: A fragmentary internal mould of a right valve, from the 333 m level (NUIF 3134).

Remarks: Preserved are the dorsal and central portions of the mould, including imprints of the umbo, both auricles and the central part of the disc. The auricles are sub-equal in size, the anterior one being slightly larger; their oblique dorsal margins meet their anterior and posterior margins, respectively, almost at right angles. On the disc, faint imprints of commarginal growth lines are visible. These characters conform to the common morphology of *Entolium*. The poor preservation prevents from specific determination.

Subclass Heterodonta Neumayr, 1884

Order Myida Stoliczka, 1870

Family Pleuromyidae Zittel, 1895

Genus *Pleuromya* Agassiz, 1842

Type species: Not validly defined.

Remarks: Agassiz (1842) had not designated a type species. Both *Mya gibbosa* J. de C. Sowerby, 1823 selected by Herrmannsen (1847) and *Pleuromya elongata* Agassiz selected by Stoliczka (1871) as type species were not mentioned in Agassiz' (1842) original generic description, but were included in *Pleuromya* in the part published in 1843.

519

520 *Pleuromya* sp.

521 Fig. 11C

522 Material: One double-valved specimen from 363.5 m log height (NUIF 3005). L = 47 mm; H = 32 mm.

523 Remarks: The specimen, preserved as a slightly compressed composite mould, has the typical shape
524 of *Pleuromya*, i.e. elongate, faintly angulate, suboval, moderately inflated shells, with blunt, barely
525 projecting, faintly opisthogyrate umbos, situated in the anterior third of the shell. It is of average size
526 for the genus (L = 47 mm) and shows the typical ornamentation of pronounced, irregular growth
527 lines. The single individual is too poorly preserved for specific determination.

528

529 Class Cephalopoda Cuvier, 1795

530 Subclass Ammonoidea Zittel, 1884

531 Order Ammonitida Hyatt, 1889

532 Family Dorsoplanitidae Arkell, 1950

533 Genus *Dorsoplanites* Semenov, 1898

534 Type species: *Ammonites dorsoplanus* Vischniakoff, 1882, by subsequent designation (Roman, 1938).

535 Diagnosis: Adult conch small to very large (D < 50 mm to > 500 mm), discoidal, subinvolute to
536 subevolute. Whorls ovate to subtrapezoidal in cross-section; venter rounded. Aperture simple or
537 moderately widened. Ribs rectiradiate to moderately prorsiradiate; commonly biplicate, often
538 triplicate or with intercalated secondary ribs later in ontogeny. Secondaries crossing venter in young
539 individuals; later in ontogeny often fading out near to or distinctly before venter. Density of ribbing

usually decreasing with ontogeny. Constrictions occur in some species. Suture typically perisphinctoid.

Remarks: Semenov (1898) introduced *Dorsoplanites* as a subgenus of *Perisphinctes* without providing a diagnosis or description. The new subgenus was listed in a table of ammonite occurrences in Russia, and seven species were included. While numerous additional species were subsequently assigned to *Dorsoplanites*, published diagnoses of the genus are generally terse and often vague. The diagnosis given above is based on personal communication with Mikhail Rogov (Moscow; February, 2019) and various published descriptions (e.g. Vischniakoff, 1882; Spath, 1936; Mesezhnikov, 1984; Wright et al., 1996). From the Sverdrup Basin, several mostly poorly preserved specimens of *Dorsoplanites* were figured and described by Frebold (1961) and Jeletzky (1966). These are discussed below.

Dorsoplanites maximus Spath, 1936

Figs 12A, 13

v*1936 *Dorsoplanites maximus*, sp. nov.: Spath, p. 71, pl. 26, fig. 1; pl. 28, fig. 1; pl. 32, fig. 3; pl. 37, fig. 6.

1961 *Dorsoplanites* sp. indet.: Frebold, p. 23, pl. 20, fig. 1.

1966 *Dorsoplanites* sp. indet. ex gr. *D. panderi* (Michalski 1890): Jeletzky, p. 23, pl. 8, fig. 1.

Material: One giant, well-preserved specimen (NUIF 3012) and two more or less fragmentary specimens (NUIF 2984, 3002), all from the 307 m horizon.

Description: Conch very large (maximum diameter DM_1 > 450 mm), moderately to thickly discoidal (conch shape index CSI = 0.4), moderately compressed (whorl width index WWI = ca. 0.73), subevolute (umbilical width index UWI = 0.45). Whorl expansion rate low (WER = 1.63). Whorls

563 moderately to strongly embracing (imprint zone rate IZR = 0.28). Whorl cross-section subtrapezoidal,
564 with well-rounded shoulders and venter; whorl width not clearly established.

565 Prominent primary ribs distantly spaced; prorsiradiate; distinctly proconcave on inner third of whorl,
566 straightening outwardly, biplicate, branching at approximately mid height. Each pair of biplicate
567 secondaries joined by an additional, equally strong, intercalated secondary rib, resulting in triplicate
568 pattern; secondaries crossing the venter in young individuals. Expression of ribs declining during
569 ontogeny; secondaries gradually becoming less distinct on penultimate whorl of largest specimen,
570 finally fading out beyond first half of ultimate whorl, at a diameter of approximately 400 mm.
571 Primary ribs on second half of ultimate whorl distinct on inner third of whorl only. Number of
572 primary ribs per whorl variable throughout ontogeny: NUIF 3012, ultimate whorl = 34, penultimate
573 whorl = 33, antepenultimate whorl = 39, fourth last whorl = 32; NUIF 2984, ultimate whorl = 35.
574 Suture lines not preserved.

575 Remarks: Specimen NUIF 3012 is approximately 450 mm wide, and thus close to the maximum size
576 documented for *Dorsoplanites*. It seems that nearly the entire conch is preserved, although the
577 aperture is broken. Commonly, traces are left on the moulds, where additional whorl sections broke
578 off; no such traces are visible on the ultimate whorl of NUIF 3012. No suture lines are preserved, and
579 the full length of the body chamber cannot be determined. With an umbilical width index of 0.45,
580 the specimen only just qualifies as subevolute, on the margin to evolute; the majority of the species
581 in *Dorsoplanites* have a narrower umbilicus. Specimen NUIF 3012 is one of the best-preserved large
582 specimens of *Dorsoplanites* published, and the second well-preserved specimen, NUIF 2984, is also
583 very large. The type material of most of the 40 or so nominal species and subspecies of
584 *Dorsoplanites* comprises small specimens that reach less than 150 mm in diameter. Consequently,
585 the individuals from the Rollrock Section preserve ontogenetic stages that were rarely documented
586 before, and comparison with published material is rather difficult.

Assigning our material to *Dorsoplanites maximus* Spath, 1936 instead of establishing a new species is probably a rather conservative approach and argues for allowing a certain degree of intraspecific variability in dorsoplanitid ammonites. Several forms of *Dorsoplanites* that are similar with regard to conch shape, number of primary ribs – between 31 and 39 – and ribbing pattern – biplicate, with intercalated secondaries – have been documented from the *Dorsoplanites maximus* Zone. The holotype of *Dorsoplanites maximus*, figured by Spath (1936, pl. 26, fig. 1, pl. 28, fig. 1), has a maximum diameter of approximately 170 mm, and 33 to 34 primary ribs per whorl. The ribs are sharper and more pronounced than in our specimens. To some degree, this may be a matter of preservation, since some specimens from the Rollrock Section are markedly compressed, while Spath's (1936) material consists of close-to-perfect 3D moulds. To a similar degree, this may be a function of ontogeny, since rib strength generally decreases with age; this process already seems to have started in the relatively small holotype of *D. maximus*. However, in other specimens of approximately the same size, e.g. *Dorsoplanites flavus* Spath *sensu* Mesezhnikov (1984; D = 129 mm in diameter) or '*Dorsoplanites* sp. indet. ex gr. *D. panderi*' of Jeletzky (1966: p. 23, pl. 8, fig. 1; D = ca 130 mm), the secondaries are already weakly expressed or have largely faded at this growth stage. Frebold (1961) figured two specimens from Slidre Fiord near Eureka (Ellesmere Island; Fig. 1), which have 35 primary ribs on the last whorl. '*Dorsoplanites* sp. indet. ex gr. *D. panderi* Michalski' (Frebold, 1961: p. 23, pl. 17, fig. 2) and '*Dorsoplanites* sp. indet.' (Frebold, 1961: p. 23, pl. 20, fig. 1) are approximately 70 mm and 130 mm in diameter, respectively. The smaller specimen does not preserve any secondary ribs, and is thus regarded as indeterminable at species level. The larger specimen has biplicate ribs and intercalated secondaries, which, with regard to strength, are somewhere in between our material and Spath's (1936) type lot; this specimen is placed in *D. maximus* here. Two further specimens of *Dorsoplanites* from Slidre Fiord were figured by Jeletzky (1966). *Dorsoplanites* cf. *gracilis* Spath, 1936 (Jeletzky, 1966: p. 21, pl. 8, fig. 10) is a fragment preserving only the inner whorls, at a diameter of approximately 70 mm. The specimen has 36 primary ribs per whorl, which are all simple biplicate. Since no specimens of *D. maximus* at a similar

growth stage are available, it is unknown whether juveniles of this species already have intercalated secondaries. '*Dorsoplanites* n. sp. ex aff. *crassus* Spath 1936?' (Jeletzky, 1966: p. 20, pl. 8, fig. 11; fragmentary, D = approximately 130 mm) is so poorly preserved that it is difficult to establish whether it had simple biplicate ribs (this is suggested by Jeletzky's tentative assignment), or additional intercalated ones; it is obvious, however, that the secondaries are already weakly expressed at this growth stage.

Spath's (1936) type specimen classifies as thickly discoidal. The specimens from the Rollrock Section seem slightly slenderer, but are too strongly compressed to confidently assess their width.

An external mould of one aptychus was discovered on the back of the concretion that enclosed the giant *Dorsoplanites maximus* (Fig. 12B). The specimen closely resembles several aptychi of dorsoplanitid ammonites referred to *Praestriaptychus* Trauth, 1927 by Rogov and Mironenko (2016), but is much too small for the giant ammonite on the same rock slab. We thus assume that it belonged to another specimen of *Dorsoplanites*.

Age: *Dorsoplanites maximus* is the index of the middle Tithonian (middle Volgian) *Dorsoplanites maximus* Zone of northern Siberia (Rogov and Zakharov, 2009).

Dorsoplanites sachsi Michailov, 1966

Fig. 14

*1966 *Dorsoplanites sachsi* Michailov sp. nov.: Michailov, 42, pl. 12, fig. 2; pl. 13, fig. 1.

2009 *Dorsoplanites sachsi* Michlv.: Rogov and Zakharov, 1894, fig. 3.4.

Material: Two fragmentary external moulds from the 307 m horizon (NUIF 3015, 3016).

Description: Conch moderately large (DM_1 = approximately 80 mm), subinvolute (UWI = approximately 0.25). Additional conch parameters unavailable, due to poor preservation.

Primary ribs sharp, prominent, distantly spaced (20 to 21 ribs on last whorl), prorsiradiate, slightly to moderately proconcave, biplicate. Each pair of biplicate secondaries joined by an additional, equally strong intercalated secondary rib, resulting in triplicate pattern. Suture lines not preserved.

Remarks: The two specimens are relatively poorly preserved external moulds. Nevertheless, they show several features distinctive of *Dorsoplanites sachsi*. The conch is subinvolute and the umbilicus thus markedly narrower than in other species of *Dorsoplanites*. Furthermore, only 20 to 21 primary ribs per whorl result in a much coarser ribbing pattern than in other species of this genus. This coarseness in appearance, however, is subdued by the presence of three secondary ribs per primary rib on the outer half of the whorl.

Age: *Dorsoplanites sachsi* is part of the typical ammonite assemblage of the middle Tithonian (middle Volgian) *Dorsoplanites maximus* Zone of northern Siberia and Svalbard (Rogov and Zakharov, 2009). The same assemblage is now documented from Arctic Canada.

Dorsoplanitidae indet.

Fig. 15

Material: One fragment from 296.8 m log height (NUIF 2980); four fragmentary specimens (NUIF 2985, 3000, 3001, 3010) and two fragments (NUIF 3011, NUIF 3158) from 307 m log height.

Remarks: Several fragmentary and/or distorted ammonite specimens were collected together with the *Dorsoplanites* described above, and one specimen also from a horizon ten meters below. These individuals are too poorly preserved for specific and essentially also generic determination, and are thus kept in open nomenclature. Some of the fragments may belong to *Dorsoplanites maximus*. However, the specimens in figures 15A and 15F probably only have approximately 25 primary ribs (much less than *D. maximus*), but a distinctly wider umbilicus than *D. sachsi*. Moreover, the outer

part of the whorl preserved in specimen 15A may indicate simple bifurcate ornament. Displayed is also a drawing (Fig. 15D) of part of one suture line of specimen 15E.

Family Craspeditidae Spath, 1924

Subfamily Subcraspeditinae Rogov, 2014

Genus *Praetollia* Spath, 1952

Type species: *Praetollia maynci* Spath, 1952, by original designation.

Diagnosis: Conch moderately large (D < 90 mm), subinvolute, strongly discoidal; venter narrowly rounded. Ribs almost rectiradiate to slightly prorsiradiate; faintly proconcave or sigmoidal. Aperture simple. Primary and secondary ribs of almost equal strength throughout ontogeny; relatively sharp. Primary ribs bifurcating or trifurcating approximately at mid height of whorl, with additional secondaries intercalated, attaining a rib coefficient of 3.0 to 3.5. Conch fully costate in adulthood. Suture lines typically perisphinctoid.

Praetollia maynci Spath, 1952

Fig. 16B, C.

1952 *Praetollia maynci*, sp. nov.: Spath, p. 13, pl. 1, figs 1–4; pl. 2, figs 1, 2; pl. 3, figs 1–5; pl. 4, figs 2, 6, 7.

?1952 *Praetollia aberrans*, sp. nov.: Spath, p. 15, pl. 3, fig. 7.

1984 *Praetollia* (*Praetollia*) *maynci* Spath 1952 var. *aberrans* Spath 1952: Jeletzky, p. 221, pl. 5, fig. 3.

Material: One specimen (NUIF 3014) from 355 m log height.

Description: Conch moderately large (DM_1 = approximately 67 mm), subinvolute (UWI = approximately 0.28), markedly discoidal, judging from only faint compression. Additional conch parameters unavailable, due to poor preservation.

Primary ribs only slightly stronger than secondaries, almost rectiradiate, faintly proconcave, bifurcate, with an additional secondary associated with each pair. Number of primary ribs unknown, due to poor preservation. Ornament of approximately 72 secondary ribs on ultimate whorl, suggesting there were 24 or slightly less primary ribs.

Remarks: Spath (1952) figured more than 20 specimens of *Praetollia maynci*, which overall show little variability. The conch is subinvolute and rather discoidal. The primary ribs are densely spaced and sharp, and bifurcate when reaching the ventral half of the whorl flank. Another secondary rib becomes intercalated slightly later between the pairs. Each primary rib is thus usually associated with three secondary ribs in adult specimens. Unlike in many other Polyptychitidae, primary and secondary ribs are rather equal in strength and elevation, resulting in a very dense and regular ribbing pattern, which has been compared to that in *Berriasella* by Spath (1952). With a rather similar conch shape and more than 70 evenly spaced secondary ribs, the single specimen from the Rollrock Section fits well into the variability of *Praetollia maynci*. Jeletzky (1984) figured a single specimen determined as '*Praetollia* (*Praetollia*) *maynci* Spath 1952 var. *aberrans* Spath 1952' from Gibbs Fiord on Axel Heiberg Island, which we think falls into the variability of *Praetollia maynci*. *Praetollia aberrans* Spath, 1952 co-occurs with abundant typical *P. maynci* in Greenland, but is based on a single specimen. To establish its status as an independent species, the holotype needs to be restudied.

Age: *Praetollia maynci* is the index of the *Praetollia maynci* Subzone of the *Chetaites sibiricus* Zone of Northern Siberia and the Subpolar Urals, and of the *Praetollia maynci* Zone of East Greenland. It marks the onset of the Ryazanian regional stage, and corresponds to the upper *Berriasella jacobi* /

lower *Subthurmannia occitanica* zones of the middle lower Berriasian (cf. Zakharov and Rogov, 2008).

Genus *Borealites* Klimova, 1969

Type species: *Borealites fedorovi* Klimova, 1969, by original designation.

Diagnosis: Conch moderately large to very large (90 to 240 mm), discoidal, subinvolute to subevolute. Whorls rounded-oval to oval in cross-section; venter broadly to narrowly rounded. Aperture simple. Primary ribs generally slightly prorsiradiate, faintly to markedly proconcave; initially biplicate, branching at about midpoint of flank; very soon in ontogeny either triplicate with one or two additional secondary ribs intercalated, or rather biplicate with two or more additional intercalated secondary ribs. Secondaries crossing venter with a forward bend. Further into ontogeny, secondaries starting to lose connection to primaries and fading out, first on mid flank, later in some species completely. Primary ribs on lower third of flank distinctly thickened and raised, becoming gradually more proconcave; also gradually fading out with ontogeny in some species, but much later than secondaries. Constrictions occurring in some species.

Remarks: Igolnikov (2014) provided a comprehensive description and discussion of *Borealites*. There is no consensus on the validity and phylogenetic relationships of *Borealites* Klimova, 1969 and *Pseudocraspedites* Casey, Mesezhnikov and Shul'gina, 1977, which are treated as subgenera in several recent studies (Wierzbowski et al., 2011; Igolnikov, 2014; Galloway et al., 2020), and the material described herein is not suited to help. Igolnikov (2014) assigned specimens with 2.5 to 4.5 secondary ribs per primary to *Borealites*, and those with 4.5 to 7 secondaries per primary, resulting in a finer and denser ornament, to *Pseudocraspedites*, which seems rather arbitrary. We thus prefer to treat *Pseudocraspedites* as a synonym of *Borealites*.

Borealites fedorovi Klimova, 1969

Figs 17–19

*1969 *Borealites fedorovi* Klimova gen. et. sp. nova: Klimova, p. 130, pl. 1, figs 1-3.

1973 *Praetollia antiqua* sp. nov.: Jeletzky, p. 75, pl. 4, fig. 1; pl. 5, fig. 1; pl. 7, fig. 1.

1984 *Craspedites* (*Craspedites*) n. sp. aff. *subditus* (Trautschold 1877): Jeletzky, p. 221, pl. 5, fig. 5; pl. 6, fig. 1?.

1984 *Praetollia* (*Praetollia*) *fedorovi*: Jeletzky, p. 233.

2009 *Craspedites* cf. *thurrelli* Casey: Rogov and Zakharov, p. 1900.

Material: One almost complete, adult specimen (NUIF 3064) and seven more or less fragmentary specimens (NUIF 2993, 2994, 2997, 3041, 3043, 3044, 3046), all from the 363.5 m horizon.

Description: Conch large to very large (D_{max} = 210 mm); discoidal; weakly to moderately compressed; subinvolute (UWI = 0.29). Whorl expansion rate low (WER = 1.54). Whorls very strongly embracing (IZR = 0.49). Venter broadly to narrowly rounded. Extent of body chamber not established, but certainly more than 315°.

Primary ribs slightly prorsiradiate, almost straight to faintly proconcave, raised and sharp, bifurcating at approximately mid height of whorl, with one or two additional secondaries per primary intercalated. Secondary ribs markedly prorsiradiate, faintly proconcave, sharp and prominent, crossing the venter in a distinct forward bend. At mid-size (D = ca 100 mm) connections of primary and secondary ribs start to become rather indistinct, and fade further with growth. Later in ontogeny, primary ribs markedly strengthened and raised, forming proconcave lunate bullae. Secondary ribs fading entirely at a diameter of approximately 170 mm, primary ribs near 200 mm. Ultimate whorl of NUIF 3064 with 16 primary ribs; penultimate whorl with 17 primary and 71 secondary ribs, resulting in a rib coefficient (RC) of 4.2.

Remarks: Jeletzky (1973) described this species under the name *Praetollia antiqua*, based on material from near Buchanan Lake on Axel Heiberg Island (locality no. 3 on Fig. 1A). At that time, he was obviously unaware of Klimova's (1969) study, but later corrected his mistake, and placed *Praetollia antiqua* in the synonymy of *Praetollia fedorovi* (see Jeletzky, 1984). Apparently, he did not adopt the genus name *Borealites*, for which he gave no further explanation. An excellent description of the early growth stages of *Borealites fedorovi* is available from Jeletzky (1973), but all of the specimens described by Klimova (1969) and Jeletzky (1973) are below 100 mm in diameter, and thus nowhere near the size of our material.

Jeletzky (1984) figured two specimens determined as *Craspedites* (*Craspedites*) n. sp. aff. *subditus* (Trautschold, 1877) from the Rollrock Section. We think, at least one of these (plate 5, figure 5) represents a young individual of *Borealites fedorovi*, while the second one (pl. 6, fig. 1) is too poorly preserved to be determined. Jeletzky (1984: 221) claimed that 'reliable differentiation […] of this specimen [i.e. Jeletzky's plate 5, figure 5] from *Praetollia* Spath 1952 [including *Borealites* Klimova, 1969, in Jeletzky's view] depends on the much more primitive character of its suture line'. However, Jeletzky (1979: 6) himself admitted difficulties in recognising an uninterrupted evolutionary trend in the suture lines of the Craspeditidae, and the referred suture line (Jeletzky, 1979, text-fig. 1L) seems rather similar to those of other craspeditids. Moreover, the subtleties of the suture line, only present near its junction to the shell wall, may easily have been obscured by surficial erosion. Rogov and Zakharov (2009) referred the same specimen to *Craspedites* cf. *thurrelli* Casey, 1973. *Craspedites thurrelli* is based on a single, slightly crushed specimen from eastern England (Casey, 1973: pl. 5, fig. 4), which is significantly more involute, more quickly expanding in whorl height, and less coarsely and prominently ribbed than the Canadian individual.

The smallest specimen of *Borealites fedorovi* from Rollrock has a diameter close to 80 mm (Fig. 17C) and earlier growth stages are poorly documented in our material. At the other end of the spectrum, only one individual from the Rollrock Section is adult and well preserved. We have kept this

776 specimen in three parts, which document subsequent stages of ontogeny and can easily be
777 reassembled (Figs 18, 19). The inner part, at a diameter of 115 mm, is fully costate and closely
778 matches the type material of Klimova (1969, pl. 1) and Jeletzky (1973, pl. 4, fig. 1, pl. 5, fig. 1, pl. 7,
779 fig. 1) in morphology. The second part comprises one full whorl, including slightly less than two
780 thirds of the last whorl. It documents the transition from a fully costate conch to a stage where the
781 secondary ribs have faded and the primaries are reduced to lunate bullae on the inner third of the
782 whorl. The third part, representing the last third of the last whorl, is entirely unornamented.

783 The general ribbing pattern of *Borealites fedorovi* is best inferred from the smaller specimens (Fig.
784 17). The smallest fragments, representing individuals of a size of approximately 80 to 90 mm in
785 diameter, have distinctly bifurcate (Figs 17A, C) or trifurcate ribs (Fig. 17D), with one or two
786 additional secondaries intercalated, resulting in rib coefficients of 3.75, 3.3 and 3.6, respectively, at
787 this stage. Larger specimens (D = 110 to 120 mm) have 3.7 (Fig. 17F, G), 4.2 (Fig. 19A) or 4.5 (Fig.
788 17B) secondary ribs per primary. All these values are well in the range given by Igolnikov (2014) for
789 adult *Borealites*, but indicate a large degree of intraspecific variability.

790 The conch parameters of *Borealites* (*Pseudocraspedites*) sp. from Buchanan Lake on Axel Heiberg
791 Island, figured by Galloway et al. (2020, fig. 3e–g) are slightly different from our large specimen (D_{max}
792 = 164 mm; UWI = 0.32; IZR = 0.41; rib coefficient = 4.6), but its secondary ribs seem to fade at a
793 similar size. We are unsure whether these values are still within the variability of *Borealites fedorovi*.
794 The fragmentary *Borealites* sp. from the same locality (Galloway et al., 2020, fig. 3h, i) shows the
795 same ribbing pattern as our specimens at similar size and most probably represents *Borealites*
796 *fedorovi*.

797 Klimova (1972) described another three species of *Borealites* (*B. radialis*, *B. mirus* and *B. explicatus*)
798 from the same unit and locality at the Yatriya River in the Subpolar Urals where the type species,
799 *Borealites fedorovi* Klimova, 1969, was found. All four species are highly similar in appearance, and,
800 if applying a biological rather than typological species concept, are certainly synonymous. However,

Igolnikov (2014) stated that the whereabouts of Klimova's type material are unknown, and a revision of the genus is beyond the scope of our study.

Age: *Borealites fedorovi* occurs in the lower Berriasian (Ryazanian) *Hectoroceras kochi* Zone in Siberia (Igolnikov, 2014).

Borealites sp.

Figs 20, 21

Material: Four more or less fragmentary specimens from 356 m (NUIF 3031), 357 m (NUIF 3013) and 363.5 m (NUIF 2992, 3004) in the log.

Description: Conch very large (D = 240 mm), extremely discoidal, subevolute (UWI = 0.42); whorls rather strongly embracing (IZR = 0.44). Body chamber extending for approximately 315°, or more. Number of primary ribs and corresponding rib coefficient rather variable; 14 primary ribs on both antepenultimate and penultimate whorls, increasing to 20 primaries on ultimate whorl. Where counting of secondaries is possible on ultimate whorl, a rib coefficient of only 4.6 (13 primaries; 60 secondaries) is attained, as opposed to 6.2 (14 primaries; 87 secondaries) on the penultimate whorl and >5.1 (14 primaries; >71 secondaries) on the antepenultimate whorl.

D1 = 240; uw = 100; wh = 78; ah = 44; 20 primaries on ultimate whorl; 14 on penultimate and antepenultimate whorls.

Remarks: This species is clearly different from *Borealites fedorovi* in several aspects. It is much more evolute (UWI = 0.42, as opposed to 0.29), has a significantly higher average rib coefficient (RC = 5.3 as opposed to 4.2), and is fully (although weakly) costate to a diameter of 240 mm (as opposed to the loss of secondaries at D = 170 mm in *B. fedorovi*). The species was collected at 356, 357 and 363.5 m, while *Borealites fedorovi* occurs only at 363.5 m. Only the largest, figured specimen, NUIF

824 3013, is well enough preserved for full description, but is too strongly compressed to assign a species
825 name.

826 Age: *Borealites* sp. first appears only one metre above *Praetollia maynci* and co-occurs with
827 *Borealites fedorovi* less than 10 m above. Accordingly, the species marks the transition from the
828 *Chetaites sibiricus* Zone to the *Hectoroceras kochi* Zone in the Rollrock Section, indicating an early
829 Berriasian (Ryazanian) age.

830

831 Subcraspeditinae indet.

832 Fig. 16A

833 Material: One fragmentary specimen (NUIF 3166) from 355 m log height.

834 Description: Conch large (DM_1 > 130 mm), presumably extremely discoidal (specimen markedly but
835 not too badly compressed), evolute (UWI = approximately 0.54). Specimen fully septate, i.e. body
836 whorl missing. Ornamented with densely and regularly spaced, almost rectiradiate, slightly
837 proconcave to sigmoidal ribs. Primary ribs bifurcating approximately at mid height of whorl, with
838 additional secondaries intercalated. Primaries and secondaries of equal strength.

839 Remarks: The specimen is very similar to *Praetollia maynci* (which occurs in the same horizon) in
840 ornamentation and in its poor inflation, but the conch is distinctly more evolute. The poor
841 preservation prevents confident assignment at genus or species level.

842

843 Order Belemnitida Zittel, 1895

844 Family Cylindroteuthididae Stolley, 1919

845 Subfamily Cylindroteuthidinae Stolley, 1919

Remarks: The taxonomy of the subfamily Cylindroteuthidinae has been controversial over the last 60 years. Besides *Cylindroteuthis*, earlier studies assigned the genera *Cylindroteuthis* and *Spanioteuthis* to the subfamily (e.g. Dzyuba, 2005). Here we follow the concept of Dzyuba (2011), who included two genera, *Cylindroteuthis* and *Arctoteuthis*, in the Cylindroteuthidinae. The third genus, *Spanioteuthis*, was assigned to the new subfamily Spanioteuthidinae. These revised Cylindroteuthidinae are characterised by large, elongate rostra with a moderately long apical groove, which are cylindrical to cylindroconical both in outline (= ventral or dorsal view) and profile (= lateral view). The alveolus is very shallow. Only *Arctoteuthis* is identified in the present study.

Genus *Arctoteuthis* Saks and Nal'nyaeva, 1964

Type species: *Cylindroteuthis septentrionalis* Bodylevsky, 1960, by original designation.

Diagnosis (following Saks and Nal'nyaeva, 1964): Rostrum slender, elongate to very elongate cylindroconical. Alveolus shallow, approximately 0.2 times the length of the rostrum.

Stratigraphic range: Kimmeridgian to Hauterivian (for details see Saks and Nal'nyaeva, 1964; Mutterlose et al. in press).

Arctoteuthis cf. *porrectiformis* (Anderson, 1945)

Fig. 22A–D

cf. *1945 *Cylindroteuthis porrectiformis* Anderson, n. sp.: Anderson; p. 988, pl. 9, fig. 3.

cf. 1964 *Cylindroteuthis* (*Arctoteuthis*) *porrectiformis* Anderson: Saks & Nal'nyaeva, p. 77, pl. 12, figs 1-3; pl. 13, figs 1, 2; text-fig. 18.

In press *Arctoteuthis* cf. *porrectiformis* (Anderson, 1945): Mutterlose et al., p. 3, fig. 2I, J.

Material: Two specimens from 410.5 m (NUIF 2996) and 425 m (NUIF 3062) in the log.

Diagnosis: Rostrum slender, elongate. Outline symmetrical (ventral view); apex and acutely conical; slightly asymmetrical in profile (lateral view). Transverse section dorsoventrally depressed in stem and apex, laterally slightly compressed in alveolar region.

Description: Both specimens are fragmentary, the tip of the apex and the alveolus are missing. The better-preserved specimen (NUIF 3062) is large (10.6 cm long), elongate and very slender. It has an acutely conical apex. The outline (ventral view) is symmetrical, the profile (lateral view) slightly asymmetrical. Transverse sections are slightly depressed in both the stem and apex. The characteristic shallow alveolus is not preserved. The apex has a ventral groove; its extension onto the stem is accentuated by weathering. Specimen NUIF 2996 shows lateral lines in the stem (Fig. 22A) and a ventral depression (Fig. 22B).

Stratigraphic range: lower to upper Berriasian (upper Volgian to Ryazanian) in Siberia and California; Valanginian (?) in Arctic Canada (Mutterlose et al., in press; this study, see discussion).

Geographic distribution: Siberia, California, Arctic Canada.

Arctoteuthis cf. *harabylensis* (Saks and Nal'nyaeva, 1964)

Fig. 22E, F

cf. *1964 *Cylindroteuthis* (*Arctoteuthis*) *harabylensis* sp. nov.: Saks and Nal'nyaeva, p. 80, pl. 15, figs 1-3, pl. 16, figs 1, 2, text-fig. 19.

In press *Arctoteuthis* cf. *harabylensis* (Saks & Nalnyaeva, 1964): Mutterlose et al., p. 3, fig. 2G, H.

Material: A single specimen from scree in the upper part of the Deer Bay Formation (NUIF 3139).

Diagnosis: Rostrum large and elongate, symmetrical and cylindrical to cylindriconical in outline (ventral view). Long, deep apical groove extending into stem region. Profile (lateral view) symmetrical; apex acute.

892 Stratigraphic range: Valanginian to lower Hauterivian in Siberia; Valanginian in British Columbia, and
893 (?) in Arctic Canada (Mutterlose et al. in press; this study, see discussion).

894 Geographic distribution: Siberia, British Columbia, Arctic Canada.

895

896 7 Discussion

897 7.1 Biostratigraphy

898 As a result of the dearth of macrofossils in the Upper Jurassic to Lower Cretaceous interval in the
899 Sverdrup Basin, biostratigraphic correlation with the remainder of the Boreal Realm is relatively
900 poorly constrained. Dinoflagellate cysts and foraminifera offer only limited insight. This is because
901 the intra-basin zonation schemes developed by Davies (1983) and Wall (1983), respectively, have not
902 been correlated to other parts of the Arctic, the precision of the ages determinable from these
903 fossils is limited. With regard to macrofossils, *Buchia* occurrences in the Sverdrup Basin are generally
904 correlatable to the established Panboreal zonation (Zakharov, 1981; see also Jeletzky, 1984; Rogov
905 and Zakharov, 2009). However, the correlation of ammonite horizons is often hampered by the lack
906 of well-preserved material (Rogov and Zakharov, 2009). According to Jeletzky (1984), the Rollrock
907 Section has the most comprehensive macrofossil record of the Jurassic-Cretaceous transition
908 interval in the Sverdrup Basin. The macrofauna described herein is richer and better preserved than
909 the material previously reported, and has a greater stratigraphic range, owing to the discovery of
910 several additional levels containing macrofossils. Most of these horizons are now confidently
911 assigned to widely recognised biozones, providing a discontinuous but robust biostratigraphic
912 framework for the succession.

913 In stratigraphic order, from oldest to youngest, the following biozones are present in the Rollrock
914 Section (Fig. 23):

915 (1) The 192 m to 197 m interval in the log is assigned to the middle lower Tithonian (lower Volgian)
916 *Buchia rugosa* Zone, based on the occurrence of the zonal index species, *Buchia rugosa*. This biozone
917 is known to occur in Alaska, the Subpolar Urals, the central Russian Platform, the Russian Far East
918 and adjacent China, and potentially also northern Siberia (see Zakharov, 1981; Rogov and Zakharov,
919 2009 and references therein). From the Sverdrup Basin, the *Buchia rugosa* Zone is recorded for the
920 first time herein.

921 (2) Jeletzky (1984) mentioned *Laugeites*? sp. and *Dorsoplanites* cf. *gracilis* from his lowest
922 macrofossil horizon in the Rollrock Section. This level corresponds to the lower middle Tithonian
923 *Dorsoplanites gracilis* Zone of East Greenland (= upper *Dorsoplanites ilovaiskii* Zone of northern
924 Siberia; see Wierzbowski et al., 2017), and is potentially represented in the 296.8 m horizon of our
925 section, where indeterminate dorsoplanitids were found.

926 (3) A concretion horizon at 307 m in Figure 6 is assigned to the middle Tithonian *Dorsoplanites*
927 *maximus* Zone, based on the occurrence of the zonal index species, *Dorsoplanites maximus*, together
928 with *Dorsoplanites sachsi*. *Buchia mosquensis*, which is a long-ranging, early to middle Tithonian
929 species, also occurs in this horizon. The *Dorsoplanites maximus* Zone is recorded from Northern
930 Siberia, the Subpolar Urals and Svalbard, and can be correlated to the *Epipallasiceras pseudapertum*
931 Zone of East Greenland, where *Dorsoplanites maximus* has its type locality (e.g. Rogov and Zakharov,
932 2009). This is the first time the *Dorsoplanites maximus* Zone has been recorded from the Sverdrup
933 Basin. However, several of the poorly preserved *Dorsoplanites* figured by Frebold (1961) and Jeletzky
934 (1966), and mentioned from the Rollrock Section by Jeletzky (1984), are thought to belong to this
935 zone.

936 (4) A monospecific shell pavement of *Buchia terebratuloides* at 333.5 m in the log is assigned to the
937 *Buchia terebratuloides* Zone of Zakharov (1981) and Jeletzky (1984). *Buchia terebratuloides* is long-
938 ranging, occurring throughout the late Tithonian to early Berriasian (Zakharov, 1981). The species
939 has been recorded from the central Russian Platform, the Russian Arctic Islands, the Russian Far

East, California and East Greenland (Zakharov, 1981; Rogov and Zakharov, 2009), and was reported from the Canadian Arctic before (Jeletzky, 1984). The interval of *Buchia terebratuloides* encompasses the *Taimyroceras taimyrensis* Zone, and thus also the Jurassic-Cretaceous boundary, as interpreted herein. *Taimyroceras canadensis*, which represents this ammonite zone at Slidre Fiord on central Ellesmere Island (Jeletzky, 1966), has so far not been found in the Rollrock Section.

(5) Jeletzky (1984) figured several poorly preserved, compressed and considerably weathered outer whorl fragments of craspeditid ammonites, collected from two horizons approximately 60 and 80 m above the dorsoplanitids noted above. He assigned these to *Craspedites* (*Subcraspedites*) cf. *sowerbyi*, *C.* (*S.*) aff. *preplicomphalus* and *Craspedites* (*Craspedites*) aff. *subditus* (referred to *Craspedites* cf. *thurelli* by Rogov and Zakharov, 2009). As a result, Jeletzky (1984, p. 219) inferred a considerable thickening of the earlier Late Tithonian part (more than 70 m) in the Rollrock Section, when compared with the condensed succession at Slidre Fiord (less than 10 m). In our opinion, however, the above-mentioned ammonite fragments were misidentified (see systematic palaeontology section), and the respective horizons correspond to the 355 to 363.5 m interval in Figure 6. The lowest macrofossil level of this interval has yielded a specimen of *Praetollia maynci* and a second, indeterminate subcraspeditine ammonite. Additionally, *Buchia unschensis*, *B. volgensis* and a well-preserved specimen of *Buchia okensis* were collected from this horizon. This assemblage is indicative of the lower middle Berriasian *Praetollia maynci* Zone of East Greenland, corresponding to the *Chetaites sibiricus* Zone of Northern Siberia and the Subpolar Urals (e.g. Zakharov and Rogov, 2008). Furthermore, *Buchia okensis* is the index species of the *Buchia okensis* Zone, which overlaps parts of the *Chetaites sibiricus* Zone and the overlying *Hectoroceras kochi* Zone.

(6) At 356 m and 357 m, *Borealites* sp. occurs, and is accompanied by *Buchia okensis* at 356 m. *Borealites* is common in the middle and upper parts of the *Hectoroceras kochi* Zone in the Subpolar Urals, and in its middle part in Northern Siberia.

964 (7) *Borealites* sp. and *Buchia okensis* also occur at 363.5 m, where several specimens of *Borealites*
965 *fedorovi* were collected. This species has its type locality in the Subpolar Urals, where it occurs in the
966 middle to upper part of the *Hectoroceras kochi* Zone (Klimova, 1969; Zakharov and Rogov, 2008).
967 Furthermore, *Borealites fedorovi* had previously been recorded from Buchanan Lake on Axel Heiberg
968 Island in the Canadian Arctic (Jeletzky, 1973, 1984). This horizon is the highest level yielding
969 ammonites in the Rollrock Section.

970 (8) Belemnites assigned to *Arctoteuthis* cf. *porrectiformis* occur at 410.5 m and 425 m. This species
971 was previously recorded from lower to upper Berriasian strata in Siberia and California (Mutterlose
972 et al. in press). In the Rollrock Section, the two specimens were found in beds containing
973 glendonites, which have so far mainly been reported from the Valanginian part of the Deer Bay
974 Formation (Kemper, 1975; Kemper and Schmitz, 1975, 1981; Grasby et al., 2016). In the same
975 interval, fossilised wood is abundant, which is another characteristic of the Valanginian succession in
976 the Sverdrup Basin (Kemper, 1975). Moreover, the belemnites bracket the occurrence of an external
977 mould of a *Buchia*, which was preserved in a particularly friable concretion and could not be saved.
978 Based on field observation, this specimen presumably represented *Buchia keyserlingi*, which would
979 indicate a Valanginian age (Zakharov, 1981). We thus assume that the beds containing *Arctoteuthis*
980 cf. *porrectiformis* are early Valanginian in age.

981 (9) An additional belemnite, *Arctoteuthis* cf. *harabylensis*, was collected from scree in the higher part
982 of the section, and must have fallen from above 400 m. *Arctoteuthis* cf. *harabylensis* was previously
983 reported from the Valanginian of British Columbia and Siberia, where it extends into the Hauterivian
984 (Saks and Nalnyaeva, 1964, 1972, 1973). Given that the Upper Valanginian to Hauterivian interval in
985 the Sverdrup Basin is represented by predominantly fluvial-deltaic strata of the Isachsen Formation
986 (e.g. Embry, 1985a; Galloway et al., 2015), a Valanginian age is inferred for this belemnite.

987

988 ## 7.2 Macrofossil record and faunal relationships

989 The macrofossil species found in the Rollrock Section are not endemic to the Sverdrup Basin.
990 Instead, these fossils link the succession in Arctic Canada to adjacent and distant parts of the Boreal
991 Realm. The closest links of the ammonite fauna are to Northern Siberia (e.g. Rogov and Zakharov,
992 2009), and the respective zonation scheme is consequently applied herein. Most of the species
993 recorded from the Rollrock Section also occur in eastern Greenland (Spath, 1936, 1952; Kelly et al.,
994 2015; Möller et al., 2015), the Subpolar Urals (Mesezhnikov, 1984; Rogov and Zakharov, 2009) and
995 Svalbard (Rogov and Zakharov, 2009; Wierzbowski et al., 2011). However, the ammonite fauna of
996 the Canadian Arctic appears significantly more impoverished compared to the assemblages reported
997 from these other areas. *Buchia* zones generally have a longer duration than ammonite zones. Most
998 *Buchia* zones start with the first occurrence of an index species (which usually extends into one or
999 several zones above) and terminate with the onset of the index species of the overlying zone. Some
1000 are acme zones, or abundance zones, however, and have no sharp boundaries (e.g. Zakharov, 1981;
1001 Rogov and Zakharov, 2009). Given that individual *Buchia* species only occur in one or a few very
1002 closely spaced horizons in the Rollrock Section, and, with the exception of *B. terebratuloides*, are
1003 never very abundant, we have chosen to display cumulative species ranges rather than zones in
1004 Figure 23. The resulting succession, although superficially more complete than the ammonite
1005 zonation, is similarly discontinuous.

1006 The macrofossil record of the Upper Jurassic to lowermost Cretaceous interval in the Sverdrup Basin
1007 is restricted to a few horizons where ferruginous concretions enclose fossils. Jeletzky (1971a-c, 1973,
1008 1984) and Kemper (1975) considered the dearth and low diversity of macrofossils to be the result of
1009 climatic fluctuations causing punctuated extinction and colonisation events. However, there is a
1010 continuous record of dinoflagellate cysts and agglutinating foraminifera in the Sverdrup Basin
1011 throughout this time (e.g. Davies, 1983, 1985; Wall, 1983). While dinoflagellate cysts generally
1012 preserve well under anoxic conditions, prolonged anoxia in the water column would certainly have
1013 led to barren intervals. Moreover, normal marine, more or less well-oxygenated conditions at the
1014 seafloor are inferred from the presence of foraminifera, and the Sverdrup Basin was well connected

to the Arctic Ocean during these times (e.g. Sømme et al., 2018). Consequently, the Sverdrup Basin was likely inhabited by a biota common to the Late Jurassic and earliest Cretaceous Arctic seas, including ammonites, bivalves and various other aquatic invertebrates and vertebrates. The absence of most of these animals from the fossil record is more likely to be a function of diagenesis, not a primary ecological absence. Given that no calcareous nannofossils, no tests of calcareous foraminifera and no carbonate skeletons of macrofossils are preserved, the Ringnes and Deer Bay formations were almost certainly subject to (early?) diagenetic carbonate dissolution. This may be explained by the solubility of carbon dioxide in seawater, which is inversely correlated with temperature. As a result, cold Arctic waters contain more dissolved CO_2 and are more acidic than warmer waters (higher content of HCO_3^- ions, lower pH), which promotes the dissolution of carbonate (e.g. Chierici and Fransson, 2009). Consequently, carbonate skeletons are dissolved more quickly in Arctic seawater once their protective organic compounds are lost during decay. The few horizons that do preserve fossils likely represent intervals of favourable taphonomic conditions, where sediment was lithified before the shells dissolved.

We thus propose that the presence of species that are shared with other parts of the Boreal Realm is a result of continuous faunal exchange rather than of recurrent, punctuated invasions of the Sverdrup Basin. In horizons where ammonites do occur, species diversity may be underestimated, due to poor preservation. However, climate, in particular sea water temperatures, may also have played a role in ammonite distribution, considering that the Rollrock area was situated much further north than most of the regions mentioned above, and that cold conditions are evident from the persistent occurrence of dropstones and glendonites (see palaeoclimate section below). Zakharov and Rogov (2003) have interpreted migration patterns of Boreal molluscs during the Late Jurassic and earliest Cretaceous (see also Kemper, 1975). However, due to the dearth of data from Arctic Canada (see also Mutterlose et al., 2in press), their scheme is difficult to apply, and the underlying causes of the low diversities observed cannot be rigorously assessed.

7.3 Dropstones, glendonites and palaeoclimate

The Rollrock Section is a testimony to the Arctic extremes of the global environmental perturbations occurring across the Jurassic-Cretaceous transition. The entirety of the mudstone-prone Deer Bay Formation is characterised by the occurrence of abundant, scattered, well-rounded chert or more rarely quartz pebbles, reaching up to 100 mm in size, and thus conforming to the definition of dropstones (Bennett et al., 1996). From the Sverdrup Basin, dropstones were first described by Embry (1991: 429), who suggested that they were transported by seasonally forming ice rafts. Several observations argue in favour of Embry's (1991) interpretation. The dropstones from the Rollrock Section are generally well rounded and polished, but striation and faceting were not observed. They occur scattered, but are strikingly abundant over a large time interval, from the early Tithonian to the middle Valanginian, in a depositional environment at considerable distance from the shore. Following the criteria outlined by Bennett et al. (1996), gastroliths and clasts fallen from tree roots or kelp holdfasts, which both tend to occur in clusters and are relatively rare, are thus confidently ruled out. The size range of clasts transported by icebergs is usually much greater than at Rollrock, and striation and faceting is common. While part of the area of Ellesmere Island may have been glaciated during the latest Jurassic and earliest Cretaceous (e.g. Vickers et al., 2019), these observations point to seasonally forming ice rafts as the most likely vector for dropstone deposition in the Deer Bay Formation.

The presence of two silicified rugose corals as dropstones indicates that Upper Palaeozoic strata were exposed during the time of deposition of the Deer Bay Formation. Silicified corals commonly occur in the Pennsylvanian to Cisuralian Belcher Channel Formation and less commonly in the Pennsylvanian Nansen Formation (Thorsteinsson, 1974). Both units crop out in the area around Tanquary Fiord (Mayr and Trettin, 1996). This suggests that, compared with the Late Palaeozoic,

either the sea level was lower, or at least the coastlines were significantly different during the study interval.

In the upper part of the Deer Bay Formation, glendonites occur together with the dropstones. Glendonites are aggregates of pseudomorphs after the metastable carbonate ikaite, and are most commonly found in high-latitude organic rich mudstones (see Grasby et al., 2017 for a summary), although they are occasionally recorded from more temperate settings (e.g. Teichert and Luppold, 2013). For the Deer Bay Formation, the high palaeo-latitude together with fossil evidence, high-latitude palaeotemperature reconstructions and host-rock geochemistry strongly support that the glendonites formed during cold intervals (Kemper, 1975; Kemper and Schmitz, 1975, 1981; Grasby et al., 2017). Kemper (1975) further advocated that the accumulation of driftwood in the upper Deer Bay Formation was promoted by low rates of biofouling, supporting the hypothesis of cold climatic conditions.

In forthcoming studies of dinoflagellate and foraminifer assemblages, as well as geochemical proxies from the Rollrock Section, we hope to address the palaeoclimatic fluctuations of the study interval in greater depth, and potentially unravel relationships with favourable taphonomic conditions and macrofossil distribution.

8 Conclusions

The Rollrock Section on northern Ellesmere Island provides the most comprehensive outcrop record of the Jurassic-Cretaceous transition interval in the Sverdrup Basin of the Canadian Arctic, and is globally one of the northernmost exposures of such rocks. More than 500 m of a continuously exposed mudstone-dominated succession are almost evenly split into the lower, Oxfordian to lower Tithonian Ringnes Formation and the overlying, lower Tithonian to middle Valanginian Deer Bay Formation, grading into the sand-dominated Isachsen Formation above. In the absence of other

lithologic distinctions, the top of a coarsening-upward interval, above which dropstones are common, is taken as the lower boundary of the Deer Bay Formation.

Macrofossils are documented from 15 horizons in the Rollrock Section, and significantly improve the biostratigraphy of the Tithonian and Berriasian in the Sverdrup Basin. *Buchia rugosa* occurs in three levels within the Ringnes Formation, and indicates an early Tithonian age for the upper part of this unit. The overlying Deer Bay Formation yielded nine horizons with biostratigraphically relevant macrofauna. Dorsoplanitid ammonites occur in two closely spaced levels. *Dorsoplanites maximus* and *D. sachsi* at 307 m indicate the middle Tithonian *Dorsoplanites maximus* Zone. Abundant *Buchia terebratuloides* at 333.5 m are late Tithonian to early Berriasian in age, and are the most accurate marker of the Jurassic-Cretaceous boundary in the Rollrock Section. At 355 m, *Praetollia maynci* indicates a late early Berriasian age and marks the onset of the Boreal Ryazanian regional stage. *Borealites* sp. (356, 357 and 363.5 m) and *Borealites fedorovi* (363.5 m) correspond to the lowermost upper Berriasian *Hectoroceras kochi* Zone. The beds with *Borealites* are thought to represent the '*Subcraspedites*' and '*Craspedites*' horizons in the literature, and are considerably younger than previously thought, i.e. middle Berriasian instead of latest Tithonian in age. Additionally, belemnites of the genus *Arctoteuthis* from two horizons (410.5 and 425 m), co-occurring with glendonites and abundant fossilised wood in this interval, suggest a Valanginian age for the higher part of the succession.

The dearth of Late Jurassic and earliest Cretaceous macrofossils in the Rollrock Section, and more generally in the Sverdrup Basin, is largely attributed to diagenetic loss, since normal marine oxygenated conditions appear to occur throughout the study interval. The sparse fossil dataset precludes a comprehensive assessment of climatic influences on fossil occurrences and migration patterns.

9 Acknowledgements

Working in the Arctic would not be possible without manifold support. Our sincere thanks go to the following people in Canada who helped to make our research a success: Sylvie LeBlanc (Department of Culture and Heritage, Iglooik, Canada); Jane Chisholm (Parks Canada, Iqaluit, Canada); John Innis (Universal Helicopters); the rangers of Parks Canada at Quttinirpaaq National Park (Ellesmere Island, Canada); the Polar Continental Shelf Programme team at Resolute (Cornwallis Island, Canada); Margaret Currie, Laura Smyk and Kieran Sheperd (all Canadian Museum of Nature, Ottawa, Canada). Alex Chavanne (California, USA) joined our team as an excellent field assistant, helped logging and sampling the Rollrock Section and found the giant *Dorsoplanites* specimen. Sarah Wallace-Jones (Sedgwick Museum, Department of Earth Sciences, University of Cambridge, UK) provided access to preparation labs. Magdalena Biszczuk (CASP) prepared the maps in Figure 1; and Michael Pointon (CASP) polished the English. Mikhail Rogov (Geologicheskij Institut, Rossijskaja Akademija Nauk, Moscow) greatly helped by sharing expert knowledge regarding ammonites of the Jurassic-Cretaceous boundary interval and by providing literature. CASP's industry sponsors are acknowledged for funding the Canadian Arctic Islands Project. Peter Alsen (Geological Survey of Denmark and Greenland, Copenhagen, Denmark) and Terence Poulton (Natural Resources Canada, Calgary, Canada) provided careful and detailed reviews, which greatly improved the manuscript.

10 References

Agassiz, L. 1842–1845. Études critiques sur les mollusques fossils. Monographie des Myes. Wolfrath, Neuchâtel, I–III, 1–142, appendice, 1842; IV–IX, 143–230, 1843; X–XII, 231–287, 1845.

Anderson, F. 1945. Knoxville Series in the California Mesozoic. The Geological Society of America Bulletin 56, 909–1014.

Arkell, W.J. 1950. A classification of the Jurassic ammonites. Journal of Paleontology 24, 354–364.

1136 Balkwill, H.R. 1983. Geology of Amund Ringnes, Cornwall and Haig-Thomas islands, District of
1137 Franklin. Geological Survey of Canada, Memoir 390, 1–76.

1138 Balkwill, H.R., Wilson, D.G., Wall, J.H. 1977. Ringnes Formation (Upper Jurassic), Sverdrup Basin,
1139 Canadian Arctic Archipelago. Bulletin of Canadian Petroleum Geology 25, 1115–1144.

1140 Bennett, M.R., Doyle, P., Mather, A.E. 1996. Dropstones: their origin and significance.
1141 Palaeogeography, Palaeoclimatology, Palaeoecology 121, 331–339.

1142 Beurlen, K. 1944. Beiträge zur Stammesgeschichte der Muscheln. Sitzungberichte der Mathematisch-
1143 Naturwissenschaftlichen Abteilung der Bayerischen Akademie der Wissenschaften zu
1144 München 1944, 133–145.

1145 Bieler, R., Mikkelsen, P.M., Collins, T.M., Glover, E.A., González, V.L., Graf, D.L., Harper, E.M., Healy,
1146 J., Kawauchi, G.Y., Sharma, P.P., Staubach, S., Strong, E.E., Taylor, J.D., Tëmkin, I., Zardus, J.D.,
1147 Clark, S., Guzmán, A., McIntyre, E., Sharp, P., Giribet, G. 2014. Investigating the bivalve tree of
1148 life – an exemplar-based approach combining molecular and novel morphological characters.
1149 Invertebrate Systematics 28, 32–115.

1150 Bodylevsky, V.J. 1960. Novye pozdnejurskie belemnity Severnoj Sibiri [New Late Jurassic belemnites
1151 of Northern Siberia]. In: Markovskii, B.P. (Ed.), Novye vidy drevnikh rastenii i
1152 bespozvonochnykh SSSR, 2 [New species of prehistoric plants and invertebrates of the USSR;
1153 Part 2]. Ministerstva Geologii i Okhran' Nedr, Vsesoiuznyi Nauchno-Issledovatel'skii,
1154 Gosgeoltekhizdat, Moskva, 193–195. [in Russian].

1155 Brideaux, W.W., Fisher, M.J. 1976. Upper Jurassic - Lower Cretaceous dinoflagellate assemblages
1156 from Arctic Canada. Geological Survey of Canada, Bulletin 259, 1–53.

1157 Buch, L. von 1844. Über einige neue Versteinerungen aus Moskau. Neues Jahrbuch für Mineralogie,
1158 Geognosie, Geologie und Petrefaktenkunde 1844, 536–539.

1159 Casey, R. 1973. The ammonite succession at the Jurassic-Cretaceous boundary in eastern England.
1160 In: Casey, R., Rawson, P.F. (Eds.), The Boreal Lower Cretaceous. The proceedings of an
1161 international symposium organised by Queen Mary College (University of London) and the
1162 Institute of Geological Sciences, 17-30 September 1972. Seel House Press, Liverpool, 193–266.

1163 Casey, R., Mesezhnikov, M.S., Shul'gina, N.I. 1977. Sopostavlenie pogranichny otlozhenij Jury i mela
1164 Anglii, Russkoj Platformy, Priopoljarnogo Urala i Sibiri [Correlation of the Jurassic/Cretaceous
1165 boundary beds of England, Russian Platform, Subpolar Urals and Siberia. Izvestija Akademii
1166 Nauk SSSR, Serija Geologicheskaja, 7, 14–33. [in Russian]

1167 Chamney, T.P. 1968. Foraminifera useful for determining the Jurassic-Cretaceous boundary in Arctic
1168 America. Geological Survey of Canada, Paper 68-1B, 82–83.

1169 Chamney, T.P. 1971. New species of Foraminifera, Cretaceous-Jurassic boundary, Arctic America.
1170 Geological Survey of Canada, Bulletin 192, 95–113.

1171 Chierici, M., Fransson, A. 2009. Calcium carbonate saturation in the surface water of the Arctic
1172 Ocean: undersaturation in freshwater influenced shelves. Biogeosciences 6, 2421–2432.

1173 Cox, L.R. 1953. Lower Cretaceous Gastropoda, Lamellibranchia and Annelida from Alexander Island
1174 (Falkland Islands Dependencies). Scientific Reports of the British Antarctic Survey, Falkland
1175 Islands Dependencies Survey 4, 1–14.

1176 Cuvier, G. 1795. Second mémoire sur l'organisation et les rapports des animaux à sang blanc, dans
1177 lequel on traite de la structure des mollusques et de leur division en ordre, lu à la société
1178 d'Histoire Naturelle de Paris, le 11 Prairial an troisième [30 May 1795]. Magazin
1179 Encyclopédique, ou Journal des Sciences, des Lettres et des Arts, 1795 [1. année] 2, 433–449.

1180 Davies, E.H. 1983. The dinoflagellate Oppel-zonation of the Jurassic-Lower Cretaceous sequence in
1181 the Sverdrup Basin, Arctic Canada. Geological Survey of Canada, Bulletin 359, 1–59.

1182 Davies, E.H. 1985. Dinoflagellate cyst occurrences of the Jurassic-Lower Cretaceous sequence in the
1183 Sverdrup Basin, Arctic Canada. Geological Survey of Canada, Open File 1153, 1–28.

1184 Dörhöfer, G. 1979. Distribution and stratigraphic utility of Oxfordian to Valanginian miospores in
1185 Europe and North America. American Association of Stratigraphic Palynologists, Contributions
1186 Series 5B, 101–132.

1187 Doyle, P., Kelly, S.R.A., 1988. The Jurassic and Cretaceous belemnites of Kong Karls Land, Svalbard.
1188 Norsk Polarinstitutt, Skrifter 189, 1–77.

1189 Dzyuba, O.S. 2005. Systematics and phylogeny of the boreal family Cylindroteuthidae: Problems
1190 solved and unsolved. In: Košťák, M., Marek, J. (Eds.), 2nd International Symposium – Coleoid
1191 cephalopods through time, Prague, September 26-28, 2005, abstracts volume, 64–67.

1192 Dzyuba, O.S., 2011. Subfamily classification within the Cylindroteuthididae (Belemnitida). News of
1193 Palaeontology and Stratigraphy, 16–17, 103–108. (Supplement to journal).

1194 Dzyuba, O.S., 2012. Belemnites and biostratigraphy of the Jurassic–Cretaceous boundary deposits of
1195 northern East Siberia: new data on the Nordvik Peninsula. Stratigraphy and Geological
1196 Correlation 20, 53–72.

1197 Embry, A.F. 1984b. The Wilkie Point Group (Lower-Upper Jurassic) Sverdrup Basin, Arctic Islands.
1198 Geological Survey of Canada, Paper 84–1B, 299–308.

1199 Embry, A.F. 1985a. Stratigraphic subdivision of the Isachsen and Christopher formations (Lower
1200 Cretaceous), Arctic Islands. Geological Survey of Canada, Paper 85–1B, 239–246.

1201 Embry, A.F. 1985b. New stratigraphic units, Middle Jurassic to lowermost Cretaceous succession,
1202 Arctic Islands. Geological Survey of Canada, Paper 85–1B, 269–276.

1203 Embry, A.F. 1986b. Stratigraphic subdivision of the Awingak Formation (Upper Jurassic) and revision
1204 of the Hiccles Cove Formation (Middle Jurassic), Sverdrup Basin, Arctic Islands. Geological
1205 Survey of Canada, Paper 86–1B, 341–349.

1206 Embry, A.F. 1991. Mesozoic history of the Arctic Islands. In: Trettin, H.P. (ed). Geology of the
1207 Innuitian Orogen and Arctic Platform of Canada and Greenland. Geology of Canada 3,
1208 Geological Survey of Canada, Ottawa & Geological Society of America, 369–433.

1209 Embry, A.F. 2019. Triassic history of the Tanquary High in NE Sverdrup Basin, Canadian Arctic
1210 Archipelago. In: Piepjohn, K., Strauss, J.V., Reinhardt, L., McClelland, W.C. (Eds.), Circum-Arctic
1211 structural events: tectonic evolution of the Arctic margins and trans-Arctic links with adjacent
1212 orogens. Geological Society of America, Special Paper 541, doi: 10.1130/2018.2541(14).

1213 Embry, A.F., Beauchamp, B. 2008. Chapter 13. Sverdrup Basin. In: Miall, A.D. (Ed.). Sedimentary
1214 basins of the world. University of Toronto, 451–471.

1215 Embry, A.F., Beauchamp, B. 2019. Chapter 14. Sverdrup Basin. In: Miall, A.D. (Ed.). The Sedimentary
1216 Basins of the United States and Canada, 2nd Edition. Elsevier, New York, 559–592.

1217 Fischer von Waldheim, G. 1837. Oryctographie du gouvernement de Moscou. Auguste Semen,
1218 Moscou, I–XVII, 1–202.

1219 Frebold, H. 1961. The Jurassic faunas of the Canadian Arctic. Middle and Upper Jurassic ammonites.
1220 Geological Survey of Canada, Bulletin 74, 1–43.

1221 Frebold, H. 1964. Illustrations of Canadian Fossils, Jurassic of western and Arctic Canada. Geological
1222 Survey of Canada, Paper 63–4, 1–104.

1223 Frebold, H. 1975. The Jurassic faunas of the Canadian Arctic. Lower Jurassic ammonites,
1224 biostratigraphy and correlations. Geological Survey of Canada, Bulletin 243, 1–24.

1225 Galloway, J.M., Sweet, A.R., Swindles, G.T., Dewing, K., Hadlari, T., Embry, A.F., Sanei, H. 2013.
1226 Middle Jurassic to Lower Cretaceous paleoclimate of Sverdrup Basin, Canadian Arctic
1227 Archipelago inferred from the palynostratigraphy. Marine and Petroleum Geology 44, 240–
1228 255.

1229 Galloway, J.M., Vickers, M.L., Price, G.D, Poulton, T., Grasby, S.E., Hadlari, T., Beauchamp, B.,
1230 Sulphur, K. 2020. Finding the VOICE: organic carbon isotope chemostratigraphy of Late
1231 Jurassic – Early Cretaceous Arctic Canada. Geological Magazine, doi:
1232 10.1017/S0016756819001316.

1233 Gradstein, F.M., Ogg, J.G., Schmitz, M.D., Ogg, G.M. 2012. The geologic time scale 2012. Volume 2.
1234 Elsevier, Oxford, 437–1144.

1235 Grasby, S.E., McCune, G.E., Beauchamp, B., Galloway, J.M. 2017. Lower Cretaceous cold snaps led to
1236 widespread glendonite occurrences in the Sverdrup Basin, Canadian High Arctic. GSA Bulletin
1237 129, 771–787.

1238 Gray, J.E. 1854. A revision of the arrangement of the families of bivalve shells (Conchifera). Annals
1239 and Magazine of Natural History, series 2, 14 (79), 408–418.

1240 Grey, M., Haggart, J.W., Smith, P.L. 2008. Variation in evolutionary patterns across the geographic
1241 range of a fossil bivalve. Science 322, 1238–1241.

1242 Grey, M., Haggart, J.W., Smith, P.L. 2010. Morphological variability in time and space: an example of
1243 patterns with buchiid bivalves (Bivalvia, Buchiidae). Palaeontology 53, 1269–1280.

1244 Hadlari, T., Midwinter, D., Galloway, J.M., Dewing, K., Durbano, A.M. 2016. Mesozoic rift to post-rift
1245 tectonostratigraphy of the Sverdrup Basin, Canadian Arctic. Marine and Petroleum Geology
1246 76, 148–158.

1247 Håkansson, E., Birkelund, T., Piasecki, S., Zakharov, V. 1981. Jurassic – Cretaceous boundary strata of
1248 the extreme Artic (Peary Land, North Greenland). Bulletin of the Geological Society of
1249 Denmark 30, 11–42.

1250 Hallam, A. 1986. The Pliensbachian and Tithonian extinction events. Nature 319, 765–768.

1251 Haq, B.U. 2014. Cretaceous eustasy revisited. Global and Planetary Change 113, 44–58.

1252 Harrison, J.C., Jackson, M.P.A. 2014. Tectonostratigraphy and allochthonous salt tectonics of Axel
1253 Heiberg Island, central Sverdrup Basin, Arctic Canada. Geological Survey of Canada, Bulletin
1254 607, 1–124.

1255 Harrison, J.C., St-Onge, M.R., Petrov, O.V., Strelnikov, S.I., Lopatin, B.G., Wilson, F.H., Tella, S., Paul,
1256 D., Lynds, T., Shokalsky, S.P., Hults, C.K., Bergman, S., Jepsen, H.F., Solli, A. 2011. Geological
1257 map of the Arctic. Geological Survey of Canada, Map 2159A.

1258 Herrle, J.O., Schröder-Adams, C.J., Davis, W., Pugh, A.T., Galloway, J.M., Fath, J. 2015. Mid-
1259 Cretaceous High Arctic stratigraphy, climate, and Oceanic Anoxic Events. Geology 45, 403–
1260 406.

1261 Herrmannsen, A.N. 1846–1849, 1852. Indices generum malacozoorum primordia. Nomina
1262 subgenerum, generum, familiarum, tribuum, ordinum, classium; adjectis auctoribus,
1263 temporibus, locis systematicis atque literariis, etymis, synonymis. Praetermittuntur Cirripedia,
1264 Tunicata et Rhizopoda. Fischer, Cassellis; vol. 1, I–XXVII, 1–637; vol. 2, XXX–XLII, 2–717;
1265 Supplementa et Corrigenda, I–IV, 1–140.

1266 Heywood, W.W. 1955. Arctic piercement domes. Transactions of the Canadian Institute of Mining
1267 and Metallurgy 58, 27–32.

1268 Heywood, W.W. 1957. Isachsen area, Ellef Ringnes Island, District of Franklin, Northwest Territories.
1269 Geological Survey of Canada, Paper 56–8, 1–36.

1270 Houša, V., Pruner, P., Zakharov, V.A., Kostak, M., Chadima, M., Rogov, M.A., Šlechta, S., Mazuch, M.
1271 2007. Boreal–Tethyan Correlation of the Jurassic–Cretaceous boundary interval by magneto-
1272 and biostratigraphy. Stratigraphy and Geological Correlation 15, 297–309.

1273 Hyatt, A. 1889. Genesis of the Arietidae. Smithsonian Contributions to Knowledge 26 (673), I–XII, 1–
1274 238.

1275 Igolnikov, A.E. 2014. A new species of the genus *Borealites* Klimova, 1969 (Ammonitida,
1276 Craspeditidae) from the Boreal Berriasian of Siberia. Paleontologicheskii Zhurnal, 2014 (3), 40–
1277 48. [in Russian; English translation, Paleontological Journal 48, 255–265]

1278 International Commission on Zoological Nomenclature 1957. Opinion 492, Suppression under the
1279 plenary powers of the family-group name “Aucellidae” Lanusen, 1897, and rejection of an
1280 application for use of the same powers to validate the generic name “*Aucella*” Keyserling,
1281 1846, by suppressing the generic name “*Buchia*” Rouillier, 1845 (Class Lamellibranchia).
1282 Opinions and Declarations rendered by the International Commission on Zoological
1283 Nomenclature 17 (14), 209-254.

1284 Jeletzky, J.A. 1964. Illustrations of Canadian fossils. Lower Cretaceous marine index fossils of the
1285 sedimentary basins of western and Arctic Canada. Geological Survey of Canada, Paper 64–11,
1286 1–101.

1287 Jeletzky, J.A. 1965a. Late Upper Jurassic and early Lower Cretaceous fossil zones of the Canadian
1288 Western Cordillera, British Columbia. Bulletin, Geological Survey of Canada 103, 1–70.

1289 Jeletzky, J.A. 1965b. *Thorsteinssonoceras*, a new craspeditid ammonite from the Valanginian of
1290 Ellesmere Island, Arctic Archipelago. Geological Survey of Canada, Bulletin 120, 1–16.

1291 Jeletzky, J.A. 1966. Upper Volgian (latest Jurassic) ammonites and buchias of Arctic Canada.
1292 Geological Survey of Canada, Bulletin 128, 1–51.

Jeletzky, J.A. 1970. Marine Cretaceous biotic provinces and paleogeography of western and Arctic Canada: Illustrated by a detailed study of ammonites. Geological Survey of Canada, Paper 70–22, 1–92.

Jeletzky, J.A. 1971a. Marine Cretaceous biotic provinces of western and Arctic Canada. Proceedings of the North American Paleontological Convention, September 1969, Part L, 1638-1659.

Jeletzky, J.A. 1971b. Biochronology of Jurassic-Cretaceous transition beds in Canada. Geological Survey of Canada, Paper 71–16, 1–8.

Jeletzky, J.A. 1971c. Jurassic–Cretaceous transition beds in Canada. Collogue du Jurassique, Luxembourg 1967. Mémoires du Bureau de Recherches Géologiques et Minières 75, 701–707.

Jeletzky, J.A. 1973. Biochronology of the marine boreal latest Jurassic, Berriasian and Valanginian in Canada. In: Casey, R., Rawson, P.F. (Eds.). The Boreal Lower Cretaceous: the proceedings of an international symposium organised by Queen Mary College, University of London, and the Institute of Geological Sciences, 17–30 September, 1972. Geological Journal, Special Issue 5, 41–80.

Jeletzky, J.A. 1979. Eurasian craspeditid genera *Temnoptychites* and *Tollia* in the Lower Valanginian of Sverdrup Basin, District of Franklin, with comments on taxonomy and nomenclature of Craspeditidae. Geological Survey of Canada, Bulletin 299, 1–89.

Jeletzky, J.A. 1984. Jurassic - Cretaceous boundary beds of western and Arctic Canada and the problem of the Tithonian-Berrisian stages in the Boreal Realm. In: Westermann, G.E.G. (Ed.). Jurassic-Cretaceous biochronology and biogeography of North America. Geological Association of Canada, Special paper 27, 175–255.

Jeletzky, J.A. 1986. *Pseudoeuryptychites*: a new polyptychitinid ammonite from the Lower Valanginian of the Canadian and Eurasian Arctic. Geological Survey of Canada, Paper 86–1B, 351–361.

1317 Jeletzky, J.A., Kemper, E. 1988. Comparative paleontology and stratigraphy of Valanginian
1318 Polyptychitinae and Simbirskitinae in Sverdrup Basin (Arctic Canada) and Lower Saxony Basin
1319 (northwest Germany). Geological Survey of Canada, Bulletin 377, 1–355.

1320 Johnson, C.D., Hills, L.V. 1973. Microplankton zones of the Savik Formation (Jurassic), Axel Heiberg
1321 and Ellesmere islands, District of Franklin. Bulletin of Canadian Petroleum Geology 21, 178–
1322 218.

1323 Kelly, S.R.A., Gregory, F.J., Braham, W., Strogen, D.P., Whitham, A.G. 2015. Towards an integrated
1324 Jurassic biostratigraphy for eastern Greenland. Volumina Jurassica 13, 43–64.

1325 Kemper, E. 1975. Upper Deer Bay Formation (Berriasian-Valanginian) of Sverdrup Basin and
1326 biostratigraphy of the Arctic Valanginian. Geological Survey of Canada, Paper 75–1B, 45–54.

1327 Kemper, E. 1977. Biostratigraphy of the Valanginian in Sverdrup Basin, District of Franklin. Geological
1328 Survey of Canada, Paper 76–32, 1–6.

1329 Kemper, E. 1987. Das Klima der Kreidezeit. In: Kemper, E. (Ed.), Das Klima der Kreidezeit.
1330 Geologisches Jahrbuch, Reihe A 96, 1–186.

1331 Kemper, E., Jeletzky, J.A. 1979. New stratigraphically and phylogenetically important olcostephanid
1332 (Ammonitida) taxa from the uppermost Lower and Upper Valanginian of Sverdrup Basin,
1333 N.W.T. Geological Survey of Canada, Paper 79–18, 1–25.

1334 Kemper, E., Schmitz, H.H. 1975. Stellate nodules from the Upper Deer Bay Formation (Valanginian)
1335 of Arctic Canada. Geological Survey of Canada, Paper 75–1C, 109–119.

1336 Kemper, E., Schmitz, H.H. 1981. Glendonite – Indikatoren des polarmarinen Ablagerungsmilieus.
1337 Geologische Rundschau 70, 759–763.

1338 Klimova, I.G. 1969. O rannem Berriase Zapadnoj Sibiri [About the Early Berriasian of Western
1339 Siberia]. Geologija I Geofizika 1969 (4), 128–132. [in Russian]

1340 Klimova, I.G. 1972. Ammonites of Western Siberia. In: Saks, V.N. (Ed.), The Jurassic-Cretaceous
1341 boundary and the Berriasian Stage in the Boreal Realm [Granitsa yury i mela i Berriasskii yarns
1342 v boreal'nom poyase]. Akademiya Nauk SSSR, Izdatel'stvo "Nauka" Sibirskoe Otdelenie,
1343 Novosibirsk. [in Russian; English translation published by Israel Program for Scientific
1344 Translations, Keter Publishing, Jerusalem, 1975]

1345 Klug, C., Korn, D., Landman, N.H., Tanabe, K., De Baets, K., Naglik, C. 2015. Describing ammonoid
1346 conchs. In: Klug, C., Korn, D., De Baets, K., Kruta, I., Mapes, R.H. (Eds.), Ammonoid
1347 paleobiology: from anatomy to ecology. Topics in Geobiology 43, 3–24.

1348 Lahusen, J. 1888. Ueber die russischen Aucellen. Mémoires du Comité Geologique 8, 1–46. [in
1349 Russian and German]

1350 Linnaeus, C. 1758. Systema naturae per regna tria naturae, secundum classes, ordines, genera,
1351 species, cum characteribus, differentiis, synonymis, locis. Editio decima, reformata. Laurentius
1352 Salvius, Holmiae, 1–824.

1353 Lippert, P. 2004. A cold start to the Cretaceous, defining climate history near to the North Pole.
1354 Journal of Undergraduate Research 2, 42–48.

1355 Lopez-Mír, Schneider, S., Hülse, P. 2018. Fault activity and diapirism in the Mississippian to Late
1356 Cretaceous Sverdrup Basin: New insights into the tectonic evolution of the Canadian Arctic.
1357 Journal of Geodynamics 118, 55–65.

1358 Mayr, U., Trettin, H.P. 1996. Geology, Tanquary Fiord, District of Franklin, Northwest Territories.
1359 Geological Survey of Canada, Map 1886A, scale 1:250,000.

1360 McMillan, N.J. 1963. Geological traverse from Lightfoot River to Wading River. Geological Survey of
1361 Canada, Memoir 320, 501-512.

1362 Meek, F.B. 1865. Description of fossils from the auriferous slates of California. Geological Survey of
1363 California, Geology 1, 477–482.

1364 Mesezhnikov, M.S. 1984. Kimeridzhskii i volzhskii yarusy severa SSSR [Kimmeridgian and Volgian
1365 stages in the northern USSR]. Leningrad, Nedra, 1–224. [in Russian]

1366 Michailov, N.P. 1966. Boreal Jurassic ammonites (Dorsoplanitidae) and zonal subdivision of the
1367 Volgian stage. Trudy, Akademija Nauk SSSR, Geologicheskij Institut 151, 1–116. [in Russian]

1368 Möller, C., Mutterlose, J., Alsen, P. 2015. Integrated stratigraphy of Lower Cretaceous sediments
1369 (Ryazanian–Hauterivian) from North-East Greenland. Palaeogeography, Palaeoclimatology,
1370 Palaeoecology 437, 85–97.

1371 MolluscaBase 2019. Accessed at http://www.molluscabase.org.

1372 Mutterlose, J., Alsen, P., Iba, Y., Schneider, S. In press. Palaeobiogeography and palaeoecology of
1373 Early Cretaceous belemnites from the northern high latitudes. Proceedings of the Geologists'
1374 Association, doi: 10.1016/j.pgeola.2019.06.001.

1375 Neumayr, M. 1884 [for 1883]. Zur Morphologie der Bivalvenschlosses. Sitzungsberichte der
1376 Kaiserlichen Akademie der Wissenschaften, Mathematisch-Naturwissenschaftliche Klasse,
1377 Abteilung I, 88, 385–419.

1378 O'Brien, C.L., Robinson, S.A., Pancost, R.D., Sinninghe Damsté, J.S., Schouten, S., Lunt, D.J., Alsen, H.,
1379 Bornemann, A., Bottini, C., Brassell, S.C., Farnsworth, A., Forster, A., Huber, B.T., Inglis, G.N.,
1380 Jenkyns, H.C., Linnert, C., Littler, K., Markwick, P., McAnena, A., Mutterlose, J., Naafs, D.A.,
1381 Püttmann, W., Sluijs, A., van Helmond, N.A.G.M., Vellekoop, J., Wagner, T., Wrobel, N.E. 2017.
1382 Cretaceous sea-surface temperature evolution: Constraints from TEX_{86} and planktonic
1383 foraminiferal oxygen isotopes. Earth-Science Reviews 172, 224–247.

1384 Pavlow, 1907. Enchaînement des Aucelles et Aucellines du Crétacé Russe. Nouveaux mémoires de la
1385 Société impériale des naturalistes de Moscou 17, 1–93.

1386 Phillips, J. 1829. Illustrations of the geology of Yorkshire; or, A description of the strata and organic
1387 remains of the Yorkshire coast: accompanied by a geological map, sections, and plates of the
1388 fossil plants and animals. Wilson & Sons, York, 1–192.

1389 Pimpirev, C., Pavlishina, P. 2005. Stratigraphy, age constraints and paleoenvironmental
1390 interpretations of the Upper Jurassic – Lower Cretaceous sediments in the area of Lake Hazen,
1391 Ellesmere Island, Canadian Arctic. 80 years Bulgarian Geological Society, Proceedings of the
1392 Jubilee International Conference, Bulgarian Geological Society, Sofia, 14–17.

1393 Pocock, S.A.J. 1967. The Jurassic-Cretaceous boundary in northern Canada. Review of Palaeobotany
1394 and Palynology 5, 129–136.

1395 Pocock, S.A.J. 1976. A preliminary dinoflagellate zonation of the uppermost Jurassic and lower part
1396 of the Cretaceous, Canadian Arctic, and possible correlation in the western Canada Basin.
1397 Geoscience and Man 15, 101-114.

1398 Poulton, T.P. 1993. Jurassic stratigraphy and fossil occurrences – Melville, Prince Patrick, and Borden
1399 Islands. Geological Survey of Canada, Bulletin 450, 161–193.

1400 Price, G.D. 1999. The evidence and implications of polar ice during the Mesozoic. Earth-Science
1401 Reviews 48, 183–210.

1402 Price, G.D., Twitchett, R.J., Wheeley, J.R., Buono, G. 2013. Isotopic evidence for long term warmth in
1403 the Mesozoic. Scientific Reports 3, 1438, doi:10.1038/srep01438.

1404 Pugh, A.T., Schröder-Adams, C.J., Carter, E.S., Herrle, J.O., Galloway, J.M., Haggart, J.W., Andrews,
1405 J.L., Hatsukano, K. 2014. Cenomanian to Santonian radiolarian biostratigraphy, carbon isotope
1406 stratigraphy and paleoenvironments of the Sverdrup Basin, Ellef Ringnes Island, Nunavut,
1407 Canada. Palaeogeography, Palaeoclimatology, Palaeoecology 413, 101–122.

1408 Rogov, M.A. 2014. *Khetoceras* (Craspeditidae, Ammonoidea) – a new genus from the Volgian stage
1409 of northern middle Siberia, and parallel evolution of Late Volgian Boreal ammonites.

1410 Paleontologicheskii Zhurnal 2014 (5), 10–16. [In Russian; English version: Paleontological
1411 Journal 48, 457–464]

1412 Rogov, M.A., Mironenko, A.A. 2016. Patterns of the evolution of aptychi of Middle Jurassic to Early
1413 Cretaceous Boreal ammonites. Swiss Journal of Palaeontology 135, 139–151.

1414 Rogov, M.A., Zakharov, V.A. 2009. Ammonite- and bivalve-based biostratigraphy and Panboreal
1415 correlation of the Volgian Stage. Science in China, Series D, Earth Sciences 52, 1890–1909.

1416 Roman, F. 1938. Les ammonites jurassiques et crétacés. Essai de genera. Masson, Paris, 1–554.

1417 Rouillier, K.F. 1845. Nouveau genre *Buchia*. Bulletin de la Société Impériale des Naturalistes de
1418 Moscou 18, 289.

1419 Saks, V.N., Nal´nayeva, T.I. 1964. Upper Jurassic and Lower Cretaceous belemnites of the northern
1420 USSR. The genera *Cylindroteuthis* and *Lagonibelus*. Nauka, Leningrad, 1–204. [in Russian]

1421 Saks, V.N., Nal´nayeva, T.I. 1966. Upper Jurassic and Lower Cretaceous belemnites of the northern
1422 USSR. The genera *Pachyteuthis* and *Acroteuthis*. Nauka, Moscow, 1–260. [in Russian]

1423 Saks, V.N., Nal'nyaeva, T.I. 1972. Belemnites. In: Saks, V.N. (Ed.), The Jurassic-Cretaceous boundary
1424 and the Berriasian stage in the Boreal Realm. Nauka, Novosibirsk, 216–229. [in Russian;
1425 English translation published by Israel Program for Scientific Translations, Keter Publishing,
1426 Jerusalem, 1975].

1427 Saks, V.N., Nal'nyaeva, T.I. 1973. Belemnite assemblages from the Jurassic-Cretaceous boundary
1428 beds in the Boreal Realm. In: Casey, R., Rawson, P.F. (Eds.), The Boreal Lower Cretaceous. The
1429 proceedings of an international symposium organised by Queen Mary College (University of
1430 London) and the Institute of Geological Sciences, 17-30 September 1972. Seel House Press,
1431 Liverpool, 393–400.

1432 Schnabl, P., Pruner, P., Wimbledon, W.A.P. 2015. A review of magnetostratigraphic results from the
1433 Tithonian—Berriasian of Nordvik (Siberia) and possible biostratigraphic constraints. Geologica
1434 Carpathica 66, 489–498.

1435 Semenov, B. 1898. Versuch einer Anwendung der statistischen Methode zum Studium der
1436 Vertheilung der Ammoniten in dem russischen Jura. Annuaire géologique et minéralogique de
1437 la Russie 2, 101–122. [in Russian and German]

1438 Sha, Jingeng, Fürsich, F.T. 1994. Bivalve faunas of eastern Heilongjiang, northeastern China. II. The
1439 Late Jurassic and Early Cretaceous buchiid fauna. Beringeria 12, 3–93.

1440 Sokolov, D.N. 1908a. Aucelly Timana I Shpicbergena. Aucellen vom Timan und von Spitzbergen.
1441 Mémoires du Comité Géologique, Nouvelle série 36, 1–29.

1442 Sokolov, D.N. 1908b. Ueber Aucellen aus dem Norden und Osten von Sibirien. Résultats scientifiques
1443 de l'Éxpedition Polaire Russe en 1900–1903, sous la direction du Baron E. Toll, Section C:
1444 Géologie et Paléontologie, Livraison 3. Mémoires de l'Académie Impériale des sciences de St.-
1445 Pétersbourg, Classe Physico-Mathématique 21 (3), 1–18.

1446 Sømme, T.O., Doré, A.G., Lundin, E.R., Tørudbakken, B.O. 2018. Triassic–Paleogene paleogeography
1447 of the Arctic: Implications for sediment routing and basin fill. AAPG Bulletin 102, 2481–2517.

1448 Souaya, F.J. 1976. Foraminifera of Sun-Global Linckens Island Well P-46, Arctic Archipelago, Canada.
1449 Micropalaeontology 22, 249–306.

1450 Spath, L.F. 1924. On the Blake Collection of ammonites from Kachh, India. Memoirs of the Geological
1451 Survey of India, Palaeontologica Indica, New Series 9 (1), 1–29.

1452 Spath, L.F. 1936. The Upper Jurassic invertebrate faunas of Cape Leslie, Milne Land. II. Upper
1453 Kimmeridgian and Portlandian. Meddelelser om Grønland 99 (3), 1–180.

1454 Spath, L.F. 1952. Additional observations on the invertebrates (chiefly ammonites) of the Jurassic
1455 and Cretaceous of East Greenland. Meddelelser om Grønland 133 (4), 1–40.

1456 Stoliczka, F. 1870–1871. Cretaceous fauna of southern India, Vol. 3, The Pelecypoda, with a review of
1457 all known genera of this class, fossil and Recent. Memoirs of the Geological Survey of India,
1458 Palaeontologia Indica 6, 1–537.

1459 Stolley, E. 1919. Die Systematik der Belemniten. Jahresbericht des Niedersächsischen Geologischen
1460 Vereins 11 (1918), 1–59.

1461 Stott, D.F. 1969. Ellef Ringnes Island, Canadian Arctic Archipelago. Geological Survey of Canada,
1462 Paper 68–16, 1–44.

1463 Tan, J.T., Hills, L.V. 1978. Oxfordian – Kimmeridgian dinoflagellate assemblage, Ringnes Formation,
1464 Arctic Canada. Geological Survey of Canada, Paper 78–1C, 63–73.

1465 Teichert, B.M.A.,, Luppold, F.W. 2013. Glendonites from an Early Jurassic methane seep—Climate or
1466 methane indicators?: Palaeogeography, Palaeoclimatology, Palaeoecology 390, 81–93.

1467 Tennant, J. P., Mannion, P. D., Upchurch, P., Sutton, M. D., Price, G. D. 2017. Biotic and
1468 environmental dynamics through the Late Jurassic–Early Cretaceous transition: evidence for
1469 protracted faunal and ecological turnover. Biological Reviews 92, 776–814.

1470 Teppner, W. von 1922. Lamellibranchia Tertiaria, Anisomyaria II. In: Diener, C. (Ed.), Fossilium
1471 Catalogus, I. Animalia, 15, W. Junk, Berlin, 67–296.

1472 Thorsteinsson, R. 1974. Carboniferous and Permian stratigraphy of Axel Heiberg Island and western
1473 Ellesmere Island, Canadian Arctic Archipelago. Geological Survey of Canada, Bulletin 224, 1–
1474 115.

1475 Trauth, F. 1927. Aptychenstudien. 1. Über die Aptychen im Allgemeinen. Annalen des
1476 Naturhistorischen Museums in Wien 41, 171–259.

1477 van Hinsbergen, D.J.J., de Groot, L.V., van Schaik, S.J., Spakman, W., Bijl, P.K., Sluijs A., Langereis,
1478 C.G., Brinkhuis, H. 2015. A paleolatitude calculator for paleoclimate studies (model version
1479 2.1). Plos One, http://doi.org/10.1371/journal.pone.0126946.

1480 Vickers, M.L., Price, G.D., Jerrett, R.M., Sutton, P., Watkinson, M.P., FitzPatrick, M. 2019. The
1481 duration and magnitude of Cretaceous cold events: Evidence from the northern high latitudes.
1482 Geological Society of America Bulletin 131, 1979–1994.

1483 Vischniakoff, N. 1882. Description des Planulati (*Perisphinctes*) jurassiques de Moscou, 1ère Partie,
1484 contenant un atlas de 8 planches. Published by the author, Moscou.

1485 Wall, J.H. 1983. Jurassic and Cretaceous foraminiferal biostratigraphy in the eastern Sverdrup Basin,
1486 Canadian Arctic Archipelago. Bulletin of Canadian Petroleum Geology 31, 246–281.

1487 Wall, J.H. 2004. Mesozoic microfossil assemblages from two wells on Prince Patrick Island, Canadian
1488 Arctic Archipelago. Geological Survey of Canada, Open File 4731, 1–18.

1489 Wierzbowski, H., Anczkiewicz, R., Pawlak, J., Rogov, M.A., Kuznetsov, A.B. 2017. Revised Middle–
1490 Upper Jurassic strontium isotope stratigraphy. Chemical Geology 466, 239–255.

1491 Wierzbowski, A., Hryniewicz, K., Hammer, Ø., Nakrem, H.A., Little, C.T.S. 2011. Ammonites from
1492 hydrocarbon seep carbonate bodies from the uppermost Jurassic – lowermost Cretaceous of
1493 Spitsbergen and their biostratigraphical importance. Neues Jahrbuch für Geologie und
1494 Paläontologie, Abhandlungen 262, 267–288.

1495 Wilson, D.G. 1976. Studies of Mesozoic stratigraphy, Tanquary Fiord to Yelverton Pass, northern
1496 Ellesmere Island, District of Franklin. Geological Survey of Canada, Paper 76–1A, 449–451.

1497 Wimbledon, W.A.P. 2017. The Tithonian/Berriasian stage boundary and the base of the Cretaceous
1498 System. Berichte der Geologischen Bundesanstalt 120, 290.

1499 Wright, C.W., Callomon, J.H., Howarth, M.K. 1996. Treatise on invertebrate paleontology, Part L,
1500 Mollusca 4, revised, Volume 4, Cretaceous Ammonoidea. The University of Kansas & The
1501 Geological Society of America, Lawrence & Boulder, i–xx, 1–362.

1502 Zakharov, V.A. 1981. Bukhiidy i biostratigrafiya boreal'noi verkh-nei yury i neokoma [Buchiids and
1503 biostratigraphy of the Boreal Upper Jurassic and Neocomian]. Trudy, Akadamija Nauk SSSR,
1504 Sibirkoe Otdelenie, Institut Geologii i Geofiziki 458, 1–271. [in Russian]

1505 Zakharov, V.A. 1987. The bivalve *Buchia* and the Jurassic-Cretaceous boundary in the Boreal
1506 Province. Cretaceous Research 8, 141–153.

1507 Zakharov, V.A., Rogov, M.A. 2003. Boreal-Tethyan mollusk migrations at the Jurassic-Cretaceous
1508 boundary time and biogeographic ecotone position in the northern hemisphere. Stratigrafiya.
1509 Geologicheskaya Korrelyatsiya 11, 54–74. [in Russian; English translation in Stratigraphy and
1510 Geological Correlation 11, 152–171]

1511 Zakharov, V.A., Rogov, M.A. 2008. Let the Volgian stage stay in the Jurassic. Russian Geology and
1512 Geophysics 49, 408–412.

1513 Zittel, K. A. von 1884. Handbuch der Palaeontologie, 1. Abtheilung, Palaeozoologie, 2. Band,
1514 Mollusca und Arthropoda. München und Leipzig, R. Oldenbourg, 1–893.

1515 Zittel, K. A. von 1895. Grundzüge der Palaeontologie (Palaeozoologie), Abteilung 1, Invertebrata.
1516 München und Leipzig, R. Oldenbourg, 1–971.

1517

1518 Figure captions

1519 Figure 1. Overview of the study area. A. Geological map of the Sverdrup Basin, Queen Elizabeth
1520 Islands, Arctic Canada; modified from Harrison et al. (2011). Small black quadrangle indicates area of
1521 Figure 1B. Numbers indicate macrofossil localities of the Jurassic-Cretaceous transition interval,

adapted from Jeletzky (1984); (1) Slidre Fiord; (2) Greely Fiord; (3) Gibbs Fiord; (4) Buchanan Lake; (5) Mackenzie King Island. B. Geological map of the Ekblaw Lake area; modified from Mayr and Trettin (1996). The area of the Rollrock Section, depicted in Figure 4A, is indicated by the black rectangle.

Figure 2. Schematic Jurassic and Lower Cretaceous lithostratigraphy of the Sverdrup Basin (modified from Lopez-Mir et al., 2018, with additions from Herrle et al., 2015). Yellow and grey fills denote sandstone- and mudstone-dominated units, respectively. The dashed line marks the transition from the syn-rift to the post-rift stage, as inferred by Hadlari et al. (2016).

Figure 3. A. Submarine erosion surface at top of Sandy Point Formation, exposed at the southern side of Rollrock Valley. B. Detail of A, showing differential weathering of burrows and background sediment and potential biogenic crusts. Scale bar = 10 mm.

Figure 4. A. Overview of the Rollrock Section, exposing the dark grey, mudstone-dominated Ringnes and Deer Bay formations, capped by yellowish sandstones of the Isachsen Formation. B. Northeastern part of A, with stippled lines indicating the position of the sedimentary log.

Figure 5. Outcrop photographs. A. Central part of Deer Bay Formation, cut by a half-metre wide, vertical volcanic dyke. B. Transition from uppermost Deer Bay Formation to lower Isachsen Formation. The stippled line indicates the boundary between these formations. C. Upper part of the Ringnes Formation and a large part of the Deer Bay Formation. The stippled line indicates the boundary between these formations. The giant concretion in the centre of the image is approximately 2.5 m wide.

Figure 6 (legend plus two facing pages). Detailed sedimentary log of the Rollrock Section. Formation boundaries are indicated by stippled red lines.

Figure 7. Field photographs. A. Pear-shaped concretion on top of indurated sideritic layer at 344 m log height. B. Overview and close up (inset) of top of Ringnes Formation, with abundant dropstones

eroded from the Deer Bay Formation above; 251 m log height. C. Concretion with negative of poorly preserved dorsoplanitid ammonite at 307 m log height. D. Glendonites at approximately 410 m log height.

Figure 8. Dropstones from the Deer Bay Formation. A–C. Carboniferous/Permian silicified rugose rugose corals. A, B. Bottom and side views; NUIF 3140. C. Top view; NUIF 3063. D–G. Chert pebbles with blackish weathering cortex.

Figure 9. Drawing of a left valve of *Buchia*, illustrating the terminology used in descriptions. CL = crest line, which is an imaginary line, connecting the points of greatest inflation on the folds; F = folds; H = height; HRA = hinge rotation axis, horizontally aligned; L = length; PA = posterior auricle.

Figure 10. Bivalves from the Rollrock Section. A, B, E. *Buchia mosquensis* (Buch, 1844); 307 m horizon. A. Two double-valved specimens; NUIF 3003. B. Left lateral view of partly covered specimen in Figure 10A. E. Right valve, silicone cast; NUIF 3136. C. *Buchia rugosa* (Fischer von Waldheim, 1837); NUIF 3019; 196.8 m horizon. D, F–J. *Buchia terebratuloides* (Lahusen, 1888); 333 m horizon. D. Right valve, NUIF 3167. F. Left valve; NUIF 3008. G. Left valve with marked growth interruption at approximately one third of shell height; NUIF 3008. H, I. Several right valves with marked growth interruption at approximately one third of shell height; NUIF 3009. J. Compressed right valve; NUIF 2991. Scale bar = 10 mm.

Figure 11. Bivalves from the Rollrock Section. A, B. *Buchia unschensis* (Pavlow, 1907); 355 m horizon. A. Right valve; silicone cast; NUIF 3038. B. One left and one right valve; NUIF 3037. C. *Pleuromya* sp.; NUIF 3005; 363.5 m horizon. D–F. *Buchia okensis* (Pavlow, 1907), left valves; NUIF 3036, 3042, 3033. G, H. *Buchia volgensis* (Lahusen, 1888), double-valved specimen; NUIF 3034; 355 m horizon. G. Left lateral view. H. Right lateral view. I. *Entolium* sp.; NUIF 3134; 333 m horizon. White arrows indicate the position of the posterior auricle in figures 11A and D–F. Scale bar = 10 mm.

Figure 12. A. *Dorsoplanites maximus* Spath, 1936; 307 m horizon; NUIF 3012. Scale bar = 50 mm. B. *Praestriaptychus* sp. from backside of specimen in Figure 12A; silicone cast. Scale bar = 10 mm.

Figure 13. *Dorsoplanites maximus* Spath, 1936; 307 m horizon; NUIF 2984. A. Right lateral view. B. left lateral view of ultimate half whorl. Scale bar = 50 mm.

Figure 14. *Dorsoplanites sachsi* Michailov, 1966; external moulds; 307 m horizon. A. NUIF 3016. B. NUIF 3015. Scale bar = 10 mm.

Figure 15. Dorsoplanitidae indet. A, C. Left and right lateral view, respectively; NUIF 2985. B. NUIF 3000. D, E. Suture line reconstructed from whorl fragment below; NUIF 2980. F. NUIF 3010. Scale bar = 50 mm.

Figure 16. A. Subcraspeditinae indet.; 355 m horizon; NUIF 3166. B, C. *Praetollia maynci* Spath, 1952; 355 m horizon; NUIF 3014. B. External mould. C. Fragmentary internal mould. Scale bar = 10 mm.

Figure 17. *Borealites fedorovi* Klimova, 1969; 363.5 m horizon. A. NUIF 2993 (part). B. NUIF 2997. C. NUIF 3044. D. NUIF 3043. E. NUIF 2993 (part). F, G. Left and right lateral views; NUIF 2994. Scale bar = 10 mm.

Figure 18. *Borealites fedorovi* Klimova, 1969; 363.5 m horizon; NUIF 3064. Right lateral view of entire specimen. Scale bar = 50 mm.

Figure 19. *Borealites fedorovi* Klimova, 1969; 363.5 m horizon; NUIF 3064. A, B. Right lateral views of earlier growth stages of specimen in Figure 18. C. Reconstructed whorl cross-section of same specimen. Scale bar = 50 mm.

Figure 20. *Borealites* sp.; 357 m horizon; NUIF 3013. Right lateral view of entire specimen. The approximate position of the last suture line is indicated by a white arrow. Scale bar = 50 mm.

Figure 21. *Borealites* sp.; 357 m horizon; NUIF 3013. Right (A) and left (B) lateral views of earlier growth stages of specimen in Figure 20. Scale bar = 50 mm.

Figure 22. Belemnites from the Rollrock Section. A–D. *Arctoteuthis* cf. *porrectiformis* (Anderson, 1945). A, B. Fragmentary specimen; NUIF 2996. A. Lateral view; venter on the right. B. Ventral view. C, D. NUIF 3062; C. Lateral view; venter on the left. D. Ventral view. E, F. *Arctoteuthis* cf. *harabylensis* (Saks and Nal'nyaeva, 1964); loose from above 400 m; NUIF 3139. E. Lateral view; venter on the left. F. Ventral view. Scale bar = 10 mm.

Figure 23. Summary log and biostratigraphic interpretation of the Rollrock Section, displaying: the lithostratigraphic framework; occurrences of glendonites and dropstones; ammonites, belemnites and *Buchia* bivalves with positions in the log indicated in metres; approximate stage boundaries; and biostratigraphic zonation schemes. Northern Siberia ammonite zones are adapted from Wierzbowski et al. (2011, 2017). Eastern Greenland ammonite zones are adapted from Kelly et al. (2015), Möller et al. (2015) and Wierzbowski et al. (2017). *Buchia* ranges are adapted from Zakharov (1981) and Rogov and Zakharov (2009). Ammonite zones and *Buchia* species represented in the Sverdrup Basin are displayed in colour. Ammonite zones and *Buchia* species (presumably) represented in the Rollrock Section are indicated by (stippled) red frames.

Figure

Click here to access/download;Figure;01_Map Sverdrup.tif

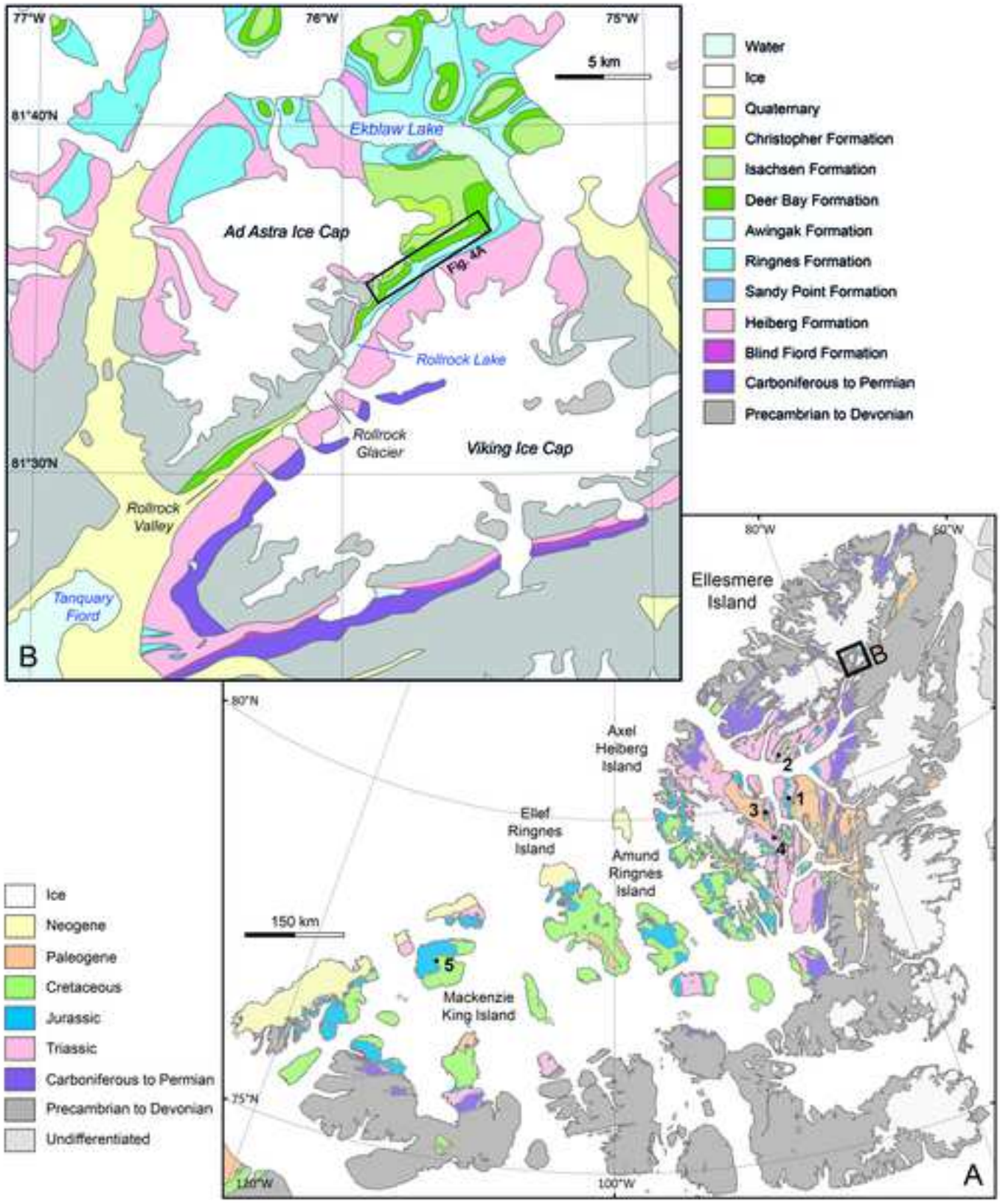

Figure

Click here to access/download;Figure;02_Lithostrat.tif

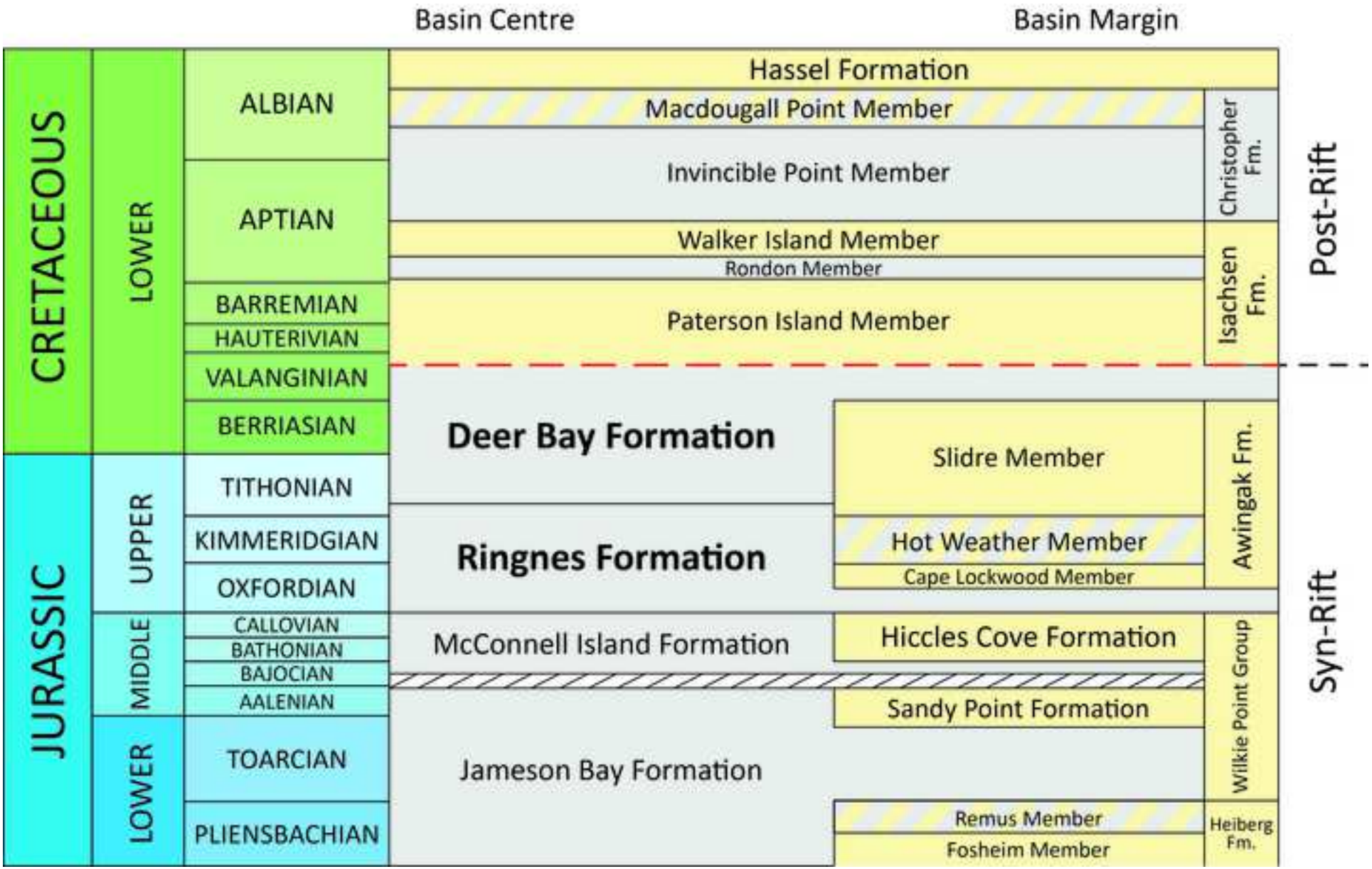

Figure

Click here to access/download;Figure;03_SandyPointTop.tif

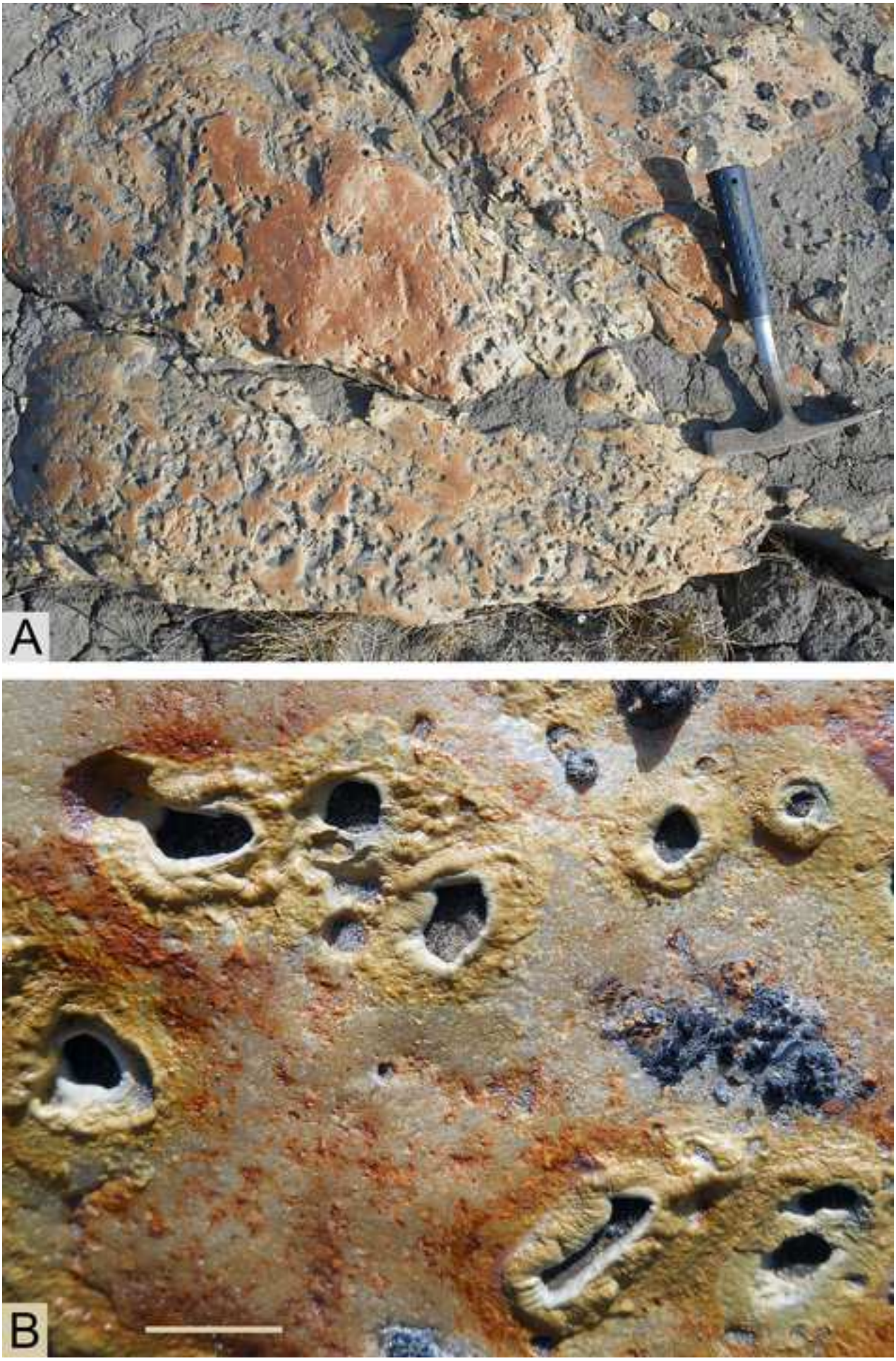

Figure

Click here to access/download;Figure;04_TheSlope.tif

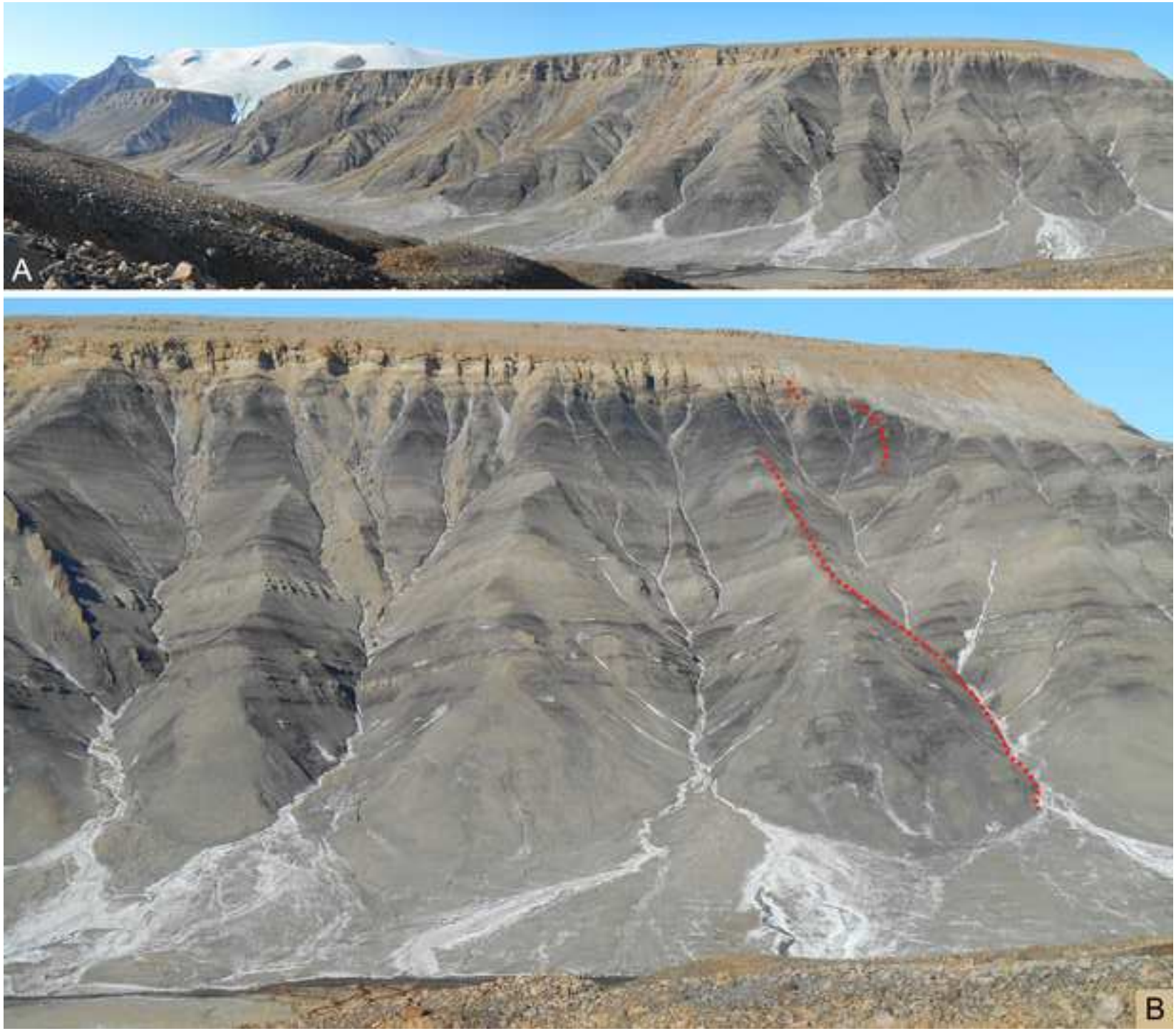

Figure

Click here to access/download;Figure;05_MidToTop.tif

Figure

Click here to access/download;Figure;06_Legend.tif

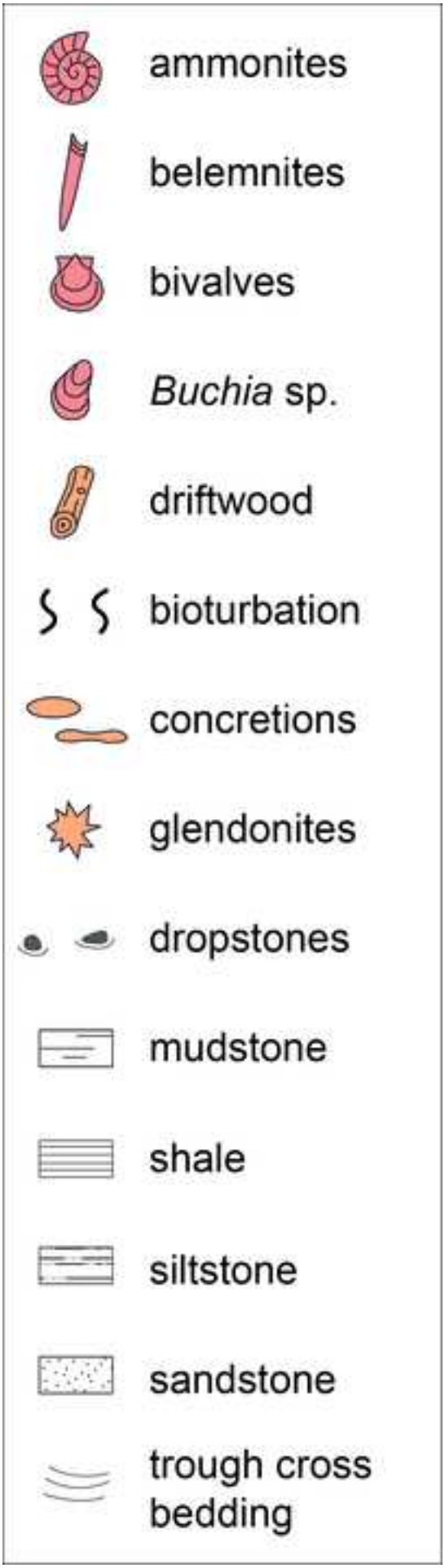

Figure

Click here to access/download;Figure;06_Rollrock Log Part 1.tif

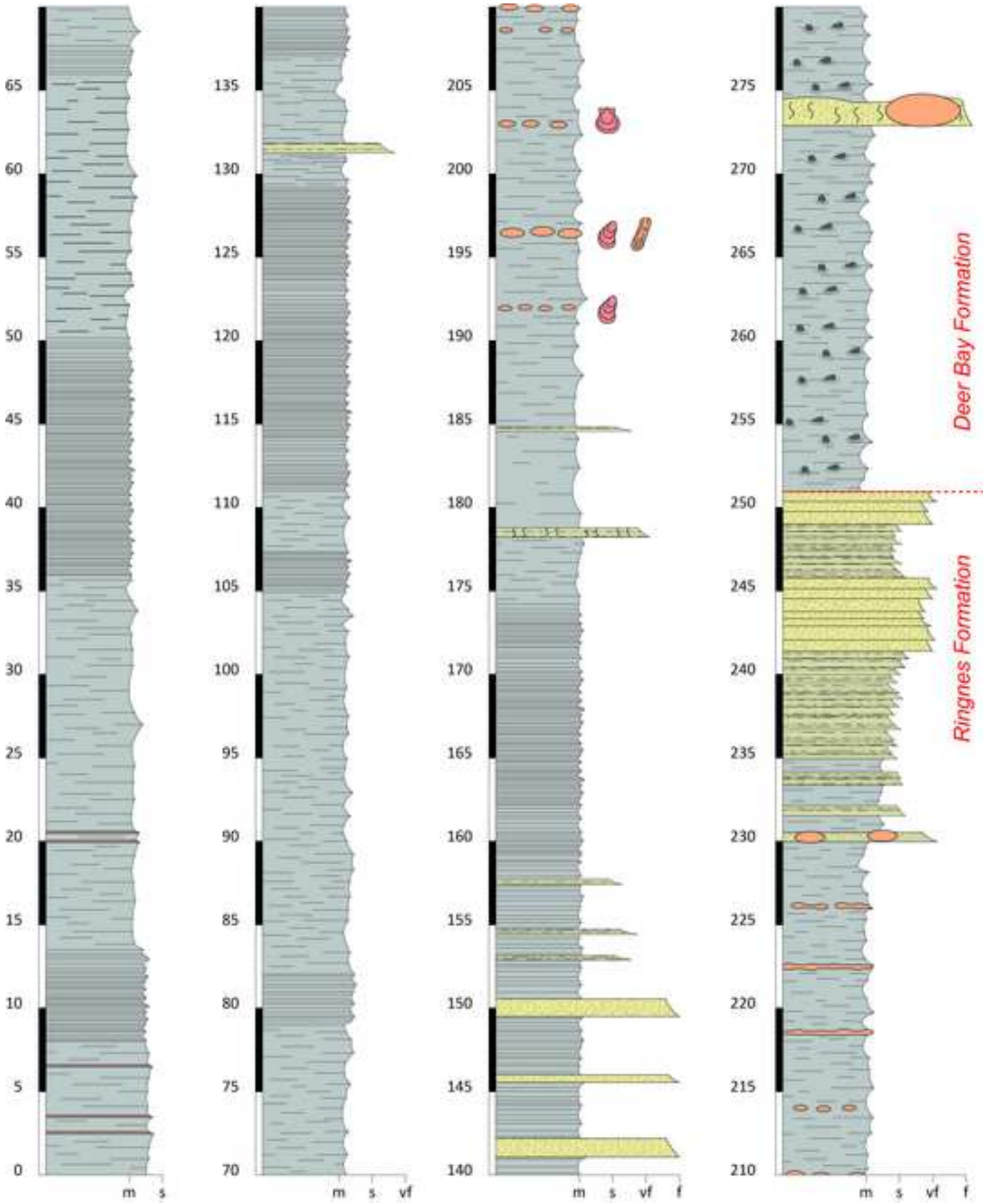

Figure

Click here to access/download;Figure;06_Rollrock Log Part 2.tif

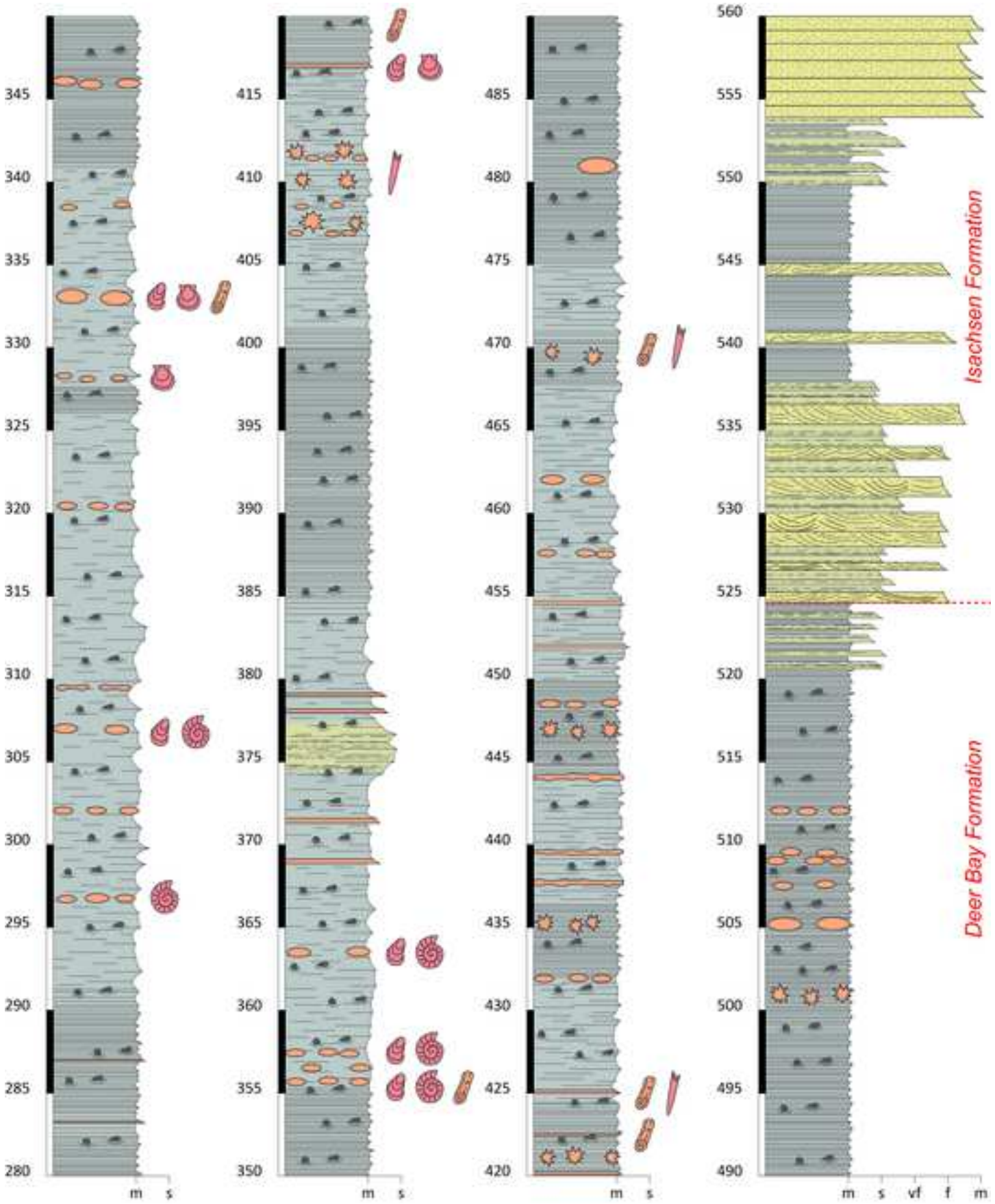

Figure

Click here to access/download;Figure;07_Outcrop_details.tif

Figure

Click here to access/download;Figure;08_Dropstones_colour.tif

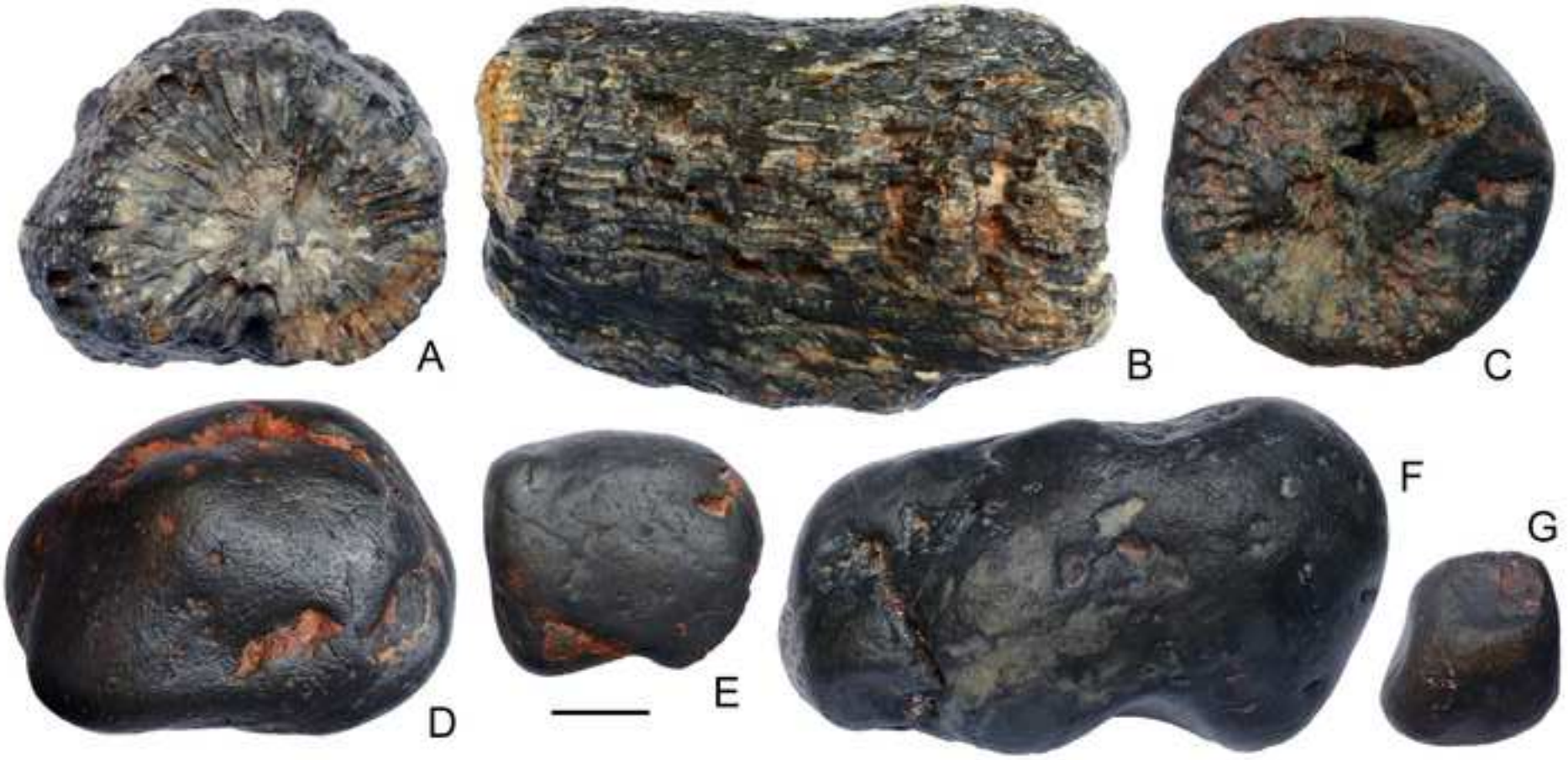

Figure

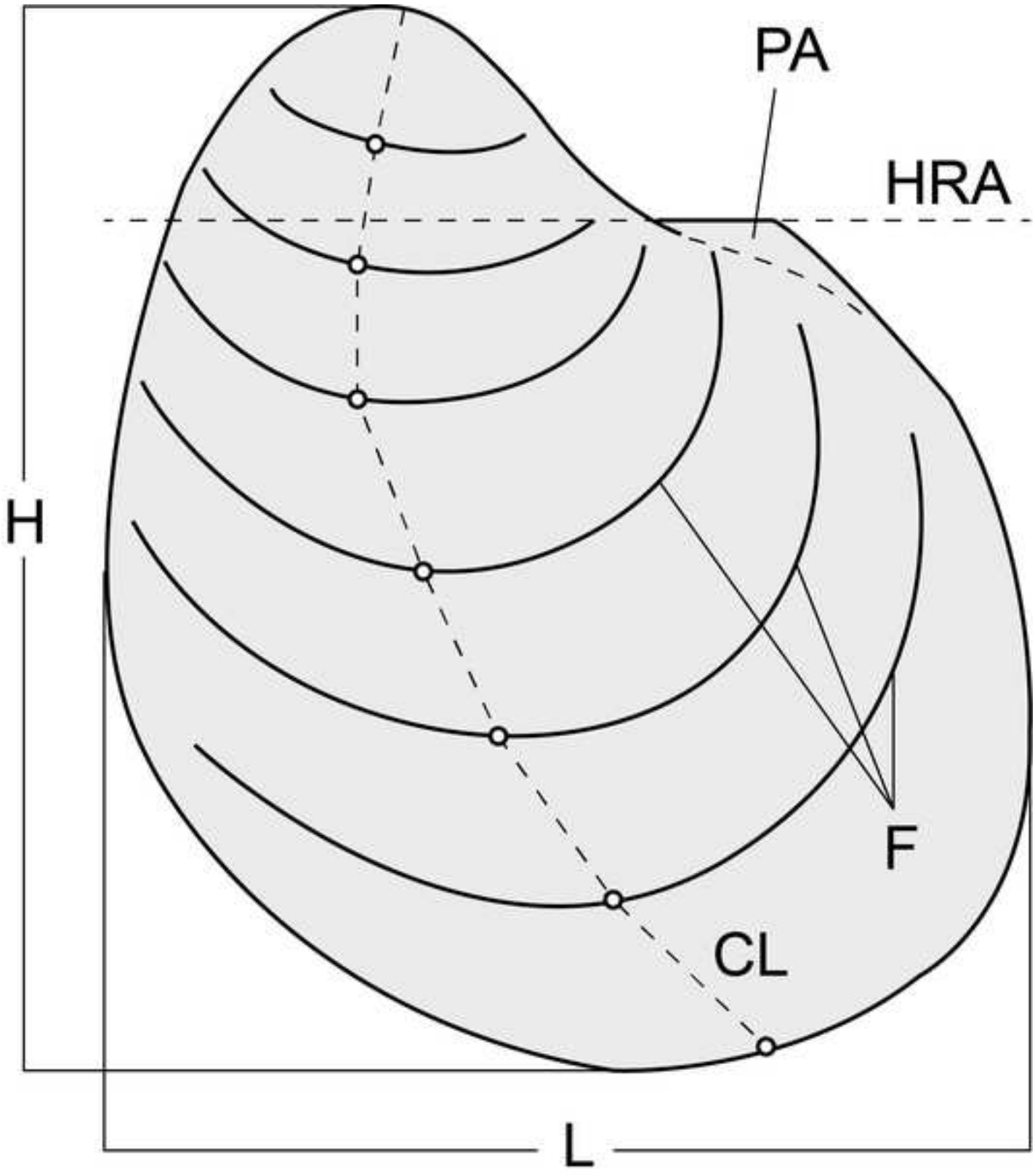

Figure

Click here to access/download;Figure;10_Bivalves_A.tif

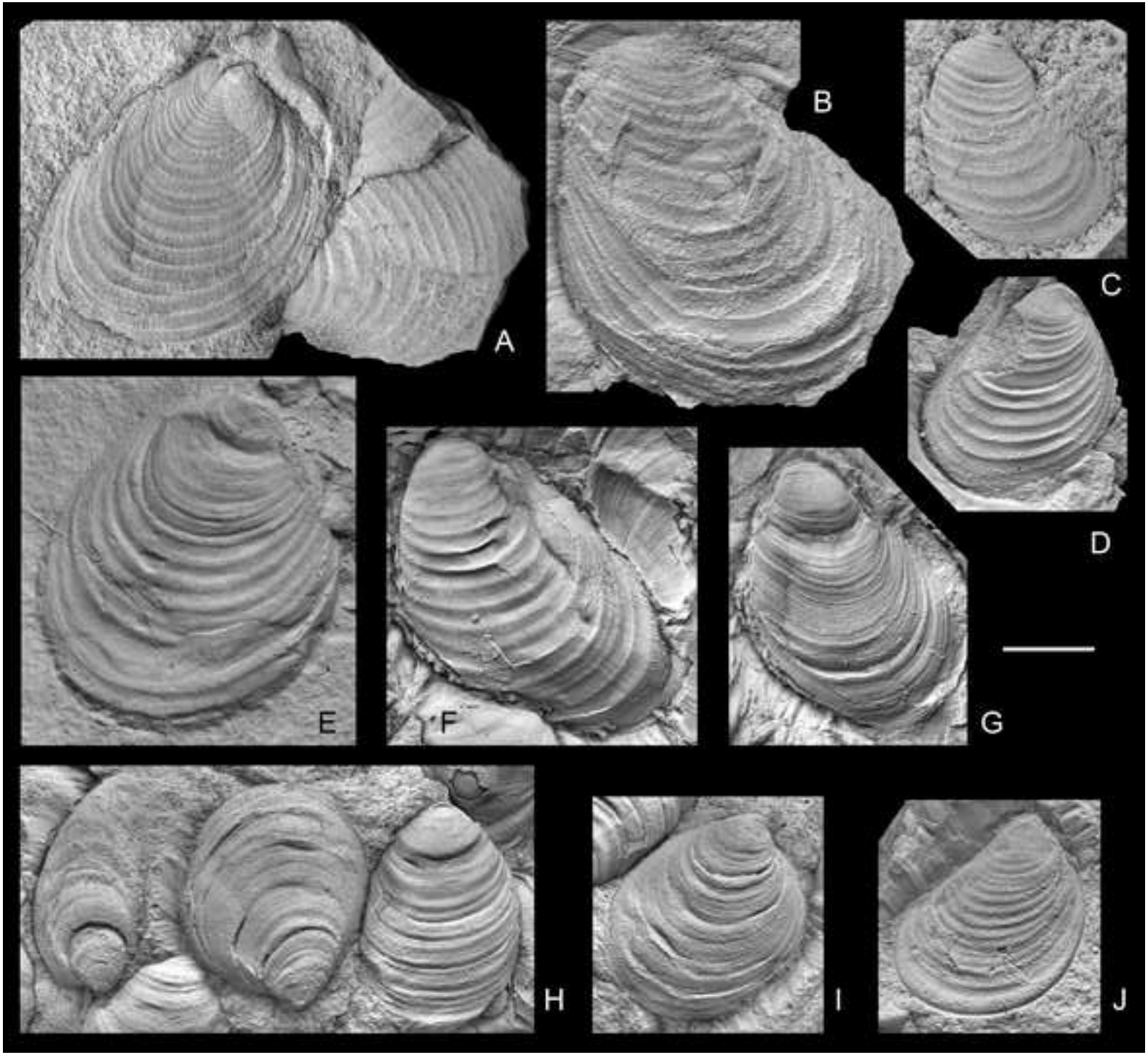

Figure

Click here to access/download;Figure;11_Bivalves_B.tif

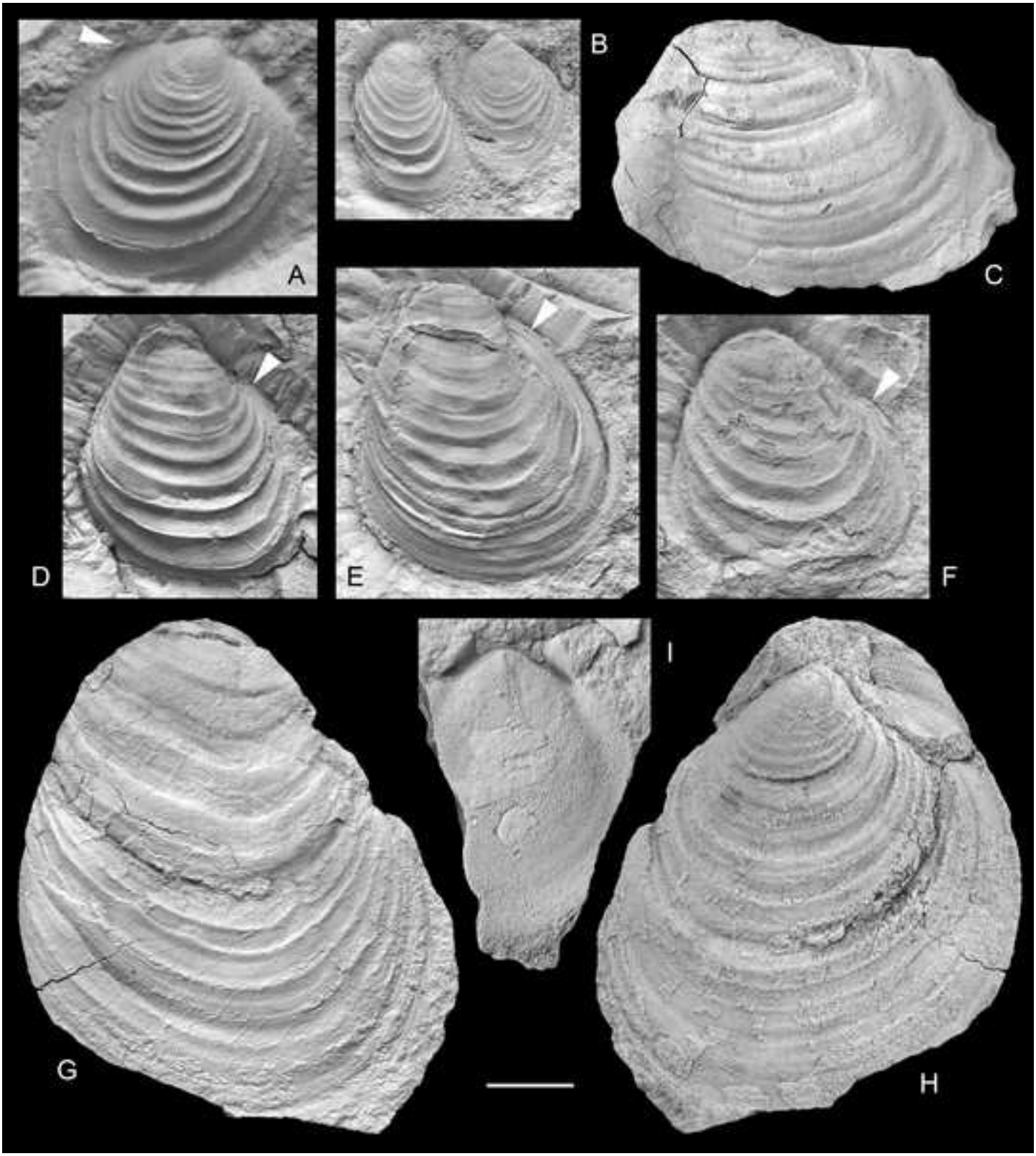

Figure

Click here to access/download;Figure;12_Dorsoplanites_maximus_A.tif

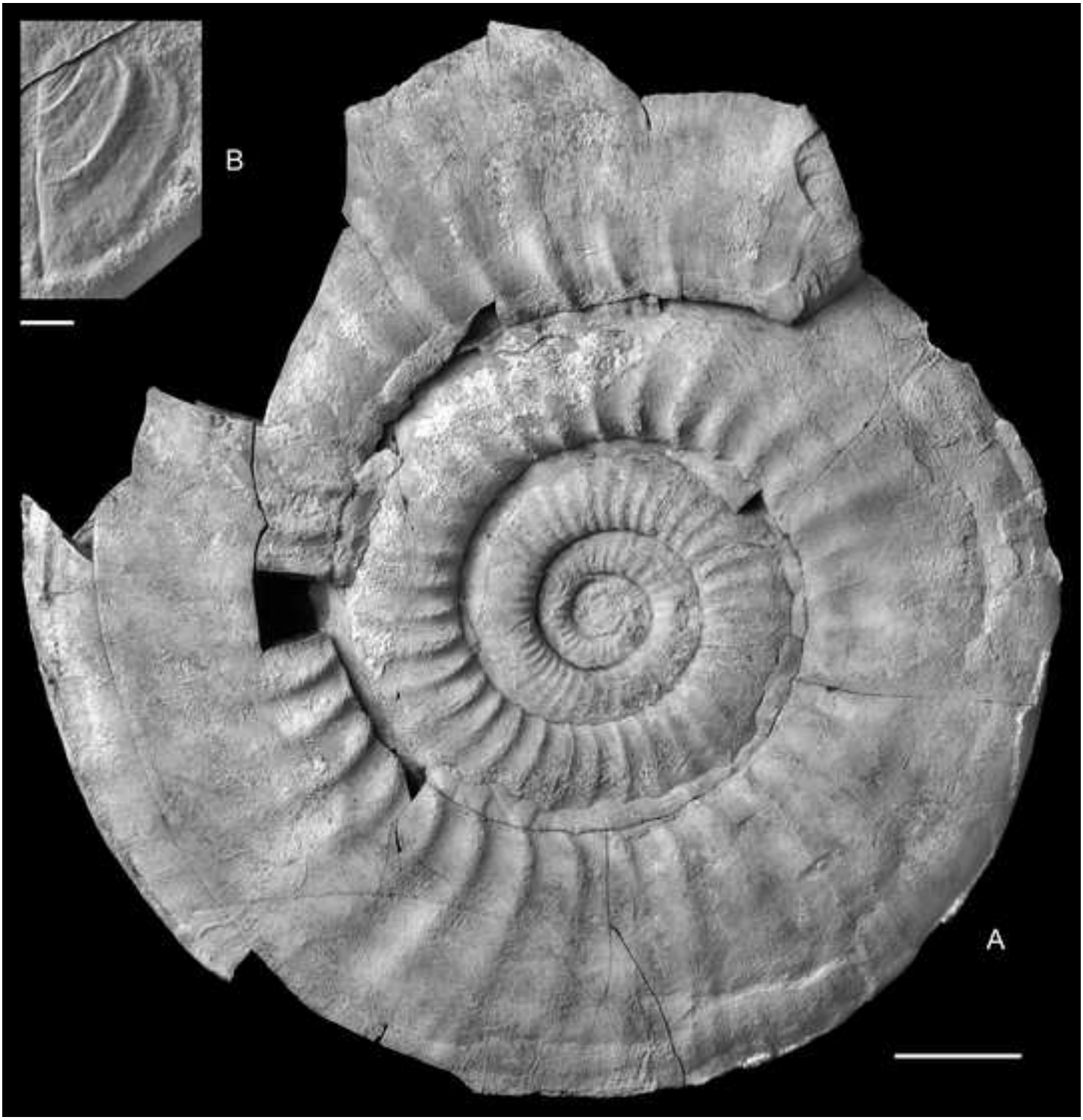

Figure

Click here to access/download;Figure;13_Dorsoplanites_maximus_B.tif

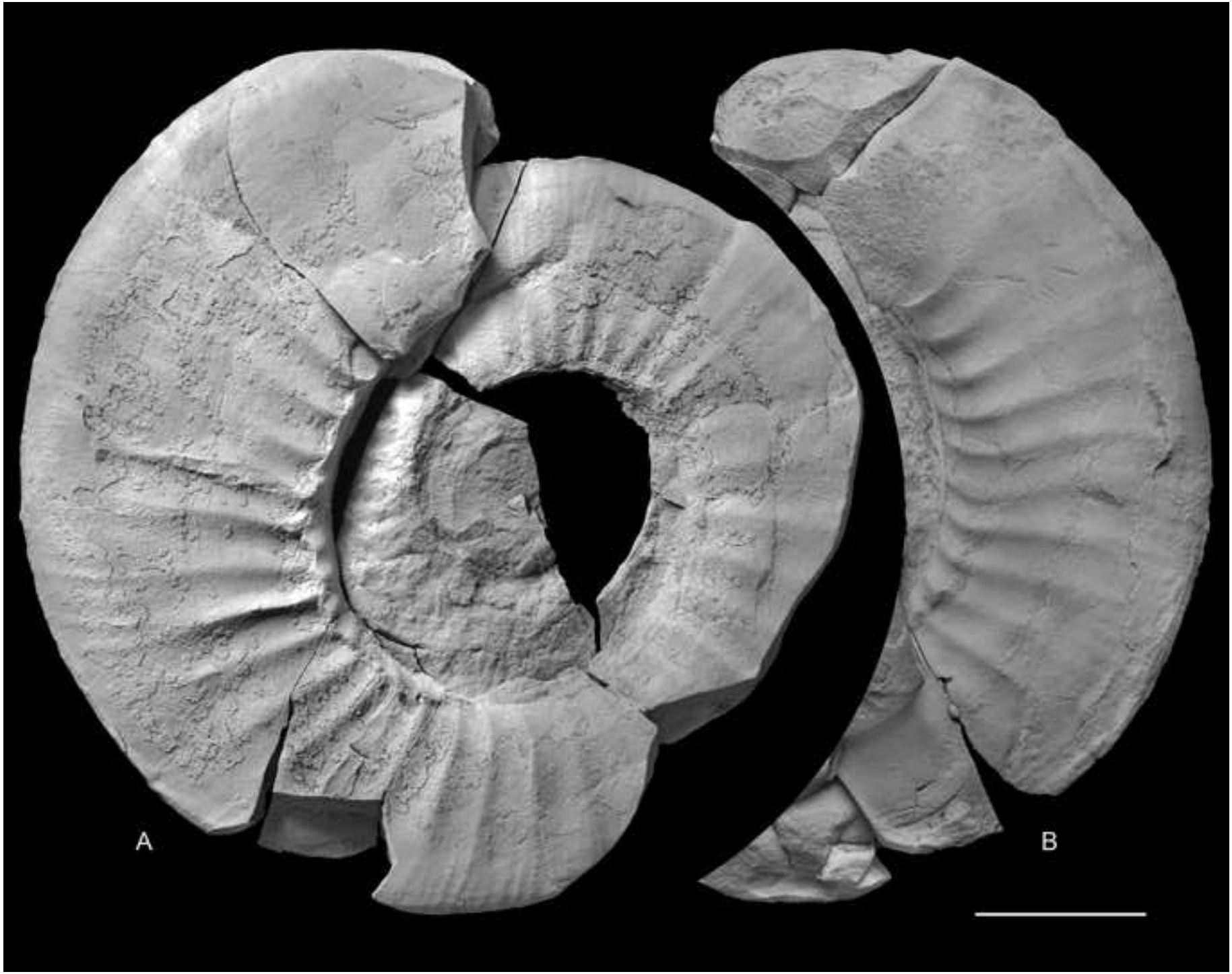

Figure

Click here to access/download;Figure;14_Dorsoplanites sachsi.tif

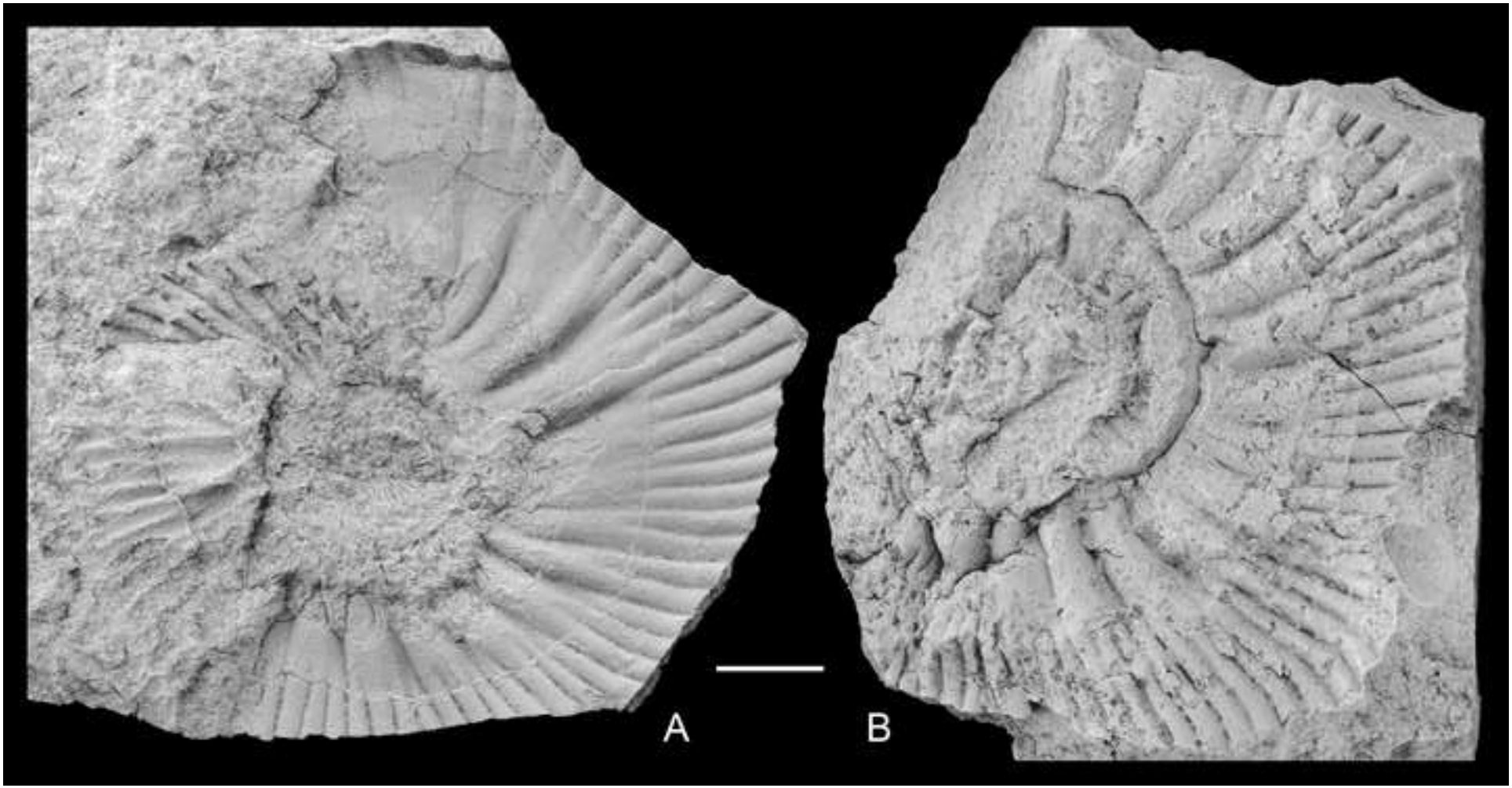

Figure

Click here to access/download;Figure;15_Dorsoplanites_sp.tif

Figure

Click here to access/download;Figure;16_Praetollia.tif

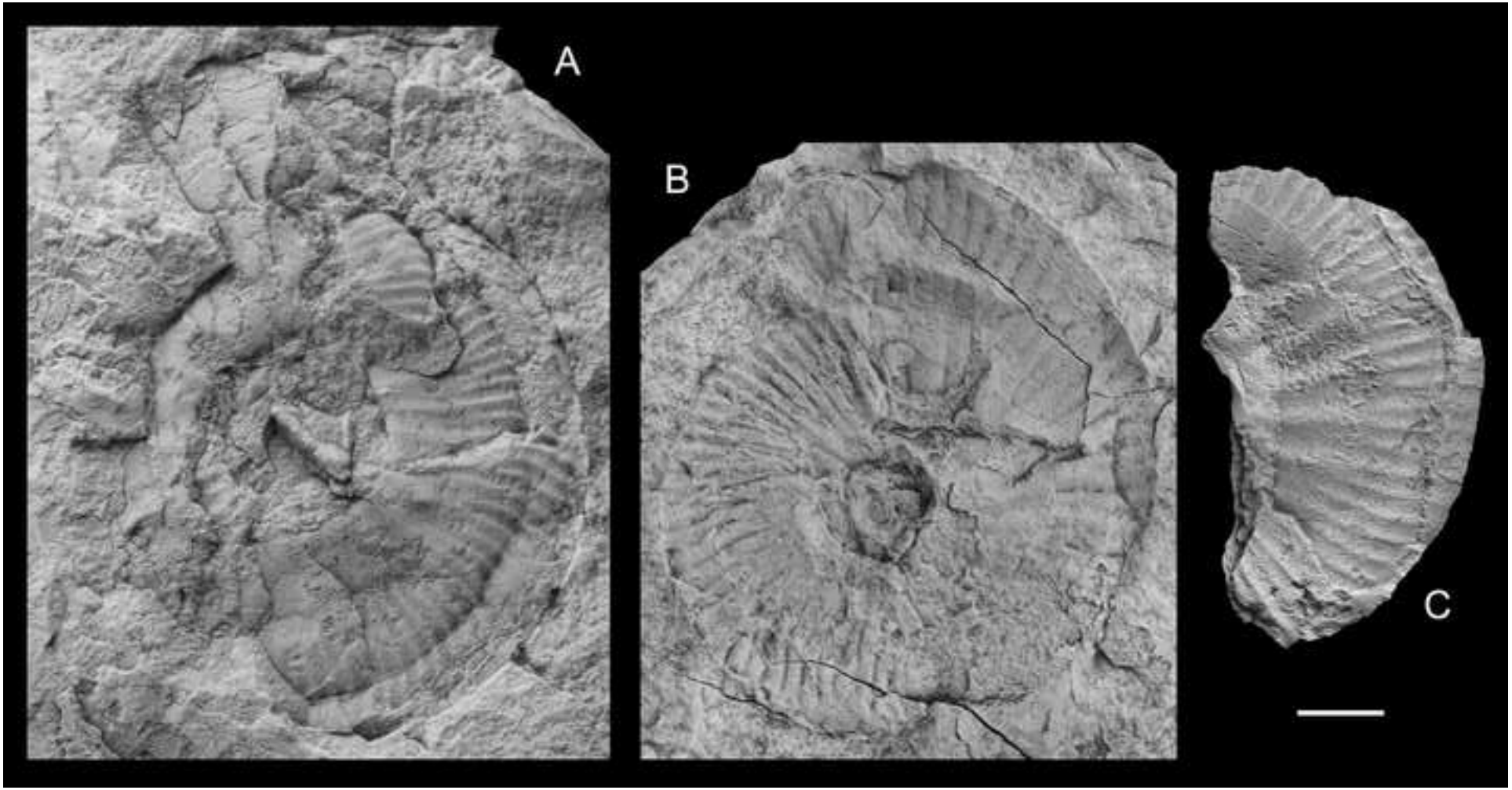

Figure

Click here to access/download;Figure;17_Borealites.tif

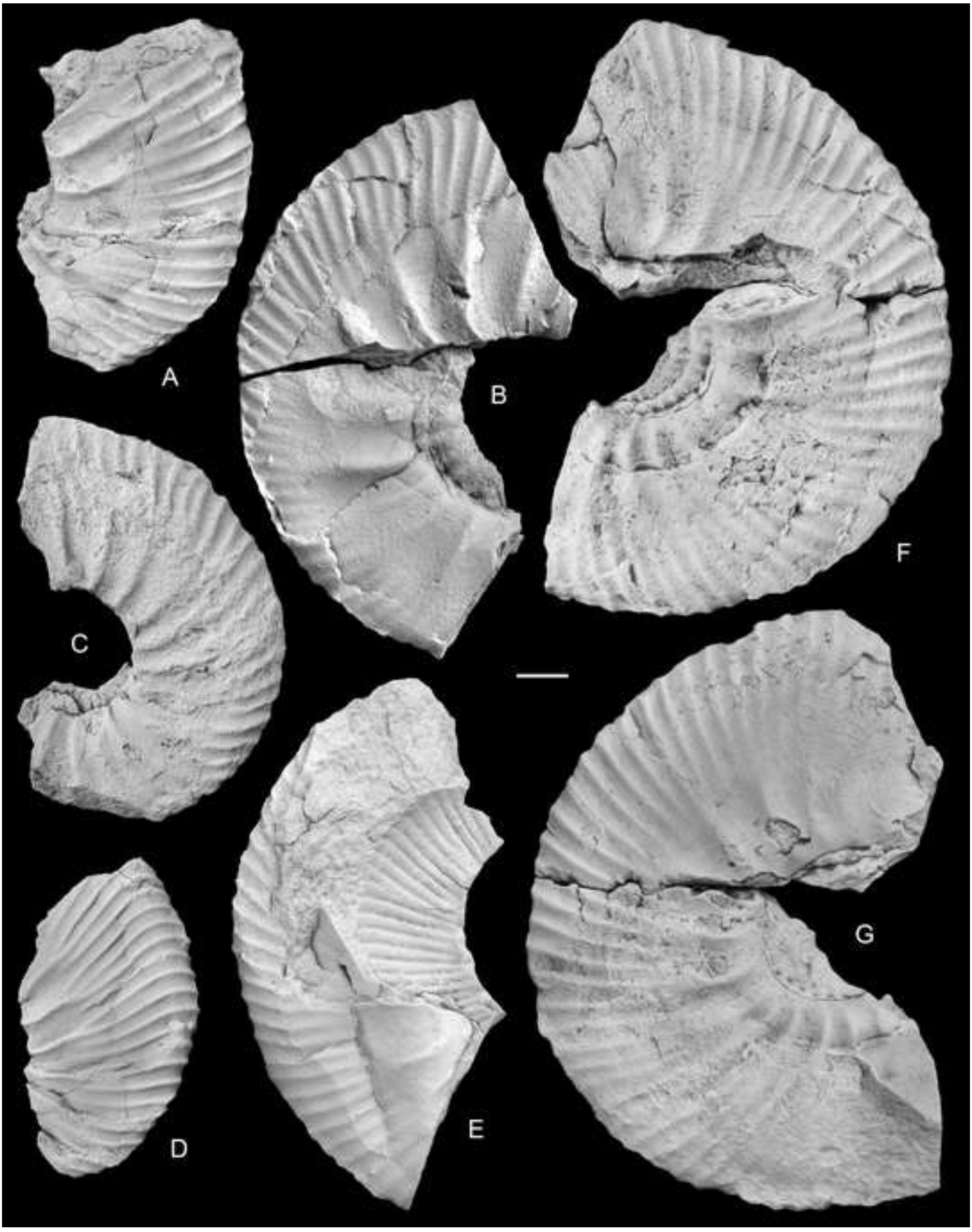

Figure

Click here to access/download;Figure;18_Borealites.tif

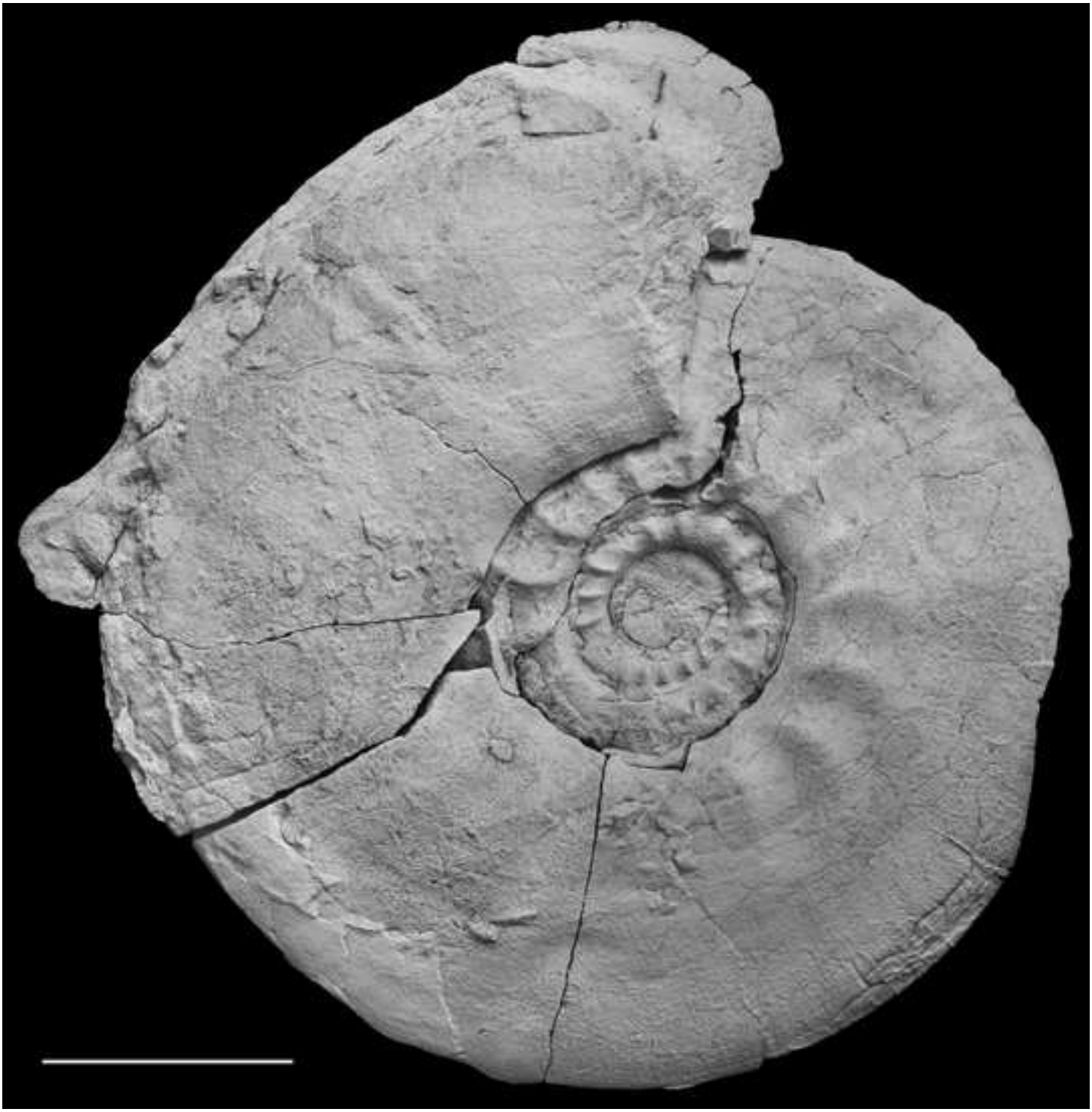

Figure

Click here to access/download;Figure;19_Borealites.tif

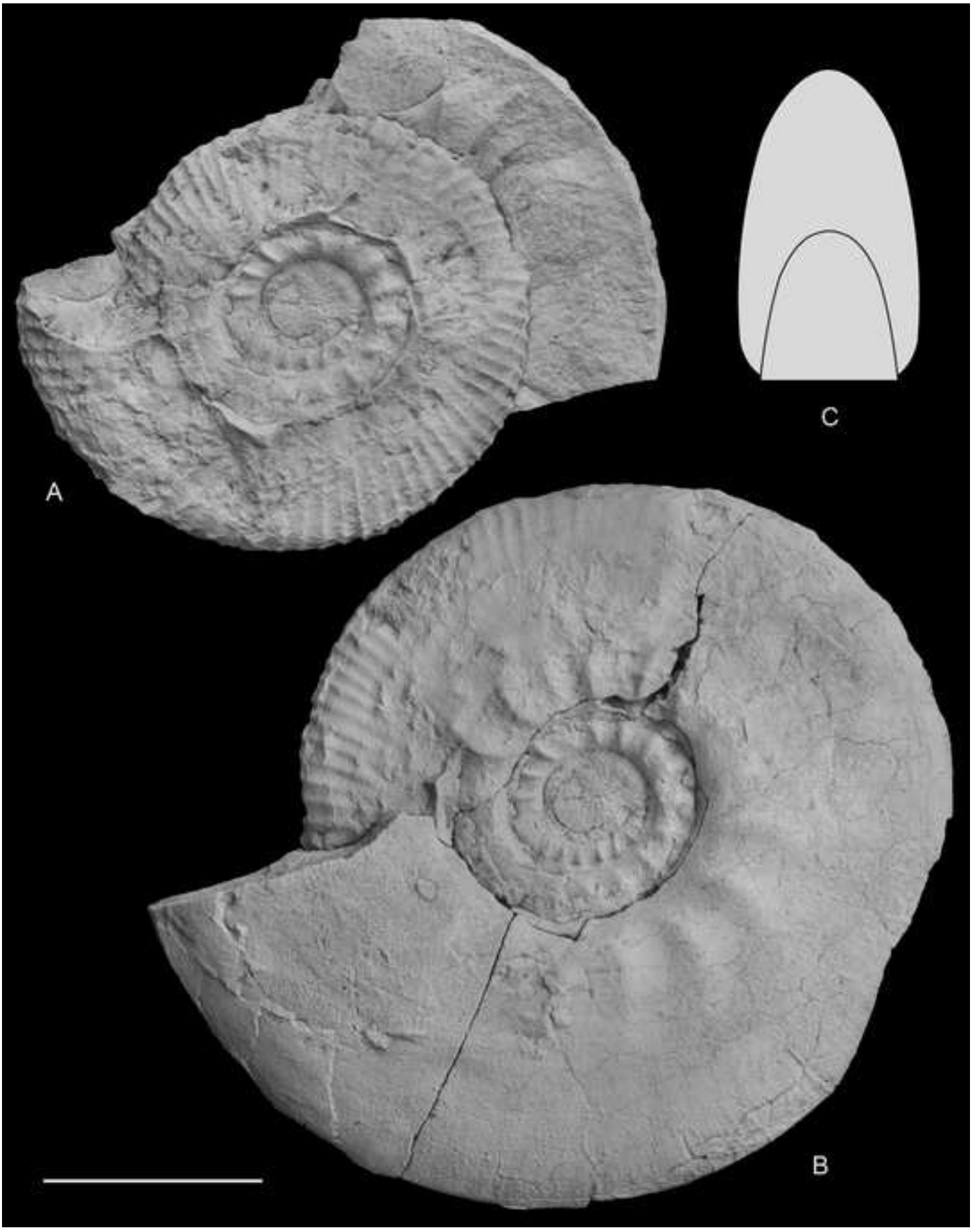

Figure

Click here to access/download;Figure;20_Borealites sp A.tif

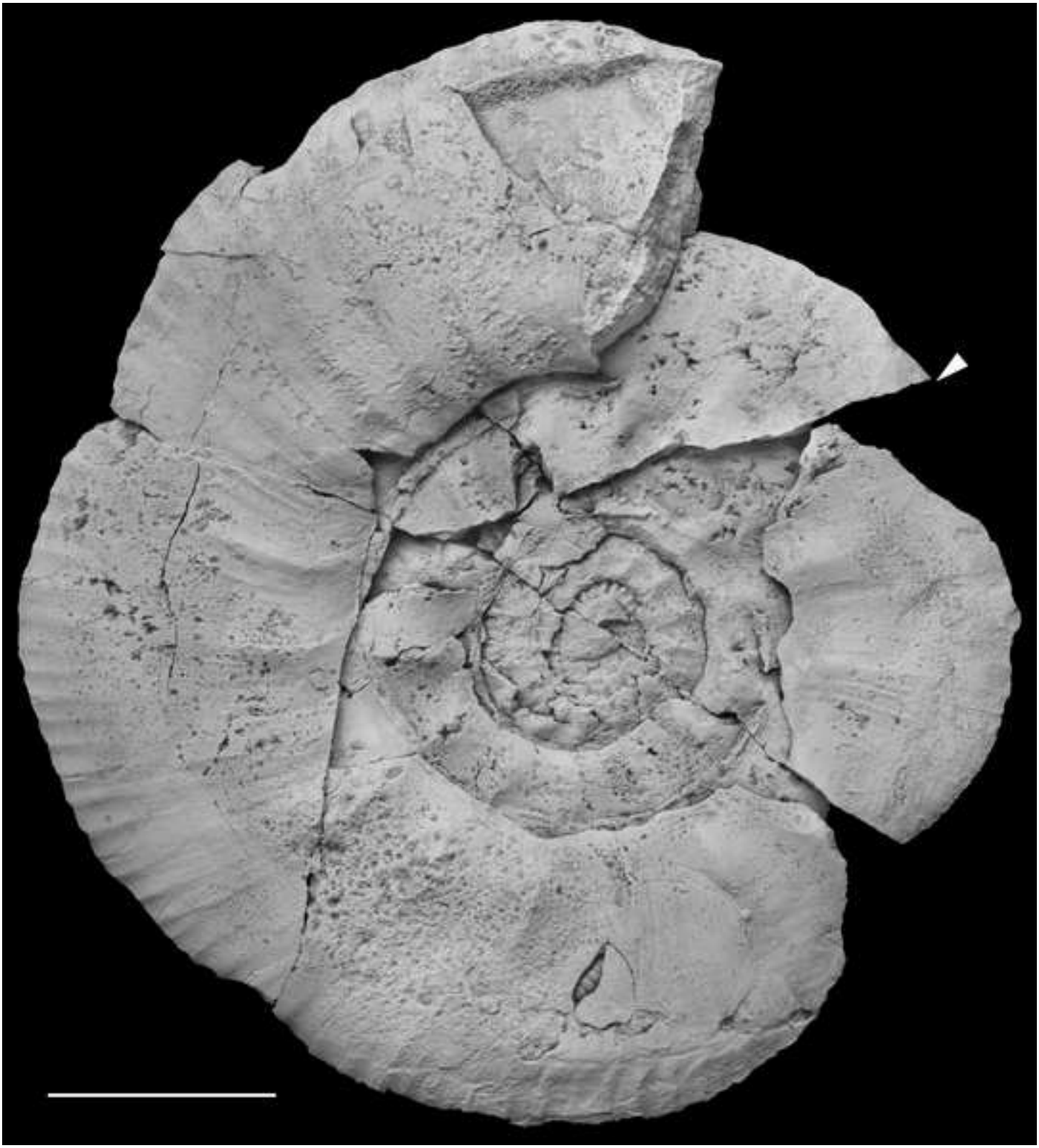

Figure

Click here to access/download;Figure;21_Borealites sp B.tif

Figure

Click here to access/download;Figure;22_Arctoteuthis.tif

Figure

Click here to access/download;Figure;23_Biostrat interpretation scaled.tif

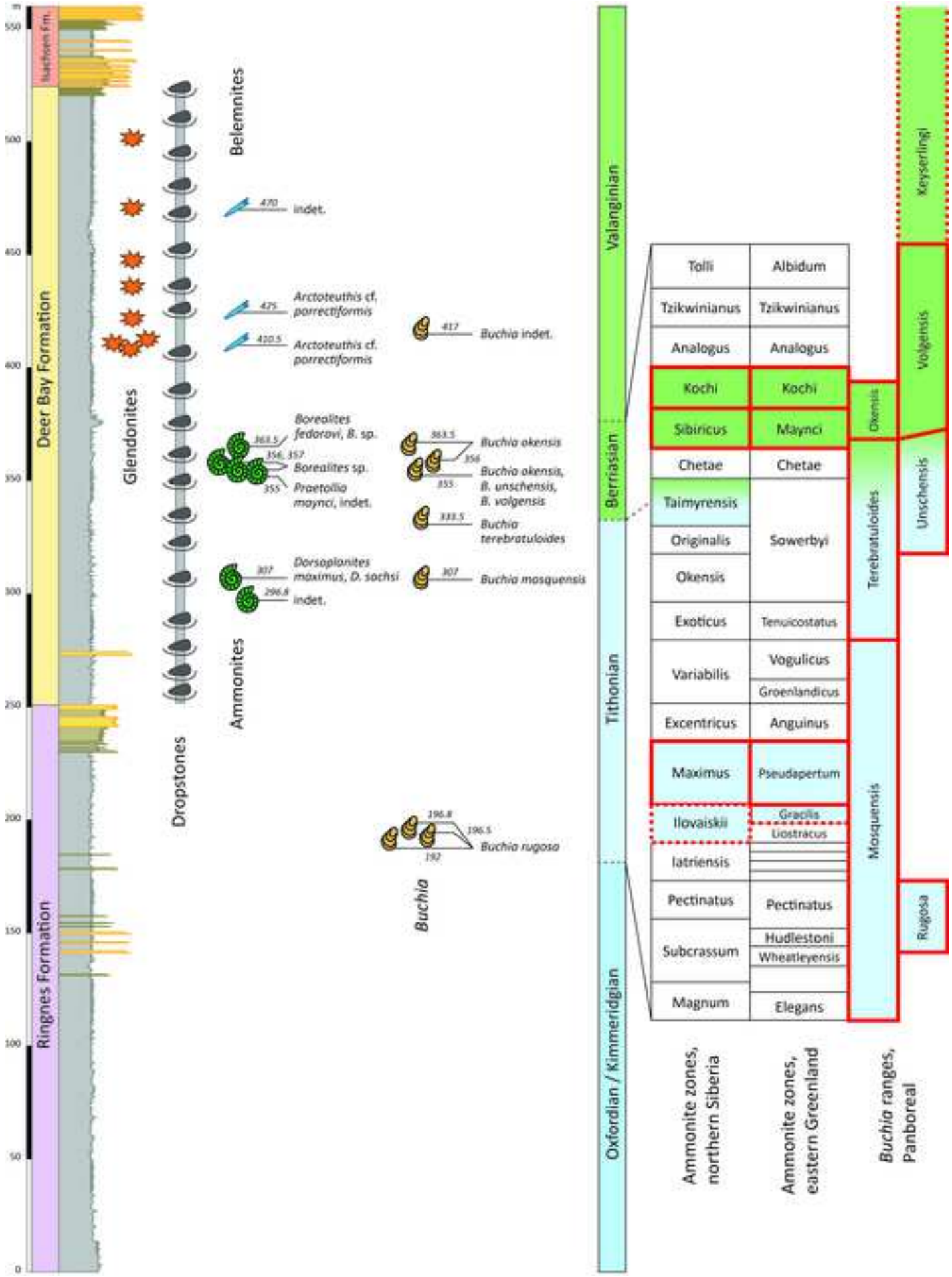

Declaration of interests

☒ The authors declare that they have no known competing financial interests or personal relationships that could have appeared to influence the work reported in this paper.

☐The authors declare the following financial interests/personal relationships which may be considered as potential competing interests: